

Electronic Thesis and Dissertation Repository

9-8-2016 12:00 AM

Esterification of Free Fatty Acid by Selected Homogeneous and Solid Acid Catalysts for Biodiesel Production

Mohamed Kaddour, *The University of Western Ontario*

Supervisor: Anand Prakash, *The University of Western Ontario*

A thesis submitted in partial fulfillment of the requirements for the Master of Engineering Science degree in Chemical and Biochemical Engineering

© Mohamed Kaddour 2016

Follow this and additional works at: <https://ir.lib.uwo.ca/etd>

 Part of the [Catalysis and Reaction Engineering Commons](#)

Recommended Citation

Kaddour, Mohamed, "Esterification of Free Fatty Acid by Selected Homogeneous and Solid Acid Catalysts for Biodiesel Production" (2016). *Electronic Thesis and Dissertation Repository*. 4345.
<https://ir.lib.uwo.ca/etd/4345>

This Dissertation/Thesis is brought to you for free and open access by Scholarship@Western. It has been accepted for inclusion in Electronic Thesis and Dissertation Repository by an authorized administrator of Scholarship@Western. For more information, please contact wlsadmin@uwo.ca.

Abstract

Biodiesel, derived from plant oils and animal fats is an attractive alternative fuel to fossil-based diesel as it is biodegradable, non-toxic, renewable, and has a low emission profile. Industrial production of biodiesel faces major challenges including limited supply of raw material and high cost of feedstock, which accounts for 60-80% of total production cost. Economic feasibility for biodiesel can be improved by using inexpensive raw materials such as waste frying oils and non-edible oils. However, these low quality feedstocks contain significant amounts of free fatty acids (FFA) which reacts with a base to produce soap hindering product separation and reduce product yield. The problem of soap formation can be avoided by adding a pretreatment step to convert FFA in oily feed to alkyl esters by esterification reaction.

This study investigates esterification of FFA using both homogeneous and heterogeneous acid catalysts under mild temperature and pressure conditions in a batch and semi-batch reactor. While homogeneous acid catalyst shows high activity leading to high conversion in less time, there is need for neutralization and water wash to remove residual acid from product. To overcome these problems solid acid catalysts were selected and tested for activity, selectivity and durability. It is demonstrated that a nonporous polymer gel type catalyst from Dow Chemical (BD 20) provides good activity and low deactivation rate compared to other catalysts. This catalyst is recommended for further testing for commercial application. Fitting kinetic models have been proposed for reactor development and modeling endeavors.

Keywords

Biodiesel, Esterification, Homogeneous catalyst, Low-quality feedstock, Semi-batch, Batch, Catalysis, Heterogeneous catalyst, SSA, Cation exchange resin, Amberlyst-15, Amberlyst BD20.

Acknowledgments

First and foremost, I would like to express my gratitude to **Pr. Shahzad Barghi** for accepting me in the program and giving me the honor and privilege to be a student at Western University. I am very thankful for his help support and guidance during the course of this learning journey.

I would like to thank my project supervisor **Pr. Anand Prakash** for his patience with me, his support, guidance and valuable suggestions. Working and learning from him was a very rewarding experience.

My sincere thanks goes to the department of Chemical and Biochemical Engineering at Western University, Staff and Teachers for the great work they are doing all year long.

I'm also very grateful for **Dr. Mark Vandersall** from the DOW Chemical Company, for his guidance and valuable advices, which were key to study the Amberlyst BD20 heterogeneous acid catalyst.

I would also like to thank **Natalia Lesmes** as she was my mentor in lab work, her help in the experimental and theory part was very valuable.

Equally this work would not be done without the valuable contribution of **Stanislas Ivanov** whose involvement in the modeling and calculation parts was of extreme importance.

Likewise, I express my gratitude to **Mr. Brian Dennis** and **Mr. Soheil Afara** the lab managers for their kindness and willingness to help in all situations, besides keeping a cool atmosphere at the engineering department.

Most importantly I would like to thank my Parents who were and are always pushing me toward continuing study, as well as my family wife and children who were very patient and supportive during this learning experience.

Table of Contents

Abstract	i
Acknowledgments.....	ii
Table of Contents	iii
List of Tables	vi
List of Figures	viii
List of Appendices	xiii
CHAPTER 1	1
1 Introduction	1
1.1 Objectives	6
1.2 Thesis Format and Structure	7
References.....	9
CHAPTER 2	11
2 Literature review	11
2.1 Background and history of Biodiesel.....	11
2.2 Advantages and Disadvantages of Biodiesel	13
2.2.1 Advantages of Biodiesel	13
2.2.2 Disadvantages of Biodiesel.....	13
2.3 Technical Properties of Biodiesel	14
2.4 Feedstock	14
2.5 Biodiesel Production.....	16
2.6 Transesterification.....	17
2.7 Esterification	18
2.8 Esterification using heterogeneous catalysts	20
2.9 Solid Acid Catalysts selected to carry out the esterification reaction.....	25

2.9.1	Silica Sulfuric Acid (SSA).....	25
2.9.2	Amberlyst 15.....	25
2.9.3	Amberlyst BD20.....	26
2.10	Patent Search for Amberlyst BD20.....	27
2.10.1	Analysis of Shah’s Patents (2013-2014).....	27
2.10.2	Analysis of Slade’s Patent (2015).....	29
2.10.3	Analysis of Coupard’s Patent (2016).....	29
2.11	Concluding remark.....	30
	References.....	32
	CHAPTER 3	37
3	Esterification Reaction using Homogeneous Catalyst.....	37
3.1	Introduction.....	37
3.2	Experimental Details.....	39
3.2.1	Materials and Chemicals.....	39
3.2.2	Equipment.....	39
3.2.3	Experimental Procedure.....	40
3.3	Results and discussion.....	43
3.3.1	Batch Mode of operation.....	44
3.3.2	Semi-Batch mode of operation.....	46
3.4	Mathematical Models.....	50
3.4.1	Models for Batch mode.....	50
3.4.2	Model for Semi-Batch mode.....	68
3.5	Conclusions.....	71
	References.....	72
	CHAPTER 4	76

4	Esterification Reaction using Heterogeneous catalyst	76
4.1	Introduction.....	76
4.2	Experimental Details.....	79
4.2.1	Materials and Chemicals.....	79
4.2.2	Silica Sulfuric Acid preparation.....	79
4.2.3	Resin Catalysts Drying and Activation:.....	81
4.2.4	Equipment.....	82
4.2.5	Experimental Procedure.....	84
4.3	Results and discussion	88
4.3.1	Catalytic screening tests.....	89
4.3.2	Selected Resin Catalysts Study.....	96
4.4	Kinetic Models for Heterogeneous Catalyst.....	103
4.4.1	First Heterogeneous Catalyst Kinetic Model.....	103
4.4.2	Second Heterogeneous Catalyst Kinetic Model	111
4.5	Conclusions.....	119
	References	120
	CHAPTER 5	127
5	Conclusions and recommendations.....	127
5.1	Summary and conclusions	127
5.2	Recommendations for Future Work.....	127
	Appendices.....	129
	List of Appendices	129
	Curriculum Vitae	140

List of Tables

Table 1-1 Status of Biofuels: Characteristics and Costs, 2013 (Foley et al., 2015)	2
Table 1-2 Biofuels global production, top 16 countries and EU-28, 2014 (Foley et al., 2015).	4
Table 2-1 Different feedstocks for production of biodiesel (Talebian-Kiakalaieh et al., 2013)...	15
Table 2-2 Heterogeneous acid catalysts used in the esterification of free fatty acids	24
Table 2-3 Structural properties of Amberlyst 15.	25
Table 2-4 Patent Search Results.	27
Table 3-1 Equilibrium conversion values	52
Table 3-2 model-fitting statistics for the first batch model.....	55
Table 3-3 estimation of the rate constants for the first batch mode kinetic model.....	55
Table 3-4 Arrhenius equation parameters for the first batch mode model	57
Table 3-5 Estimation of the reaction order	62
Table 3-6 model-fitting statistics for the second batch model.....	63
Table 3-7 Values of $k_{1\text{apparent}}$ and $k_{1\text{true}}$ for the second batch model.....	65
Table 3-8 Arrhenius Equation parameters for the second batch mode model.....	65
Table 3-9 Comparison of the kinetics parameters obtained by the second batch kinetic model with literature	67
Table 4-1 Properties of Ion Exchange Resin Catalysts.....	94
Table 4-2 Equilibrium conversion values	105
Table 4-3 Model-fitting statistics for the first heterogeneous catalyst model	107

Table 4-4 Rate constants for heterogeneous catalyst first model	108
Table 4-5 Arrhenius equation parameters for the first heterogeneous model.....	110
Table 4-6 model-fitting statistics for the second batch model	114
Table 4-7 Values of $k_{1\text{apparent}}$ and $k_{1\text{true}}$ for the second heterogeneous catalyst model.....	115
Table 4-8 Arrhenius Equation parameters for the second Heterogeneous Catalyst Model.....	116
Table 4-9 Comparison of the kinetics parameters obtained by the second heterogeneous catalyst kinetic model with literature	118
Table 0-1 Esterification reactions mass balance (Homogeneous catalyst).....	130
Table 0-2 Input requirement for Esterification reaction	133

List of Figures

Figure 1-1 Estimated Renewable Energy Share of Global Final Energy Consumption, 2013(Brower et al., 2014)	2
Figure 1-2 Biofuels Global Production, 2004-2014(Foley et al., 2015).....	3
Figure 2-1 Fatty acid alkyl esters produced through different routes (Sanchez, 2013).....	16
Figure 2-2 Transesterification of triglycerides with alcohol.....	17
Figure 2-3 Mechanism of Fisher esterification reaction by methanol	19
Figure 2-4 Simplified flow diagram of the heterogeneous process Esterfip-H .(Michel Bloch, 2006)	22
Figure 2-5 Scheme of reaction mechanism for the esterification catalyzed by ion-exchange acid	23
Figure 2-6 Comparison of Amberlyst BD20 and Sulfuric acid	26
Figure 3-1 Schematic of Experimental setup for homogeneous catalysed esterification	40
Figure 3-2 Block Flow diagram for homogeneous catalyst Esterification reaction	42
Figure 3-3 Esterification reaction (Johnson, 2016).....	44
Figure 3-4 FFA% versus. Time for Batch Mode Operation	45
Figure 3-5 Conversion% versus. Time for Batch Mode Operation	45
Figure 3-6 FFA% vs. Time for Semi-Batch Mode Operation	47
Figure 3-7 Conversion% vs. Time for Semi-Batch Mode	47
Figure 3-8 FFA Concentration profile [g/L] for Batch and Semi-Batch Mode.....	48
Figure 3-9 FFA Conversion profile [%] for Batch and Semi-Batch Mode	49

Figure 3-10 FFA conversion vs. time along with the prediction results of the first batch model	54
Figure 3-11 Determination of k_1 values for First batch mode model	56
Figure 3-12 Arrhenius Van't Hoff plot for First batch mode model.....	57
Figure 3-13 Experimental versus. Calculated FFA conversion for the First Batch mode catalyst model.....	58
Figure 3-14 Fitting curve for r_A versus. time at different temperatures.....	60
Figure 3-15 Graph of $\ln(r_A)$ versus. $\ln(C_{FFA})$ at different temperatures.....	61
Figure 3-16 conversion vs. time along with the prediction results of the second batch model	64
Figure 3-17 Determination of kinetic constants values for Second batch mode model	65
Figure 3-18 Experimental Versus. Calculated FFA conversion for the Second Batch mode catalyst model	66
Figure 3-19 FFA conversion versus time for semi-batch mode.	70
Figure 4-1 Esterification reaction to produce biodiesel (Johnson, 2016).....	77
Figure 4-2 Scheme of SSA2 synthesis.....	80
Figure 4-3 Comparison between prepared and as received resin catalysts. Reaction conditions: FFA=15%, Methanol/FFA=20:1, catalyst loading 10wt% (except prepared Amberlyst 15=20wt.%), Reaction time:90min, Temperature= 60°C.	81
Figure 4-4 SEM images of cation exchange resins: (a) Amberlyst BD20 as received, (b) Amberlyst BD20 prepared, (c) Amberlyst BD20 prepared higher magnifications, (d) Amberlyst BD20 prepared surface view, (e) Amberlyst-15 as received, (f) Amberlyst- 15 prepared, (g) Amberlyst-15 prepared at different view (h) Amberlyst-15 prepared surface view.....	82
Figure 4-5 Schematic of Experimental Set up used to experiment heterogeneous catalyst (Pal and Prakash, 2012).....	83

Figure 4-6 Schematic of an SEM (Purdue University - Scanning Electron Microscope)	84
Figure 4-7 Block flow diagram for esterification reaction using heterogeneous catalyst	85
Figure 4-8 Filtration and Decantation.....	86
Figure 4-9 Vacuum distillation setting	86
Figure 4-10 Saponification from FFAs. (Atadashi et al., 2012a, 2013).	88
Figure 4-11 Esterification Reaction (Borges and Díaz, 2012).....	89
Figure 4-12 Experimental batch runs for catalytic screening. Reaction conditions: FFA = 15 wt.% based on reaction mix, catalyst concentration 10wt.% based on FFA weight; molar ratio of methanol to FFA= 20:1, temperature= 60 °C; agitation speed=720 rpm; reaction time=90min..	90
Figure 4-13 Experimental batch runs for the catalytic activity of the SSA catalysts. (A) SSA1-200 deactivation test. (B) SSA1-35 deactivation test. (C) SSA2-35 deactivation test. (D) Summary of %conversion attained by individual silica supported catalyst after each run. Reaction conditions: FFA = 15 wt.% based on reaction mix, catalyst concentration 10wt.% based on FFA weight; molar ratio of methanol to FFA= 20:1, temperature= 60 °C; agitation speed=720 rpm; reaction time =90min.	92
Figure 4-14 Experimental batch runs for the catalytic activity of the ion exchange resins catalysts. Reaction conditions: FFA = 15 wt.% based on reaction mix, catalyst concentration 20wt.% based on FFA weight; molar ratio of methanol to FFA= 20:1, temperature= 60 °	93
Figure 4-15 Experimental batch runs for the catalytic activity of the ion exchange resins catalysts. Reaction conditions: FFA = 15 wt.% based on reaction mix, catalyst concentration 20wt.% based on FFA weight; molar ratio of methanol to FFA= 20:1, temperature= 60 °C; agitation speed=720 rpm; reaction time =240min.	94
Figure 4-16 SEM Images of catalysts: (A) Amberlyst BD20 outer surface (B) Amberlyst BD20 inner surface, (C) Amberlyst-15 outer surface, (D) Amberlyst-15 inner surface.	96

Figure 4-17 (A) and (B) catalyst reusability test for Amberlyst BD20. Reaction conditions: FFA = 15 wt.% based on reaction mix, molar ratio of methanol to FFA= 20:1, agitation speed=720 rpm; reaction time = 90min	97
Figure 4-18 Organic deposit on BD20.....	98
Figure 4-19 (A) and (B) Experimental batch runs for the catalytic activity of Amberlyst BD20 at different RPM. Reaction conditions: FFA = 15 wt.% based on reaction mix, catalyst concentration 20wt.% based on FFA weight; molar ratio of methanol to FFA= 20:1, temperature= 60 °C; reaction time = 90min.	99
Figure 4-20 (A) and (B) Experimental batch runs for the catalytic activity of Amberlyst BD20 at different catalyst loading. Reaction conditions: FFA = 15 wt.% based on reaction mix, molar ratio of methanol to FFA= 20:1, agitation speed=720 rpm, temperature= 60 ° C; reaction time = 90min.	100
Figure 4-21 (A) and (B) Experimental batch runs for the catalytic activity of Amberlyst BD20 with respect to temperature. Reaction conditions: FFA = 15 wt.% based on reaction mix, catalyst concentration 20wt.% based on FFA weight; molar ratio of methanol to FFA= 20:1, agitation speed=720 rpm; reaction time = 90min.	101
Figure 4-22 (A) and (B) Experimental batch runs for the catalytic activity of Amberlyst BD20 with respect to time. Reaction conditions: FFA = 15 wt.% based on reaction mix, catalyst concentration 20wt.% based on FFA weight; molar ratio of methanol to FFA= 20:1, agitation speed=720 rpm; temperature= 60 °C.	102
Figure 4-23 FFA conversion vs. time along with the prediction results of the first heterogeneous catalyst model	107
Figure 4-24 Determination of k_1 values for the first heterogeneous catalyst model	108
Figure 4-25 Arrhenius Van't Hoff plot for the first heterogeneous catalyst model	109
Figure 4-26 Experimental versus. calculated FFA conversion for the first heterogeneous catalyst model.....	110

Figure 4-27 conversion vs. time along with the prediction results of the second heterogeneous catalyst model	114
Figure 4-28 Determination of kinetic constants values for Second Heterogeneous Catalyst model	116
Figure 4-29 Experimental versus. Calculated FFA conversion for the Second heterogeneous catalyst model	117

List of Appendices

Appendix-A Esterification reaction mass balance (homogeneous catalyst)	130
Appendix-B Standard calculation for reaction experimental parameters	131
Appendix-C Example of calculation for First batch mode kinetic model	134
Appendix-D Example of calculation for First Second mode kinetic model	135
Appendix-E Example of calculation for Heterogeneous Catalyst First kinetic model	136
Appendix-F Example of calculation for Heterogeneous Catalyst Second kinetic model	137
Appendix-G Technical properties of Biodiesel	138
Appendix-H ASTM standards for biodiesel (B100) and petrodiesel fuels (PD)	139

CHAPTER 1

1 Introduction

All sectors of human life such as transportation, power generation, residential consumption, and industrial processes require energy. At present this energy is mainly supplied by fossil fuels like oil, coal, and natural gas. Those fuels are subject to a constant escalating demand due to the dramatic expansion in human population during the last century, industrialization, and economic development. For instance, World energy consumption doubled between 1971 and 2001, it will increase 53% by the year 2030, also World petroleum demand will increase from the current 84.4 million barrels per day to 116 million barrels per day in 2030 (Worldwide Energy Demand : Brienergy 2014). This increasing demand results in environmental concerns from pollution with its effects on human health, greenhouse gases emission and global warming. Therefore “meeting future energy demand with continued limited resources has been acknowledged to be unsustainable”(Sanchez, 2013). The aforementioned reasons triggered an extensive research for alternative energy resources that are viable by mean of they are renewable, readily available, technologically feasible, environmentally acceptable, and economically competitive (Meher et al., 2006). Examples of renewable sources for energy are: wind, solar, hydro, geothermal, marine, and biomass. One of the most worthwhile alternatives is the use of biofuels as they provide a convenient mean for distribution due to their liquid state (Sanchez, 2013). **Figure 1-1** shows the renewable energy segments of global energy consumption in 2013 (Foley et al., 2015), when they represented 19.1% of the global energy consumption while biofuels share was only 0.8% of this consumption compared to 78.3% for fossil fuels, showing the enormous potential of market development for biofuels.

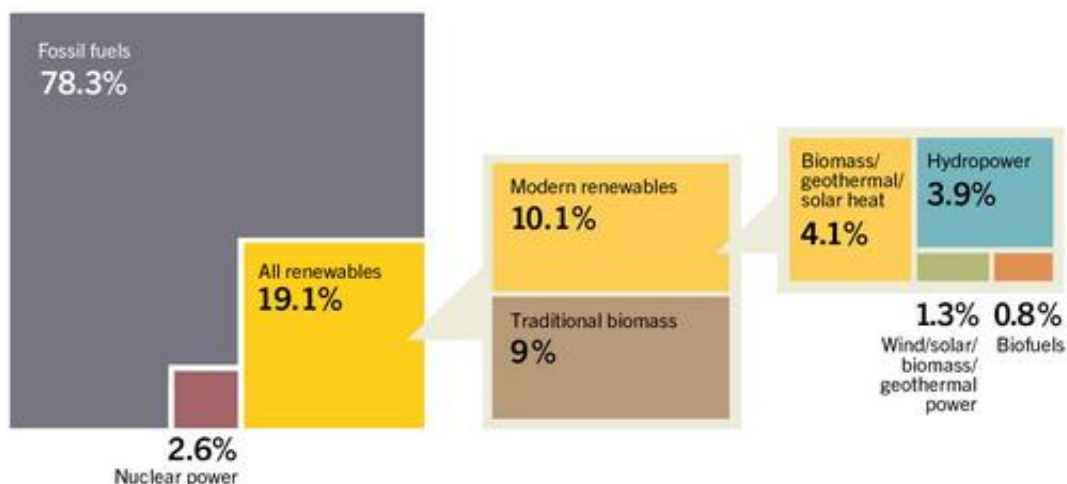


Figure 1-1 Estimated Renewable Energy Share of Global Final Energy Consumption, 2013 (Brower et al., 2014)

The major drawback on biofuels expansion is their price mainly due to the cost of the feedstock (Knothe et al., 2010). **Table 1-1** depicts the estimated production cost for two major biofuels: biodiesel and ethanol.

Table 1-1 Status of Biofuels: Characteristics and Costs, 2013 (Foley et al., 2015)

TECHNOLOGY	FEEDSTOCKS	FEEDSTOCKS CHARACTERISTICS	ESTIMATED PRODUCTION COSTS (US cents/liter)
TRANSPORT FUELS			
BIODIESEL	Soy, rapeseed, mustard seed, palm, jatropha, waste vegetable oils, animal fats	Range of feedstocks with different crop yields per hectare, hence, production costs vary widely among countries. Co-products include high-protein meals.	Soybean oil: 56-72 (Argentina); 100-120 (Global average) Palm oil: 100-130 (Indonesia, Malaysia, and other) Rapeseed oil: 105-130 (EU)
ETHANOL	Sugar cane, sugar beets, corn, cassava, sorghum, wheat (and cellulose in the future)	Range of feedstocks with wide yield. Co-products include animal feed, heat and power from bagasse residues. Advanced biofuels are not yet fully commercial and have higher costs.	Sugar cane: 82-93 (Brazil) Corn (dry mil): 85-128 (United States)

The production cost varies according to the location, labor costs, and depends on subsidies or policy incentives. Nevertheless, as it can be seen from **Figure 1-2** that biofuels production has increased 4.6 times between the year 2004 to 2013 passing from 28 to 127.7billion liters. One of the major reason being that current energy policies fosters environmental issues including environmentally friendly technologies to increase energy supplies. Governments also encourages clean and more efficient energy use. This effort is targeted toward the reduction of air pollution, and global warming by greenhouse effect (Demirbas, 2010).

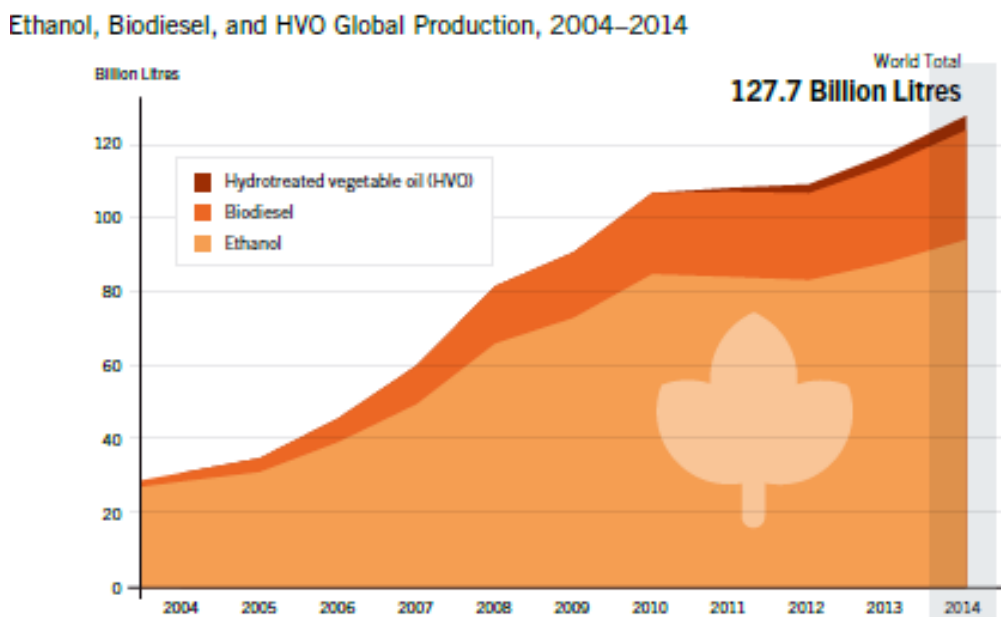


Figure 1-2 Biofuels Global Production, 2004-2014(Foley et al., 2015)

A statistical view for the distribution of biofuel production among the top 16 countries and European Union 28 countries in 2013 is shown in **Table 1-2** where it can be seen that USA and Brazil have produced 70.47% of the world production compared to 14.56% for all EU countries, meanwhile it can be noticed that USA and Brazil produces mainly ethanol with 85.95% of the world production while EU are more focused on biodiesel with 39.05% compared to USA & Brazil with 27.27% between them, this is due to the fact that diesel fuels are more used in European countries.

Table 1-2 Biofuels global production, top 16 countries and EU-28, 2014 (Foley et al., 2015).

<i>Country</i>	<i>FUEL ETHANOL</i>	<i>BIODIESEL</i>	<i>HVO</i>	<i>TOTAL</i>	<i>CHANGE RELATIVE TO 2013</i>
	Billion liters				
<i>United States</i>	54.3	4.7	1.1	60.1	+3.9
<i>Brazil</i>	26.5	3.4		29.9	+1.6
<i>Germany</i>	0.9	3.4		4.3	+0.6
<i>China</i>	2.8	1.1		3.9	+0.3
<i>Argentina</i>	0.7	2.9		3.6	+0.8
<i>Indonesia</i>	0.1	3.1		3.2	+0.9
<i>France</i>	1.0	2.1		3.1	+0.1
<i>Netherlands</i>	0.4	0.7	1.7	2.5	+0.2
<i>Thailand</i>	1.1	1.2		2.3	+0.4
<i>Canada</i>	1.8	0.3		2.1	+0.1
<i>Belgium</i>	0.6	0.7		1.3	+0.2
<i>Spain</i>	0.4	0.8		1.2	+0.1
<i>Singapore</i>	0	0	1.0	1.0	+0.1
<i>Poland</i>	0.2	0.8		1.0	+0.1
<i>Colombia</i>	0.4	0.6		1.0	No change
<i>Australia</i>	0.2	0.1		0.3	-0.1
<i>EU-28</i>	5.2	11.6	1.8	18.6	1.9
<i>World</i>	94	29.7	4	127.7	10.4

Worldwide increase in attraction for biodiesel fuels as a blending component or direct replacement for petroleum-derived diesel fuel in vehicle engines, as it is renewable, can be easily implemented and used in most diesel equipment with no or only minor modifications, it contains 90% of the energy of the petroleum diesel and has very similar physical and chemical attributes (Pal and Prakash, 2012). Furthermore, biodiesel is non-toxic, biodegradable, and suitable for sensitive environments (Demirbas, 2010).

Biodiesel is defined as mono-alkyl esters of long chain fatty acids derived from vegetable oils or animal fats which conform to ASTM D6751 specifications for use in diesel engines (Borges and Díaz, 2012; Chai et al., 2014). Biodiesel refers to the pure fuel before blending with diesel fuel. Biodiesel blends are denoted as, "BXX" with "XX" representing the percentage of biodiesel

contained in the blend for example. B20 is 20% biodiesel, 80% petroleum diesel (Kinast, 2003). More than 350 types of plants lipids can be used as fatty acid sources in addition to animal fats (Atabani et al., 2012; Talebian-Kiakalaieh et al., 2013). However, at present time soybean, rapeseed, and palm oils are the ones mainly used in biodiesel production. The use of edible oils has given rise to certain concerns as some of them are important food chain materials. Moreover, the use of land for growing fuel feedstock competes directly with their intended usage for food production (Luque et al., 2010; Atabani et al., 2012; Santacesaria et al., 2012). Transesterification also referred as alcoholysis has emerged as the most common scheme for converting vegetable oil into biodiesel of acceptable quality, this sequential reversible chemical reaction consist on the reaction between a triglyceride (TG) and a short chain alcohol in the presence of a catalyst in three consecutive steps: the triglyceride (TG) is converted to di-glyceride (DG), then to mono-glyceride (MG) and finally to glycerol with alkyl esters formed in each step (Pal and Prakash, 2012). Various alcohols can be used in the transesterification reaction such as methanol, ethanol, propanol, butanol and amyl alcohol. The most frequently used are ethanol and methanol, ethanol being preferred because it is derived from agricultural products, renewable and biologically less offensive in the environment. However, methanol is commonly employed due to its low cost and its physical and chemical advantages (polar and shortest chain alcohol) (Demirbas, 2009). The transesterification reaction requires a catalyst at mild operating conditions, acid (H_2SO_4 , para-toluene sulfonic acid (PTSA) and H_3PO_4) and alkali (KOH, NaOH, CH_3ONa) catalyst are used depending on the nature of the oil used. Though, alkali-catalyzed reactions have much higher reaction rate as it has been demonstrated that alkaline catalyst is about 4000-times faster than the acid one (Sendzikiene et al., 2004). Even though the use of alkali catalyst is conditioned by a highly refined vegetable oil as FFAs reacts easily with alkaline catalyst to form soap that prohibit the separation of biodiesel and glycerol. Also foaming in aqueous medias is caused by FFAs soaps resulting in an increase in viscosity, and formation of gels (Demirbas, 2009).

Currently biodiesel industry uses refined edible oil extensively as raw material, this high value food-grade vegetable oil yields a high purity biodiesel at high production cost due mainly to the cost of feedstock which accounts for about 80% of the overall cost in the production process (Lam et al., 2010), limiting its commercialization. In addition to that the production of biodiesel from human nutrition sources can cause a food crisis, for those reasons alternative feedstock such as: non-edible oils, waste cooking-oils (15 million tons of waste cooking /frying oil is thrown away

annually worldwide (Lee et al., 2014)), animal fats, and algal oils has been the focus of researchers. Nevertheless, their high free fatty acids and moisture content raise side reactions for instance hydrolysis and saponification resulting in a decrease in product yield.

To overcome those obstacles extensive research has been performed on various methods to improve biodiesel production from high-acid number oils. One of the most meaningful alternatives is an integrated two-step process wherein pre-esterification of FFA with acid catalyst to decrease the FFA levels to lower than 0.5wt.% considered being an acceptable level, followed by transesterification using an alkaline catalyst (Knothe et al., 2010).

1.1 Objectives

The study aims at identifying suitable catalyst for operation at relatively mild temperature and pressure conditions to improve inherent safety while minimizing environmental impact. The feedstock selected for the tests consisted of 15 wt.% of oleic acid in Canola oil which is representative of high FFA feed for biodiesel production. The research plan was mainly divided into two parts based on current information about catalysis for the esterification reaction. The main challenge of this study was identifying a suitable heterogeneous catalyst aimed at reducing overall cost of biodiesel production.

Part A: Tests with homogeneous catalysts

These tests were conducted to collect base case data for reaction at low temperature for further comparison. For these tests sulphuric acid was selected as the catalyst due to its low cost, high activity and easy availability. Effects of mixing mode and reaction time are investigated for temperature below 60°C and reaction kinetic parameters are determined.

Part B: Tests with heterogeneous catalysts

Although a number of potential heterogeneous catalysts have been reported in literature, their long term usage based on recyclability/reuse has been lacking. The deactivation rate for most heterogeneous catalysts is high and regeneration often difficult. The challenge here was identifying a catalyst with low rate of deactivation and hence lower costs and environmental impact of regeneration. A catalyst selected based on extensive testing is the main contribution of the thesis.

1.2 Thesis Format and Structure

This thesis is presented in the format of integrated-article as specified by the School of Postdoctoral Studies of the University of Western Ontario. The body of this work is written as technical papers without an abstract. Individual chapters have their own bibliographic section.

The contents of this study have been organized in five chapters:

Chapter 1 consist of a general introduction.

Chapter 2 Literature Review, main advantages of disadvantages of using biodiesel as a substitute of conventional diesel are described. This chapter examines biodiesel production processes used at a commercial scale. The esterification reaction is emphasised as a way to unlock potential low cost feedstock. The reaction mechanisms and parameters are also discussed. Furthermore, a patent search for one of the studied heterogeneous catalyst is presented.

Chapter 3 The effects of temperature, reaction time and mixing modes were investigated for esterification reaction using methanol and homogeneous catalyst H_2SO_4 , to convert FFA in the feedstock to methylesters. The esterification reaction was investigated using two different reactor configurations to evaluate the best approach leading to up to standard specification under mild conditions at lower cost. Two kinetic models have been proposed to predict the experimental data. In addition, estimates of kinetic parameters for the esterification reaction are presented.

Chapter 4 In this chapter, a search for suitable heterogeneous catalyst to carry out the esterification reaction has been conducted. The selection criteria were stability, selectivity and activity at low temperature and pressure (mild conditions: 60°C, 1atm). To accomplish this objective, four preselected heterogeneous catalysts have been evaluated. One of the preselected catalysts demonstrated high activity due to high acid site concentration, and the absence of pores resulting on enhanced reaction rate by avoiding diffusional slow down. The results show that at temperature of 60°C and reaction time of 240 minutes, heterogeneous catalyst can provide close to 97% conversion of FFA, corresponding to FFA concentration of 0.45wt.%, that is up to standard. The trade-off of increasing the reaction time compared to homogeneous catalyst is well justified, due to inherent advantages for the process in term cost and ease of separation of the

catalyst after reaction. Consequently, this catalyst is recommended for further testing for commercial application. Additionally, two kinetic models have been proposed to predict the experimental data. Finally, estimates of kinetic parameters for the esterification reaction are presented.

In Chapter 5, *Conclusions and Recommendations*, major findings are reported summarizing the contributions of this work. As a final point, recommendations for future work are proposed.

References

- Atabani, a. E.; Silitonga, a. S.; Badruddin, I. A.; Mahlia, T. M. I.; Masjuki, H. H.; Mekhilef, S. A. Comprehensive Review on Biodiesel as an Alternative Energy Resource and Its Characteristics. *Renew. Sustain. Energy Rev.* **2012**, *16* (4), 2070–2093.
- Borges, M. E.; Díaz, L. Recent Developments on Heterogeneous Catalysts for Biodiesel Production by Oil Esterification and Transesterification Reactions: A Review. *Renew. Sustain. Energy Rev.* **2012**, *16* (5), 2839–2849.
- Brower, M.; Green, D.; Hinrichs-rahlwes, R.; Sawyer, S.; Sander, M.; Taylor, R.; Giner-reichl, I.; Teske, S.; Lehmann, H.; Alers, M.; et al. *RENEWABLE 2014 GLOBAL STATUS REPORT*; Paris, 2014.
- Chai, M.; Tu, Q.; Lu, M.; Yang, Y. J. Esterification Pretreatment of Free Fatty Acid in Biodiesel Production , from Laboratory to Industry. *Fuel Process. Technol.* **2014**, *125*, 106–113.
- Demirbas, A. Progress and Recent Trends in Biodiesel Fuels. *Energy Convers. Manag.* **2009**, *50* (1), 14–34.
- Demirbas, A. Biodiesel for Future Transportation Energy Needs. *Energy Sources, Part A Recover. Util. Environ. Eff.* **2010**, *32* (September 2013), 1490–1508.
- Foley, T.; Thornton, K.; Hinrichs-rahlwes, R.; Sawyer, S.; Sander, M.; Taylor, R.; Teske, S.; Lehmann, H.; Alers, M.; Hales, D. *Renewables 2015 Global Status Report*; 2015.
- Kinast, J. a. *Production of Biodiesels from Multiple Feedstocks and Properties of Biodiesels and Biodiesel/diesel Blends. Final Report. Report 1 in a Series of 6. Subcontractor Report.*; Golden, Colorado, 2003.
- Knothe, G.; Krahl, J.; Van Gerpen, J. *The Biodiesel Handbook, 2nd Edition.*, 2nd Editio.; AOCS Press: Urbana, Illinois, 2010.
- Lam, M. K.; Lee, K. T.; Mohamed, A. R. Homogeneous, Heterogeneous and Enzymatic Catalysis for Transesterification of High Free Fatty Acid Oil (Waste Cooking Oil) to Biodiesel: A Review. *Biotechnol. Adv.* **2010**, *28* (4), 500–518.

Lee, A. F.; Bennett, J. A.; Manayil, J. C.; Wilson, K. Heterogeneous Catalysis for Sustainable Biodiesel Production via Esterification and Transesterification. *Chem. Soc. Rev.* **2014**, *43* (22), 7887–7916.

Luque, R.; Lovett, J. C.; Datta, B.; Clancy, J.; Campelo, J. M.; Romero, A. A. Biodiesel as Feasible Petrol Fuel Replacement: A Multidisciplinary Overview. *Energy Environ. Sci.* **2010**, *3* (11), 1706–1721.

Meher, L.; Vidyasagar, D.; Naik, S. Technical Aspects of Biodiesel Production by Transesterification—a Review. *Renew. Sustain. Energy Rev.* **2006**, *10* (3), 248–268.

Pal, K. D.; Prakash, A. New Cost-Effective Method for Conversion of Vegetable Oil to Biodiesel. *Bioresour. Technol.* **2012**, *121*, 13–18.

Sanchez, N. Investigation of Cost-Effective Biodiesel Production from High FFA Feedstock—Masters Thesis, The University of Western Ontario, 2013.

Santacesaria, E.; Vicente, G. M.; Di Serio, M.; Tesser, R. Main Technologies in Biodiesel Production: State of the Art and Future Challenges. *Catal. Today* **2012**, *195* (1), 2–13.

Sendzikiene, E.; Makareviciene, V.; Janulis, P.; Kitrys, S. Kinetics of Free Fatty Acids Esterification with Methanol in the Production of Biodiesel Fuel. *Eur. J. Lipid Sci. Technol.* **2004**, *106* (12), 831–836.

Talebian-Kiakalaieh, A.; Amin, N. A. S.; Mazaheri, H. A Review on Novel Processes of Biodiesel Production from Waste Cooking Oil. *Appl. Energy* **2013**, *104*, 683–710.

Worldwide Energy Demand: Brienergy 2014 <http://www.brienergy.com/worldwide-energy-demand>.

CHAPTER 2

2 Literature review

2.1 Background and history of Biodiesel

Rudolf Christian Karl Diesel (1858-1913) the inventor of biodiesel engines demonstrated the use of vegetable oil as a substitute for diesel fuel in the 19th century. “*Diesel used straight peanut oil as a fuel for demonstration purposes at the World Exhibition in Paris in 1900*”. Although this statement is widely used in literature, some source reveals that it hasn’t been stated by Rudolf Diesel. However, he believed that the utilization of biomass fuel will become a reality as future versions of his engine are designed and developed (Talebian-Kiakalaieh et al., 2013). The utilization of vegetable oil or biofuel in internal combustion engines was reported during 1920-1930, and second world war from all around the world. However, unlimited supply and low price of petroleum fuels stopped the biofuel industry from evolving, until the oil crisis in 1970s. Recent concerns about fossil fuels depletion, in addition to environmental degradation triggered the research for alternative fuels field. Among which the biodiesel seems to be a viable solution for these problems.

Direct usage of vegetable oils in diesel engines sounds attractive because they are biodegradables, have relatively high heat content (80% of diesel fuel), and are non-toxic. Conversely, it is not technically possible because of their high viscosity ranging from 10 to 17 times greater than No.2 diesel fuel (No.2 diesel fuel refer to a diesel engine fuel with 10 to 20 carbon number hydrocarbon) (Demirbas, 2009). Additionally, the low volatility of vegetable oils results on the formation of relatively high amount of ashes due to incomplete combustion. Furthermore, the reactivity of unsaturated hydrocarbon chains results on low stability against oxidation with subsequent reactions of polymerization (Robles-Medina et al., 2009).

To overcome those technical issues with vegetable oil, it has to be processed to acquire the properties necessary to be directly used in current diesel engines. Various processes have been considered to reduce the viscosity and improve the combustion characteristics of vegetable oil

such as: supercritical treatment, catalytic cracking, pyrolysis, dilution, micro emulsification, and transesterification (Demirbas, 2009; Lee and Saka, 2010; Atabani et al., 2012).

Pyrolysis and micro emulsification are cost intensive processes producing a low quality biodiesel (Robles-Medina et al., 2009). Dilution of vegetable oils can be achieved by using ethanol or diesel fuel up to 25% by volume to reduce the viscosity. However, the product creates some engines performance problems such as injector coking and more carbon deposit, thus the mixture is not suitable for long term usage due to lubricant thickening (Demirbas, 2009). Production of biofuels from catalytic cracking of oils and fats is a promising process under development (Ong and Bhatia, 2010) reported the following wt.% yields from palm Oil over HZSM-5 zeolite catalyst: bio-gasoline 49.2%, kerosene 26.1%, diesel 2.6%, gases 8.2%, and coke 1.7%. However, the operating conditions were 450°C at 1 atmosphere pressure in a catalytic micro reactor unit simulating a traditional FCC unit in oil refinery, hence pointing to the necessity to further investigate optimum process operation condition. The supercritical process although being very fast (2 minutes to complete reaction) and procuring high yield of methylesters (up to 100% conversion), it presents economical challenges due to the very stringent operating condition (200°C/7MPa to 487°C/105MPa). Finally, transesterification of vegetable oils with alcohol is considered to be the best method for biodiesel production (Atabani et al., 2012; Talebian-Kiakalaieh et al., 2013). The alcoholysis is an equilibrium chemical reaction that reduces the viscosity of vegetable oils 10 times by using an aliphatic alcohol. To date, transesterification has been the most common method employed to produce high quality biodiesel due to its simplicity and low cost (Knothe et al., 2010; Atadashi et al., 2012b).

Biofuel production and consumption due to its environmental impact has been boosted by government's implementation of new energy policies and goals. European Union targets biodiesel to represent 20% of the total diesel market by 2020. The USA aims to produce 3.3million tones of biodiesel by 2016 (Talebian-Kiakalaieh et al., 2013), while Minnesota became the first U.S state to require 5% biodiesel content in conventional petro-diesel. In 2015 the Canadian government scheduled the addition of 2% biodiesel content in diesel distillate.

2.2 Advantages and Disadvantages of Biodiesel

2.2.1 Advantages of Biodiesel

Biodiesel has many technical, environmental, and economic advantages. In term of environmental advantages, it reduces sulphur oxide emissions by 100%, polycyclic aromatic hydrocarbons by 80%, unburned hydrocarbons by 67%, carbon monoxide by 48%, and particulate matter by (75-83%) (Demirbas, 2009). Moreover, Life cycle analysis of 100% biodiesel has reported zero carbon dioxide emissions considering carbon dioxide life cycle during cultivation, production, and conversion of oil; in other words biodiesel has a closed carbon cycle (Van Gerpen, 2005; Sawangkeaw et al., 2010; Sanchez, 2013). In addition, a life cycle analysis of biodiesel indicated that overall CO₂ emission were cut by 78% compared with petroleum-based diesel fuel (Helwani et al., 2009). Biodiesel is highly biodegradable in fresh water (77-89%), as well as in soil environments (90-98%) after 28 days. Therefore, it is safe to handle, store, and transport (Demirbas, 2010). Additionally, it is the only alternative diesel fuel in which low-concentration biodiesel-diesel blends run on conventional unmodified engines the most common blend being a mix of 20% biodiesel with 80% petroleum diesel. Furthermore, biodiesel has higher combustion efficiency than petroleum diesel, higher cetane number, and improves the lubrication properties of the diesel fuel blend which reduces corrosion in engines and increases durability. Even biodiesel levels below 1% can provide up to 30% increase in lubricity (Demirbas, 2009). Finally, due to oxygen content in the chemical structure of biodiesel, combustion properties are better.

Economically speaking biodiesel is readily available, it can be made from domestically produced, renewable oilseeds crops such as rapeseed, sunflower and soybean, and it has the potential for reducing a given economy's dependency on imported petroleum and enhances energy security.

2.2.2 Disadvantages of Biodiesel

The major disadvantages of biodiesel are lower energy content compared to petroleum diesel, higher viscosity, higher pour and cloud pour, higher nitrogen oxide (NO_x) emission, lower engine speed and power, and injector coking. However, the most important drawback is the high price due to the high feedstock price which account for 70-80% of the total production cost. Without government tax incentives and subsidies industrial production of biodiesel is not economically

competitive with petroleum-based diesel fuel (Serio et al., 2007; Lee and Wilson, 2015). Alternative low quality raw materials as inedible and used oils have to be used in order to reduce the production cost of biodiesel and make it more economically worthwhile. Furthermore, the use of these alternative feedstock would avoid the competition between land usage for fuel crops against conventional agricultural cultivation (Lee et al., 2014).

2.3 Technical Properties of Biodiesel

Biodiesel is a clear amber-yellow liquid with a viscosity similar to petrodiesel; technical properties of biodiesel are shown in **Appendix-G**. Biodiesel is non-flammable and, in contrast to petrodiesel, is non-explosive, with a flash point of 423K (150°C) as compared to 337K (64°C) for petrodiesel (Demirbas, 2010; Atabani et al., 2012).

The introduction and commercialization of biodiesel in the fuel market is subject to a variety of standards in order to insure high quality and engine performances, the fuel ASTM standards of biodiesel and petrodiesel are shown in **Appendix-H**. An extensive review of biodiesel has been undergone by (Moser, 2011; Atabani et al., 2012) where detailed biodiesel characterization based on physical and chemical properties including viscosity, flash point, cetane number, and carbon residue are explained in details. Although biodiesel can be derived from numerous sources, its chemical structure is dependent on the fatty acid profile of the parent oil. Physical properties are strongly related to the degree of unsaturation and distribution within the fatty acid molecules (Sanchez, 2013). Nevertheless whatever the initial feedstock the final product should comply with the international standards (ASTM D6751, EN14217:2008).

2.4 Feedstock

Biodiesel feedstock is divided into three categories:

1. First Generation: comprises edible vegetable oil (Samir Najem Aldeen Khurshid, 2014)
2. Second generation: Non-edible vegetable oil. Animal fats such as: tallow, yellow grease, chicken fats and by-products from fish oil. Finally waste or recycle oil (Atabani et al., 2012).
3. Third generation: Micro algae, considered to be the most promising due to high oil content as well as high yield. However still not exploited due to high production cost.

All fatty acid sources as animal fats or plants lipids (more than 350 types of them) can be used in biodiesel production (Atabani et al., 2012; Talebian-Kiakalaieh et al., 2013). Other authors stated that it could be as much as 4000 vegetable species from which vegetable oil can be extracted (Santori et al., 2012). Animal fats are derived from beef and sheep tallow and poultry oil. Typical biodiesel feedstocks used in industry today depending on the location are virgin oil such as: soybean oil is commonly used in United States, palm oil in Malaysia and Indonesia, rapeseed/canola oil is used in many European countries and Canada, and *Jatropha tree (Jatropha curcas)* is used in India and Southeast Asia (Demirbas, 2010). **Table 2-1** shows various conventional and non-conventional feedstocks in biodiesel production.

Table 2-1 Different feedstocks for production of biodiesel (Talebian-Kiakalaieh et al., 2013).

Conventional Feedstock		Non-conventional Feedstock
Mahua	Soybean	Lard
Nile tilapia	Rapeseed	Tallow
Palm	Canola	Poultry fat
Poultry	Babassu	Fish oil
Tobacco seed	Brassica carinata	Bacteria
Rubber plant	Brassica napus	Algae
Rice bran	Copra	Fungi
Sesame	Groundnut	Micro-algae
Sunflower	Cynara cardunculus	Terpenes
Barley	Cotton seed	Latexes
Coconut	Pumpkin	Pongamina pinnata
Corn	Jjoba oil	Palanga
Used cooking oil	Camelina	<i>Jatropha curcas</i>
Linseed	Peanut	Sea mango
Mustard	Olive	Okra

The use of refined oil increases the production cost accounting for almost 80% of the production costs, at the same time it compromises human nutrition sources. Therefore, majority of researcher have opted to look for alternative low quality feed stock such as non-edible oils, animal fat, waste cooking oil and greases, algae oil, and microalgae. The usage of waste edible oils can reduce biodiesel production costs by 60-90% (Talebian-Kiakalaieh et al., 2013). As much as possible the biodiesel source should fulfill two requirements: low production costs and large production scale (Pinto et al., 2005).

2.5 Biodiesel Production

As shown in **Figure 2-1** there are several chemical routes to produce alky esters (biodiesel). Nevertheless, commercial processes for synthesis of FAAE only occurs from direct esterification of FFA or transesterification of triglycerides. The process selection is dictated by the feedstock quality, the type of catalyst, and the operating conditions. Generally, the path followed using refined edible vegetable oils involves pre-treatment by esterification, followed by transesterification, recovery of excess alcohol, separation of glycerol from ester-rich phase, neutralization of catalyst, and purification of FAAE.

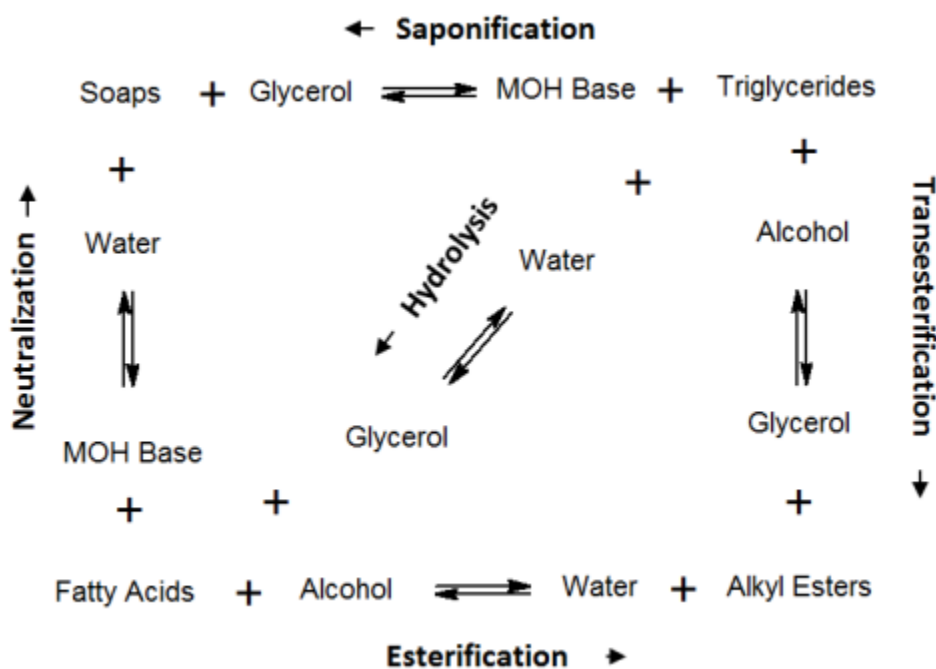


Figure 2-1 Fatty acid alkyl esters produced through different routes (Sanchez, 2013)

2.6 Transesterification

Talebian-Kiakalaieh et al., 2013, stated that “*Transesterification of vegetable oils with alcohol is the best method for biodiesel production*”. Transesterification is a reversible chemical reaction where vegetable oils, animal fat or algal oil (mainly composed of triglycerides) reacts with an aliphatic alcohol to form fatty acid alkyl esters (FAAE) and glycerol (Sanchez, 2013). The reaction is generally conducted in presence of catalyst, and consists of a sequence of three consecutive reversible reactions where triglycerides (TG) are converted to diglycerides (DG) and then diglycerides are converted to monoglycerides (MG) followed by the conversion of monoglycerides to glycerol. At each step an ester is produced and consequently three esters molecules are produced from one molecule of triglycerides (Demirbas, 2009). The overall reaction is illustrated in **Figure 2-2**, where stoichiometric coefficients indicates that three moles of alcohol are required for each mole of triglyceride. Even so, the process is carried out with excess alcohol to drive the equilibrium toward products side.

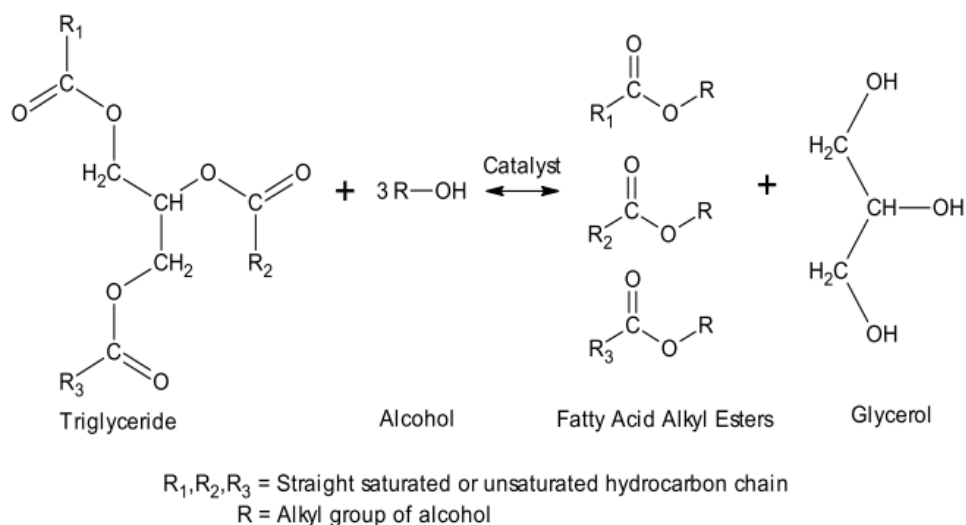


Figure 2-2 Transesterification of triglycerides with alcohol

To increase the reaction rate transesterification reaction can be achieved under supercritical conditions without catalyst since the supercritical methanol is fully miscible with the vegetable oils. The main obstacle is that the supercritical process requires severe operating condition in term of temperature

(350-400°C) and pressures (200-400 bar) (Melero et al., 2009). The other alternative is the use of different types of catalyst such as:

1. Alkaline catalyst: NaOH, KOH, NaOMe (Sodium methoxide), (Robles-Medina et al., 2009).
2. Acid catalyst: H₂SO₄, HCl, BF₃, H₃PO₄ (Melero et al., 2009).
3. Enzymatic-catalyst (lipases), (Helwani et al., 2009; Talukder et al., 2009; Santori et al., 2012; Stergiou et al., 2013)
4. Solid phase heterogeneous catalyst.(Wilson et al., 2002; Shibasaki-Kitakawa et al., 2007; Marchetti and Errazu, 2008; Feng et al., 2010; Kondamudi et al., 2011; Lee and Wilson, 2015)

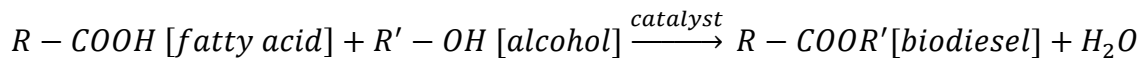
The best known and most widely used process is the one using basic catalyst (Demirbas, 2009). Practically 100% of the biodiesel produced presently is by alkaline catalyst process (Robles-Medina et al., 2009) Conversely, if the starting vegetable oil contains some small amount of free fatty acids (>0.5 wt.%) alkaline-catalyzed reactions are inhibited by FFA due saponification, which causes reduction in ester yield, difficult separation of glycerol from methyl ester, raise in viscosity, and formation of emulsion all of which creates many problems in downstream purification and methyl ester recovery.

In fact, this small amount of FFA definition differs from one author to another, values of: less than 0.5wt. %, less than 1.0wt. %, greater than 1.0wt. %, less than 2.0%, less than 3.0wt.%, and up to 5wt.% FFA have been reported (Talebian-Kiakalaieh et al., 2013). In this research value of: less than 0.5wt.% has been taken as threshold limit for FFA content.

The most important variables which significantly influence transesterification reaction are: reaction temperature, FFA content as discussed previously, water content in the oil, type of catalyst, reaction time, molar ratio of alcohol to oil, use of co-solvent, type of chemical stream of alcohol, and mixing intensity.

2.7 Esterification

Esterification, also known as Fischer esterification is an alternative chemical route to produce FAME from FFA as previously shown in Figure 2-1. This process is generally conducted under the presence of an acid catalyst and low molecular weight alcohols. The reaction may be represented by the following scheme:



The esterification reaction occurs between FFA and alcohol, in a mol-to-mol basis. Still, in order to obtain high conversion a large excess of alcohol is used (Pisarello et al., 2010).

Formation of alkyl esters is favored by the continuous removal of water from the system, as it is a reversible reaction. An interesting approach for continuous water removal has been proposed by (Coupard et al., 2016), in this patent a vertical liquid/liquid column containing the solid esterification catalyst is supplied in counter-current by an alcohol +oil feedstock. The column is claimed to be able to achieve very high conversion of FFA and avoid intermediate drying of oil for water removal. A variety of catalyst can be used but inorganic acids such as H_2SO_4 , HCl , and, H_3PO_4 are preferred due to high catalytic activity, efficiency, and low cost.

The mechanism for Fisher esterification occurs in a sequence of 4 steps as shown in **Figure 2-3**:

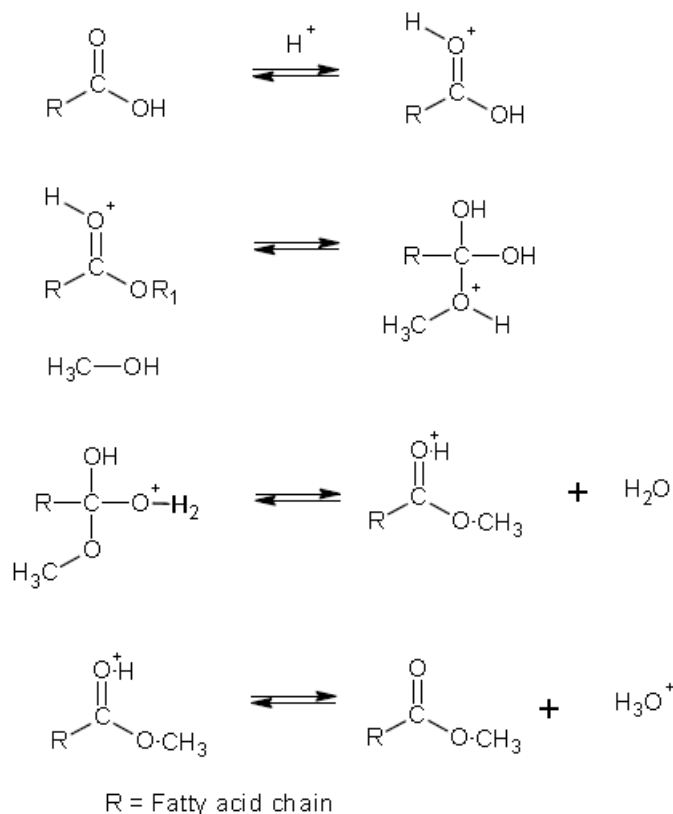


Figure 2-3 Mechanism of Fisher esterification reaction by methanol

As discussed earlier esterification can be used as a pre-treatment, prior to transesterification, to convert fatty acid oil contaminants to biodiesel to avoid saponification. By doing this, biodiesel yield would be considerably increased when low-quality oils are used as feedstock.

Both esterification and transesterification reactions are integrated on a two-step process in industry. First step is to convert the FFA into alkyl esters by esterification and then to convert the remaining triglycerides into methylesters by transesterification.

Examples of raw material with high acidity are: recycled vegetable oils (0.3-3.3%FFA), chicken fat (53%FFA), coconut oil (12%FFA), cottonseed oil (85.3%FFA), fatty acid recovered from degumming residues, residues from several industries (11.5-24.1%FFA). These raw materials can be converted to biodiesel with high yield using acid-catalyzed esterification as a first step (Pisarello et al., 2010).

2.8 Esterification using heterogeneous catalysts

An economic assessment of different biodiesel production processes (homogeneous alkali and acid catalysts, heterogeneous acid catalyst, and supercritical) has been undergone by (West et al., 2008). The study revealed that heterogeneous solid acid catalyzed process is advantageous over others. By means of it requires the lowest total capital investment and manufacturing costs, and had the only positive after tax rate-of-return. Other advantages from the use of heterogeneous catalyst for a two-step esterification-transesterification mechanism would be the ease of separation, reusability, fewer inputs into the reaction stream resulting on less wastes, as no soap would be formed (Melero et al., 2009). On the other hand heterogeneous catalysts yield of methylesters is lower compared to homogeneous catalysts (Ullah et al., 2015). Additionally, they are prone to deactivation due to many reasons such as, poisoning, leaching and coking.

A unique heterogeneous commercial process is based on Esterfip-H technology developed by the French Institute of Petroleum (IFP) (Bournay et al., 2005; Michel Bloch, 2006). In this continuous process shown in **Figure 2-4**, the transesterification reaction is carried out in two fixed bed reactors by a completely heterogeneous catalyst that consists of a mixed oxide of zinc and aluminium (zinc aluminate oxide). The process operate at 180-220°C and 62 bar corresponding to the vapor pressure of methanol at this temperature range (Santacesaria et al., 2012; Omberg, 2015).

Biodiesel yield obtained is around 100% and purity higher than 99%. However, the raw material must have very low FFA (< 0.25%) and water (< 1000ppm) content as the catalysts used is alkaline in nature and higher concentration of FFA or water in feedstock would lead to soap formation as discussed earlier (Hillion et al., 2007). Nevertheless, the development of the Esterfip-H process has triggered the aspiration to find new heterogeneous catalysts that are more efficient, moisture resistant, and eventually able to promote simultaneously the esterification of FFA along with transesterification of triglycerides.

The heterogeneous catalyst for esterification and transesterification reaction have been extensively reported in literature. Numerous recent studies have stated the technical feasibility of biodiesel production via heterogeneous catalyst among them (Helwani et al., 2009; Melero et al., 2009; Semwal et al., 2011; Romero et al., 2011; Atadashi et al., 2012b, 2013; Wilson and Lee, 2012; Santacesaria et al., 2012; Santori et al., 2012; Lee et al., 2014; Sani et al., 2014; Lee and Wilson, 2015).

Many heterogeneous acid catalysts are found to catalyze the esterification of FFAs to biodiesel. Nevertheless, two types are mainly reported:

1. sulfonic acid-functionalized solids, supported either by
 - ion-exchange organic resin
 - inorganic support
2. Inorganic metal-oxide based superacids.

The chosen catalysts in this study are among the first group. For instance, the first pair was the: Silica Sulfuric Acid based either on sulfuric or Chlorosulfonic acid attached to an inorganic support. While the other pair tested was: Amberlyst 15, Amberlyst BD20 representing the cation exchange organic resins (polymers).

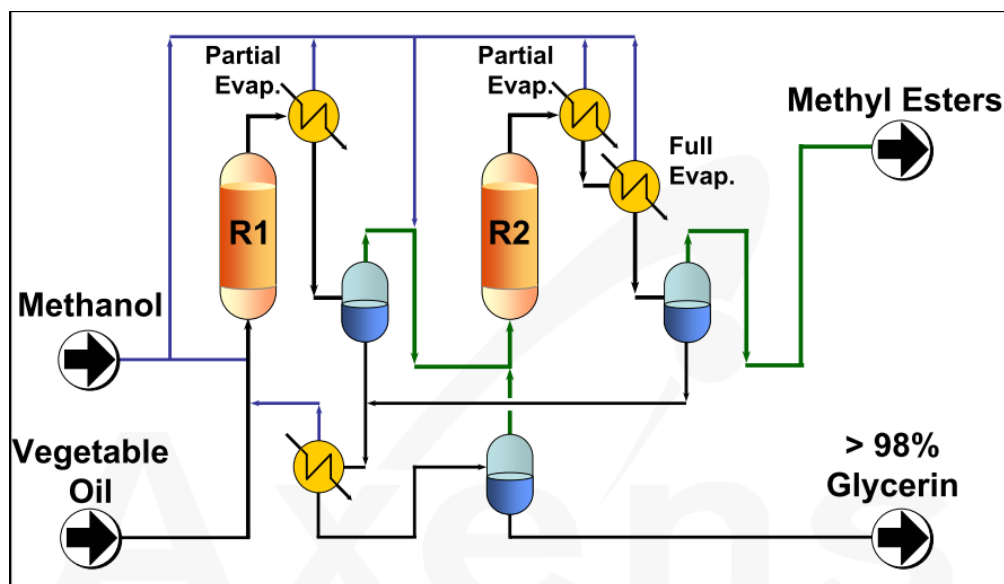


Figure 2-4 Simplified flow diagram of the heterogeneous process Esterfip-H .(Michel Bloch, 2006)

The reaction mechanism for esterification catalysed by ion-exchange resins was described by (Tesser et al., 2010). The reaction events occur through an Eley-Rideal mechanism between a protonated fatty acid and the methanol coming from liquid phase absorbed inside the resin particles. The scheme of exchange and reaction steps is shown in **Figure 2-5** where:

1. Step (a): represents the exchange between fatty acid and protonated methanol
2. Step (b): represents Eley-Rideal surface reaction that involves the protonated fatty acid and methanol. This reaction leads to the formation of protonated methylester and the corresponding amount of water that is partitioned between the internal (absorbed) liquid phase and the external (bulk) liquid phase. The water present in the internal liquid phase can then be involved in an exchange equilibrium with protonated methanol giving place to a completion on the active site, as shown by step (d).
3. Step (c): represents the exchange reaction between the protonated methylester and methanol from the internal liquid phase that, contemporarily, restore the active site with protonated methanol and release the methylester that is partitioned between the internal and the external liquid phase.

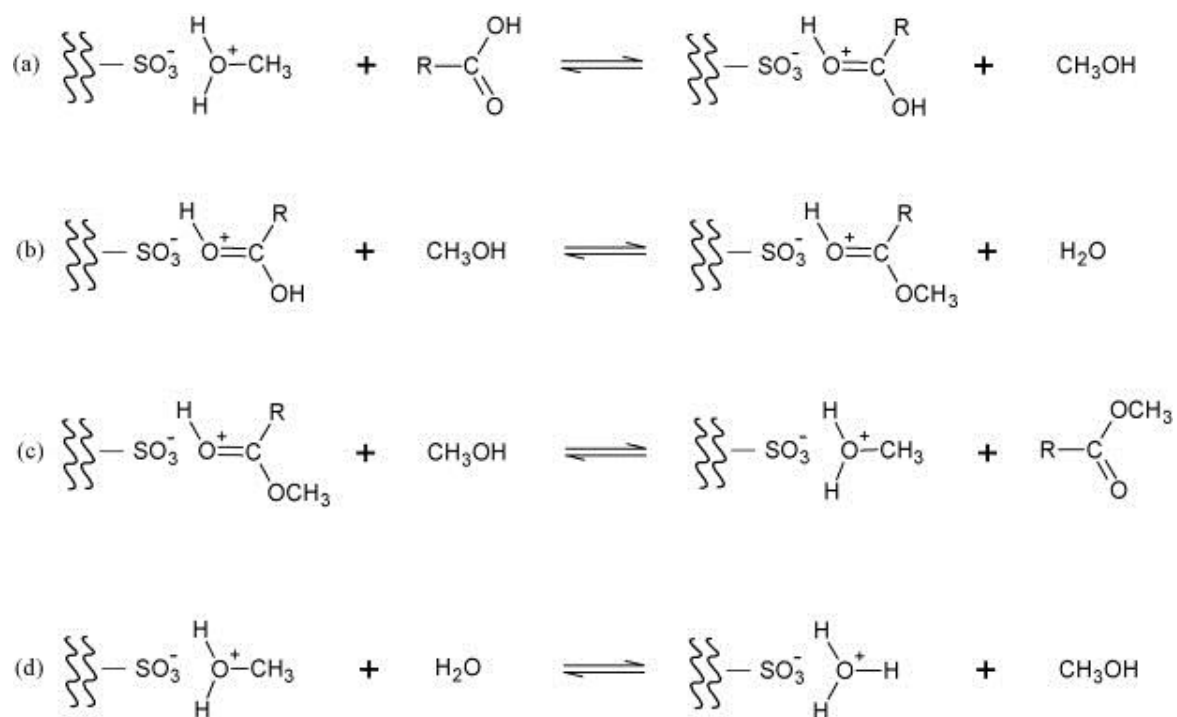


Figure 2-5 Scheme of reaction mechanism for the esterification catalyzed by ion-exchange acid

Some examples of reported solid catalysts used for esterification reaction are illustrated in

Table 2-2.

Table 2-2 Heterogeneous acid catalysts used in the esterification of free fatty acids

Acid Catalyst	Catalyst features	Reaction Conditions	FFA Conv.	Comments
Ion exchange resins. Styrene-divinyl benzene.	Amberlyst 15 4.7 meq H ⁺ g ⁻¹	Palm Fatty Acid distillate (97 wt. %) + methanol. MR = 20. t = 6 h. T = 60 °C. Cat = 30 wt.%	>95%	Resins show more swelling effect in the presence of non-polar solvent, increasing the amount of catalytic sites accessible by reaction substrates. Reusable for at least 15 reaction cycles without noticeable activity decay.
	EBD-100 5.4 meq H ⁺ g ⁻¹	Stearic acid (10 wt. %) + rapeseed oil + methanol. MR = 20. t = 6 h. T = 60 °C. Cat = 1 wt.%	>98%	Good performance in esterification of FFA. Easily regenerated.
Sulfonated solids	Sulfonated carbon 1.6 meq H ⁺ g ⁻¹	Soybean oil fatty acids (70%) + methanol. MR = 10. t = 6 h. T = 60 °C. Cat = 14 wt.%	99.5%	Prepared from Glycerol and sulfuric acid. High acid loading and surface area.
Metal oxides	Sulfated zirconia on SBA-15 1.3 meq H ⁺ g ⁻¹	Palmitic acid + methanol. MR = 80. t = 6 h. T = 68 °C. Cat = 2 wt.%	89.2%	High density of acid sites. Twice the catalyst activity obtained from unsupported sulfated zirconia. No data about deactivation behavior.
Supported heteropoly acids	H ₃ PW ₁₂ O ₄₀ / Ta ₂ O ₅	Lauric acid + ethanol. MR = 3. t = 3 h. T = 78 °C. Cat = 3 wt.%	70%	Low acid sites leaching. Reutilization tests experienced high catalytic activity decay due to poisoning caused by adsorption of chemicals on the catalytic centres. Catalysts could be regenerated.

2.9 Solid Acid Catalysts selected to carry out the esterification reaction

2.9.1 Silica Sulfuric Acid (SSA)

A wide range of important organic reactions can be efficiently catalyzed by these materials (Shah et al., 2014a, 2014b), which can be designed to provide different types of acidity as well as high degrees of reaction selectivity. The solids acids generally have high turnover numbers and can be easily separated from the organic components. In recent years the H₂SO₄ immobilized on SiO₂ was used as a catalyst for synthesis of organic compounds. However, there is still a drawback for these catalysts in terms of deactivation that needs further investigation.

2.9.2 Amberlyst 15

Amberlyst 15 is a bead form heterogeneous acid catalyst. It is a macro reticular polystyrene based ion exchange resin with strongly acidic sulfonic group (Pal et al., 2012). Thus, it serves as an excellent source of strong acid, that has been used in various acid catalyzed reactions. The catalyst is easy to measure, safe to use, and readily removable at the end of the reaction. An additional advantage is that Amberlyst 15 can be regenerated and used several times. For instance, it has been reported that it didn't lose activity after 15 runs. Talukder (Talukder et al., 2009) reported that palm fatty acid distillate (PFAD) a by-product from the palm oil refinery process, has been utilized as an alternative feedstock for biodiesel production via Amberlyst-15 catalyzed esterification with a yield up to 97% (Pal et al., 2012). The structural features of Amberlyst 15 are given in **Table 2-3**.

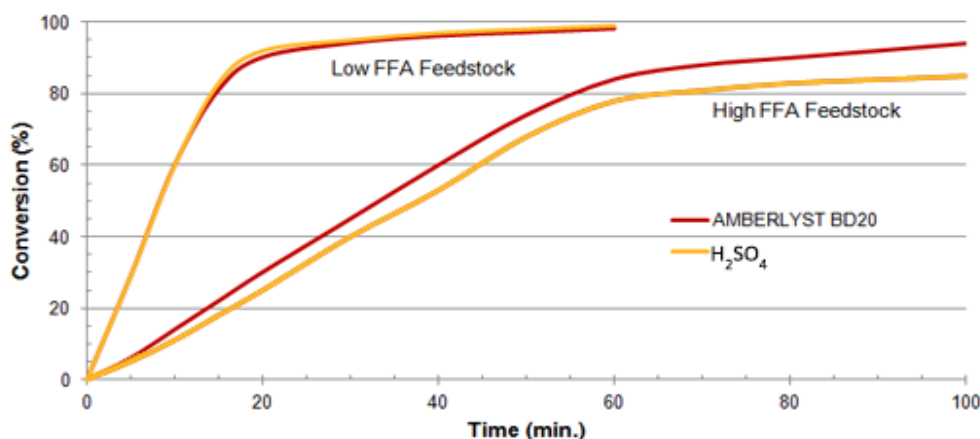
Table 2-3 Structural properties of Amberlyst 15.

<i>Ionic form as shipped</i>	Hydrogen
<i>Concentration of active sites</i>	>4.7 eq/kg
<i>Moisture holding capacity</i>	52 to 57% (H ⁺ form)
<i>Particle size</i>	0.600 to 0.850 mm
<i>Average pore diameter</i>	300Å
<i>Total pore volume</i>	0.40 mL/g
<i>Maximum operating temperature</i>	120 °C (250 °F)

2.9.3 Amberlyst BD20

Amberlyst BD20 from DOW chemical is a bead form, polymeric, heterogeneous acid catalyst. This functionalized polymer has been specifically designed for esterification of fatty acids in the production of biodiesel fuels. It allegedly outperforms all other presently available solid acid catalysts. These resins have high attraction for FFA long carbon chain due to the hydrophobic character of their polymer support (Omberg, 2015). The manufacturer reported tests on pilot plant under the following conditions: Feedstock FFA content 1-40wt.%, molar ratio of methanol to FFA 5-20, and temperature range of 85-105 °C.

When compared to sulfuric acid BD20 catalyst showed similar behavior at low FFA feed stocks. However, with higher FFA content, sulfuric acid catalysis becomes sluggish, this resulted on better performance for BD20 as shown in **Figure 2-6**. Reportedly more than 20 different oils were tested, and in each case, the catalyst was effective at converting the FFAs to the consequent esters.



Feed: 10 wt. % of pure stearic acid (> 97 %, Fluka, Germany)
in a low-acid vegetable oil (0.04 %) bought in the supermarket.

Figure 2-6 Comparison of Amberlyst BD20 and Sulfuric acid

2.10 Patent Search for Amberlyst BD20

To the best of the author knowledge there is very few study on one of the selected heterogeneous catalysts used in this study compared to other solid catalyst in literature, therefore an existing patent search has been conducted.

For the patent search the keywords: Biodiesel and BD20 have been used at the United States Patent website. The search generated 25 hits, out of which 11 has been preselected as shown in **Table 2-4** since the others focuses on different use of the catalyst as follows:

Table 2-4 Patent Search Results.

	PAT.#	Title
1	9,328,305	Catalytic processes for preparing estolide base oils
2	9,234,158	Process for pretreatment of vegetable oils by heterogeneous catalysis of the esterification of fatty acids
3	8,975,425	Catalytic processes for preparing estolide base oils
4	8,957,242	Dual catalyst esterification
5	8,637,689	Catalytic processes for preparing estolide base oils
6	8,629,291	Esterification of biodiesel feedstock with solid heterogeneous catalyst
7	8,580,119	Transesterification of biodiesel feedstock with solid heterogeneous catalyst
8	8,545,703	Production of glycerin from feedstock
9	8,545,702	Production of biodiesel from feedstock
10	8,540,881	Pretreatment, esterification, and transesterification of biodiesel feedstock
11	8,540,880	Pretreatment of biodiesel feedstock

A further screening discarded the ones treating the preparation of estolide base oils (number: 1,3, and 5 respectively). As well as number 7, and 8 treating transesterification and glycerin production respectively since these steps comes downstream of esterification in biodiesel production scheme.

2.10.1 Analysis of Shah's Patents (2013-2014)

It has to be noted that patents 6 to11 belongs to se same authors: Shah et Sunil, and assigned to Menlo Energy Management, LLC, San Francisco, CA (US). These similar in text format and contents patents (Shah and Suri, 2013a, 2013b, 2013c, 2014) describes an integrated pretreatment, esterification, and transesterification process where:

- Pretreatment process uses vacuum distillation at temperature of about 200-230°C to remove liquid impurities, then filtration to remove any solid particles above 2microns, finally an ion exchange purification resin Ambersep BD19 (DOW Chemical, USA) is used to provide a purified biodiesel feedstock by a straight flow through 2 stages guard bed column in series (lead-lag) without application of heat or pressure.
- The esterification of FFAs (Free Fatty Acids) present in the pretreated feedstock is carried through 3 stages, each stage consisting of packed bed reactors filled with solid ion exchange heterogeneous catalyst Amberlyst BD20 (DOW Chemical, USA) immobilized in solid support. Between each stage the bottom of the column is sent to a flash still in order to remove excess water and methanol. The reactors are operated at temperature of 85°C and 2.06 Bar pressure, with a reaction time of up to 75 minutes. The resulting triglyceride and biodiesel from the 3rd stage reactor has moisture and methanol content less than about 0.2% which proceeds to the transesterification process.
- The transesterification is carried out in two stage, and can include multi-stage bioreactors, with intermediate glycerin settling. The solid heterogeneous enzyme biocatalyst used include Biocatalyst A, Biocatalyst B, or a combination of both (developed by: TransBiodiesel, Israel). The reactor operates at 35°C with a residence time of 30 and 30-45min for the first and second stage respectively.

The transesterification step in Shah's patents has been mentioned for information only, as our study was focused only on the esterification step. However, it is considered that the pretreatment step mentioned is of critical importance and has to be incorporated in the process as it avoids catalyst poisoning, hence extending the catalyst commercial life up to 18 months. This can lower the actual cost of the solid catalyst, as well as the labor costs and costs of down-time associated with the plant shut-down while replacing the catalyst. On the other hand, the operating conditions for esterification mentioned in this patents (85°C, 2.06 Bar) are higher than the one studied (60°C, 1Bar).

2.10.2 Analysis of Slade's Patent (2015)

Patents No.4 belongs to the authors: Slade et al., and assigned to Renewable Energy Group, Inc., Ames, IA (US). This patent (Slade et al., 2015) describes an esterification with optional pretreatment process where:

- A combination of an homogeneous catalyst (either: Methanesulfonic acid “MSA”, sulfuric acid, phosphoric acid, and p-toluene sulfonic acid), and an heterogeneous ion exchange catalyst (either: Amberlyst BD20 from DOW Chemical, Lewatit® from Lanxess, DOWEX dry acid catalysts from DOW such as DR-2030 or M-31). The patent claims that the homogeneous catalyst prolongs the life of heterogeneous one, also their combination provide increased conversion relative to the use of either catalyst alone.
- The process provides for the use of a single, or two reactors in series. The reactors may be a continuously stirred tank (CSTR), plug-flow, mixed-flow, fixed bed, fluidized bed, batch, semi-batch, recirculating, or other reactor type.

Although the author mentioned that at any initial amount of FFA, esterification with methanol using Amberlyst BD-20 catalyst can briefly reduce the initial FFA content below 1wt.% in a single stage “*by carefully selecting certain combinations of methanol ratio, weight hourly space velocity, and reaction temperature*”. The author gives only a range of temperature: 50-150 °C, pressure: 0-10.34 Bar gage, and residence time: 2-480min for the process. All examples mentioned in the patent uses operating parameters of: 80°C and 4.13 Bar pressure, which are higher than the ones in this study.

2.10.3 Analysis of Coupard's Patent (2016)

Patents No.2 belongs to the authors: Coupard et al., and assigned to IFP Energies Nouvelles, Rueil-Malmaison (FR). This patent (Coupard et al., 2016) describes a continuous pretreatment esterification process of an oil feedstock (either raw or semi-refined) containing at most 20wt.% of FFA where:

- The reaction is carried out in a vertical counter-current liquid/liquid contactor between light phase rich in alcohol (has the lowest density by adjusting the water content in the alcohol feedstock), and heavy phase rich in oil. By this difference in density the light phase circulates from bottom to top. The reactor is filled with solid acid catalyst, in a

very preferred manner: divinylbenzene and polystyrene copolymer such as TA801 resin sold by Axens company.

- Upon contact with the catalyst, the reaction for esterification between the FFA and the alcohol contained in the light and heavy phase takes place, producing esters and water. Simultaneously the alcohol passes from the alcohol rich phase to the oil-rich phase, while the water passes from the oil rich phase to the alcohol rich phase by mass-transfer. Therefore, the water will be separated from the oil and esters formed by the reaction without the need for a separation stage, making the process more economically viable.
- The liquid/liquid contactor is operated at temperatures between 25-120°C, Pressure between 1-20 bar absolute, and time between 30-90min. The FFA conversion is greater than 98%

In the prior art the author mentioned a process using BD20 in a two stage process operating at 80°C and 20 bars, yielding a conversion of 99%. The author also mentioned that the pressure has to be kept so the alcohol will remain at liquid stage that implies a minimum of 2 bars at 70°C. Therefore this process also operates at higher temperature and pressure than the ones used in this study. The inherent process and economic advantages presented in this patent consists on the elimination of the water phase separation after reaction.

The patent analysis conducted in this section are for generated results from the search conducted at the U.S patent office and is not in any mean exhaustive of other existing technologies we are not aware of.

2.11 Concluding remark

Biodiesel is an attractive biofuel showing inherent advantages compared to petro-diesel. It is the only fuel where blended with petro-diesel that can run in conventional unmodified engines. In addition, it has higher combustion efficiency, higher cetane number and improves the lubrication properties of the diesel fuel blend resulting on reduced corrosion and increase in durability. Biodiesel is environmentally friendly as it is biodegradable, reduces pollution and has zero carbon dioxide emission life cycle.

There is a wide range of available feedstock (more than 4000 potential plants has been reported) for biodiesel production, this represent a major advantage of producing biodiesel from alternative non-edible feedstock that doesn't compete with food crops. On the other hand, it has been found that refined edible vegetable oils feedstock represents more than 75% of the overall biodiesel production cost. Therefore, tremendous effort of research has been undergone in order to reduces the raw material cost impact, by focusing on processes and catalysts able to use low cost non-edible vegetable oils, animal fats, and algal oils.

Currently biodiesel production is not economically viable without government subsidies, due to the afore mentioned reasons. Nevertheless, the production of biodiesel has grown 4.6 times between the year 2004 to 2013. The major reason being that current energy policies fosters environmental issues including the development of environmentally friendly technologies that increases energy supplies, reduces air pollution, and addresses the global warming by greenhouse effect.

The work undergone in this study is aimed toward the reduction of biodiesel cost, eventually the biodiesel price would be competitive in the near future.

References

- Atabani, a. E.; Silitonga, a. S.; Badruddin, I. A.; Mahlia, T. M. I.; Masjuki, H. H.; Mekhilef, S. A. Comprehensive Review on Biodiesel as an Alternative Energy Resource and Its Characteristics. *Renew. Sustain. Energy Rev.* **2012**, *16* (4), 2070–2093.
- Atadashi, I. M.; Aroua, M. K.; Abdul Aziz, a. R.; Sulaiman, N. M. N. The Effects of Water on Biodiesel Production and Refining Technologies: A Review. *Renew. Sustain. Energy Rev.* **2012**, *16* (5), 3456–3470.
- Atadashi, I. M.; Aroua, M. K.; Abdul Aziz, A. R.; Sulaiman, N. M. N. The Effects of Catalysts in Biodiesel Production: A Review. *J. Ind. Eng. Chem.* **2013**, *19* (1), 14–26.
- Bournay, L.; Casanave, D.; Delfort, B.; Hillion, G.; Chodorge, J. a. New Heterogeneous Process for Biodiesel Production: A Way to Improve the Quality and the Value of the Crude Glycerin Produced by Biodiesel Plants. *Catal. Today* **2005**, *106* (1–4), 190–192.
- Coupard, V.; Bournay, L.; Toth, E.; Maury, S. Process for Pretreatment of Vegetable Oils by Heterogeneous Catalyst of the Esterification of Fatty Acids. US Patent. US 9,234,158, 2016.
- Demirbas, A. Progress and Recent Trends in Biodiesel Fuels. *Energy Convers. Manag.* **2009**, *50* (1), 14–34.
- Demirbas, A. Biodiesel for Future Transportation Energy Needs. *Energy Sources, Part A Recover. Util. Environ. Eff.* **2010**, *32* (September 2013), 1490–1508.
- Feng, Y.; He, B.; Cao, Y.; Li, J.; Liu, M.; Yan, F.; Liang, X. Biodiesel Production Using Cation-Exchange Resin as Heterogeneous Catalyst. *Bioresour. Technol.* **2010**, *101* (5), 1518–1521.
- Van Gerpen, J. Biodiesel Processing and Production. *Fuel Process. Technol.* **2005**, *86*, 1097–1107.
- Helwani, Z.; Othman, M. R.; Aziz, N.; Fernando, W. J. N.; Kim, J. Technologies for Production of Biodiesel Focusing on Green Catalytic Techniques: A Review. *Fuel Process. Technol.* **2009**, *90* (12), 1502–1514.

Hillion, G.; Delfort, B.; Durand, I. Method for Producing Biofuels, Transforming Triglycerides into at Least Two Biofuel Families: FATTY ACID MONOESTERS and ETHERS And/or SOLUBLE GLYCEROL ACETALS. US 2007/0283619 A1, 2007.

Knothe, G.; Krahl, J.; Van Gerpen, J. *The Biodiesel Handbook, 2nd Edition.*, 2nd Editio.; AOCS Press: Urbana, Illinois, 2010.

Kondamudi, N.; Mohapatra, S. K.; Misra, M. Quintinite as a Bifunctional Heterogeneous Catalyst for Biodiesel Synthesis. *Appl. Catal. A Gen.* **2011**, *393* (1–2), 36–43.

Lee, A. F.; Wilson, K. Recent Developments in Heterogeneous Catalysis for the Sustainable Production of Biodiesel. *Catal. Today* **2015**, *242*, 3–18.

Lee, A. F.; Bennett, J. A.; Manayil, J. C.; Wilson, K. Heterogeneous Catalysis for Sustainable Biodiesel Production via Esterification and Transesterification. *Chem. Soc. Rev.* **2014**, *43* (22), 7887–7916.

Lee, J. S.; Saka, S. Biodiesel Production by Heterogeneous Catalysts and Supercritical Technologies. *Bioresour. Technol.* **2010**, *101* (19), 7191–7200.

Marchetti, J. M.; Errazu, A. F. Comparison of Different Heterogeneous Catalysts and Different Alcohols for the Esterification Reaction of Oleic Acid. *Fuel* **2008**, *87* (15–16), 3477–3480.

Melero, J. A.; Iglesias, J.; Morales, G. Heterogeneous Acid Catalysts for Biodiesel Production: Current Status and Future Challenges. *Green Chem.* **2009**, *11* (9), 1285–1308.

Michel Bloch. Improved Glycerin Quality via Solid Catalyst Transesterification : The Esterfip-H Process. In *European Biofuels Forum; Bio-Oil International Conference*, Ed.; 2006; pp 1–20.

Moser, B. Biodiesel Production, Properties, and Feedstocks. *Biofuels* **2011**, No. March, 285–347.

Omberg. Small-Scale Biodiesel Production Based on a Heterogenous Technology- Masters Thesis, Norwegian University of Life Sciences, 2015.

Ong, Y. K.; Bhatia, S. The Current Status and Perspectives of Biofuel Production via Catalytic Cracking of Edible and Non-Edible Oils. *Energy* **2010**, *35* (1), 111–119.

Pal, R.; Sarkar, T.; Khasnobis, S. Amberlyst-15 in Organic Synthesis. *Arkivoc* **2012**, 2012 (i), 570–609.

Pinto, A. C.; Guarieiro, L. L. N.; Rezende, M. J. C.; Ribeiro, N. M.; Ednildo, A. Biodiesel : An Overview. *J. Braz. Chem. Soc* **2005**, 16 (6), 1313–1330.

Pisarello, M. L.; Dalla Costa, B.; Mendow, G.; Querini, C. a. Esterification with Ethanol to Produce Biodiesel from High Acidity Raw Materials: Kinetic Studies and Analysis of Secondary Reactions. *Fuel Process. Technol.* **2010**, 91 (9), 1005–1014.

Robles-Medina, A.; González-Moreno, P. A.; Esteban-Cerdán, L.; Molina-Grima, E. Biocatalysis: Towards Ever Greener Biodiesel Production. *Biotechnol. Adv.* **2009**, 27 (4), 398–408.

Romero, R.; Martínez, S. L.; Natividad, R. Biodiesel Production by Using Heterogeneous Catalysts. *Altern. Fuel* **2011**, 3–20.

Samir Najem Aldeen Khurshid. Biodiesel Production by Using Heterogeneous Catalysts. MSc Thesis, Royal Institute of Technology (KTH) Stockholm, Sweden, 2014.

Sanchez, N. Investigation of Cost-Effective Biodiesel Production from High FFA Feedstock- Masters Thesis, The University of Western Ontario, 2013.

Sani, Y. M.; Daud, W. M. A. W.; Abdul Aziz, A. R. Activity of Solid Acid Catalysts for Biodiesel Production: A Critical Review. *Appl. Catal. A Gen.* **2014**, 470, 140–161.

Santacesaria, E.; Vicente, G. M.; Di Serio, M.; Tesser, R. Main Technologies in Biodiesel Production: State of the Art and Future Challenges. *Catal. Today* **2012**, 195 (1), 2–13.

Santori, G.; Di Nicola, G.; Moglie, M.; Polonara, F. A Review Analyzing the Industrial Biodiesel Production Practice Starting from Vegetable Oil Refining. *Appl. Energy* **2012**, 92, 109–132.

Sawangkeaw, R.; Bunyakiat, K.; Ngamprasertsith, S. A Review of Laboratory-Scale Research on Lipid Conversion to Biodiesel with Supercritical Methanol (2001-2009). *J. Supercrit. Fluids* **2010**, 55 (1), 1–13.

Semwal, S.; Arora, A. K.; Badoni, R. P.; Tuli, D. K. Biodiesel Production Using Heterogeneous Catalysts. *Bioresour. Technol.* **2011**, *102* (3), 2151–2161.

Serio, M. Di; Cozzolino, M.; Giordano, M.; Tesser, R.; Patrono, P.; Santacesaria, E.; Federico, N.; Universitario, C.; Angelo, M. S. From Homogeneous to Heterogeneous Catalysts in Biodiesel Production. *Ind. Eng. Chem. Res.* **2007**, *46*, 6379–6384.

Shah, G.; Suri, S. Pretreatment, Esterification, and Transesterification of Biodiesel Feedstock. US Patent. US 8,540,881, 2013a.

Shah, G.; Suri, S. Pretreatment of Biodiesel Feedstock. US Patent. US 8,540,880, 2013b.

Shah, G.; Suri, S. Production of Biodiesel from Feedstock. US Patent. US 8,545,702, 2013c.

Shah, G.; Suri, S. Esterification of Biodiesel Feedstock with Solid Heterogeneous Catalyst. US Patent. US 8,629,291, 2014.

Shah, K.; Parikh, J.; Dholakiya, B.; Maheria, K. Fatty Acid Methyl Ester Production from Acid Oil Using Silica Sulfuric Acid: Process Optimization and Reaction Kinetics. *Chem. Pap.* **2014a**, *68* (4), 472–483.

Shah, K. A.; Parikh, J. K.; Maheria, K. C. Optimization Studies and Chemical Kinetics of Silica Sulfuric Acid-Catalyzed Biodiesel Synthesis from Waste Cooking Oil. *Bioenergy Res.* **2014b**, *7* (1), 206–216.

Shibasaki-Kitakawa, N.; Honda, H.; Kuribayashi, H.; Toda, T.; Fukumura, T.; Yonemoto, T. Biodiesel Production Using Anionic Ion-Exchange Resin as Heterogeneous Catalyst. *Bioresour. Technol.* **2007**, *98* (2), 416–421.

Slade, D.; Ellens, C.; Brown, J.; Pollard, A.; Albin, B. Dual Catalyst Esterification. US Patent. US 8,957,242, 2015.

Stergiou, P.-Y.; Foukis, A.; Filippou, M.; Koukouritaki, M.; Parapouli, M.; Theodorou, L. G.; Hatziloukas, E.; Afendra, A.; Pandey, A.; Papamichael, E. M. Advances in Lipase-Catalyzed Esterification Reactions. *Biotechnol. Adv.* **2013**, *31* (8), 1846–1859.

Talebian-Kiakalaieh, A.; Amin, N. A. S.; Mazaheri, H. A Review on Novel Processes of Biodiesel Production from Waste Cooking Oil. *Appl. Energy* **2013**, *104*, 683–710.

Talukder, M. M. R.; Wu, J. C.; Lau, S. K.; Cui, L. C.; Shimin, G.; Lim, A. Comparison of Novozym 435 and Amberlyst 15 as Heterogeneous Catalyst for Production of Biodiesel from Palm Fatty Acid Distillate. *Energy and Fuels* **2009**, *23* (January), 1–4.

Tesser, R.; Casale, L.; Verde, D.; Di Serio, M.; Santacesaria, E. Kinetics and Modeling of Fatty Acids Esterification on Acid Exchange Resins. *Chem. Eng. J.* **2010**, *157* (2–3), 539–550.

Ullah, F.; Dong, L.; Bano, A.; Peng, Q.; Huang, J. Current Advances in Catalysis toward Sustainable Biodiesel Production. *J. Energy Inst.* **2015**, 1–11.

West, A.; Posarac, D.; Ellis, N. Assessment of Four Biodiesel Production Processes Using HYSYS.Plant. *Bioresour. Technol.* **2008**, *99* (14), 6587–6601.

Wilson, K.; Lee, A. F. Rational Design of Heterogeneous Catalysts for Biodiesel Synthesis. *Catal. Sci. Technol. Catal. Sci. Technol* **2012**, *2* (2), 884–897.

Wilson, K.; Lee, A. F.; Macquarrie, D. J.; Clark, J. H. Structure and Reactivity of Sol–gel Sulphonic Acid Silicas. *Appl. Catal. A Gen.* **2002**, *228* (1–2), 127–133.

CHAPTER 3

3 Esterification Reaction using Homogeneous Catalyst

3.1 Introduction

Extensive research on alternative renewable energy sources such as geothermal, solar, wind, and biomass; have been triggered by fossil fuel exhaustion, on top of the environmental concerns resulting from global warming due to greenhouse gases generated after fossil fuels combustion. Biodiesel, obtained from vegetable oils and animal fats stands for a clean and attractive alternative fuel compared to fossil-based diesel. The advantages of BD are: that it is non-toxic, biodegradable, renewable, and has a low emission profile. In fact the carbon life cycle for biodiesel is considered to be zero (Van Gerpen, 2005; Sawangkeaw et al., 2010). It consists of a combination of mono-alkyl esters of long-chain fatty acids chemically produced by transesterification of triglycerides (TG) or esterification of free fatty acids (FFA). In order to promote the reaction and improve yield a catalyst is generally required (Ma and Hanna, 1999; Meher et al., 2006). Industrial production of biodiesel confronts major challenges consisting on limited supply of raw material due to the use of high quality refined vegetable oils, on top of the cost of feedstock, which accounts for 60-80% of total production cost (Leung et al., 2010). At present, biodiesel is not economically competitive with petroleum based-fuels. The use of alternative feedstock such as waste frying oils, non-edible oils, and animal fats could address the issue of feedstock cost (Berchmans and Hirata, 2008; Atadashi et al., 2012a). However, biodiesel cannot entirely replace the petroleum-based diesel fuel. Since, if all of the vegetable oil and animal fats produced in United State for example were available to produce biodiesel, it would only replace 14% of the requirement for on-highway diesel fuel (Van Gerpen, 2005). Still, the main obstacle to use these feedstocks is that they contain significant amount of free fatty acids (FFA). These FFAs reacts with the base catalyst usually used for transesterification, and produces soap and water hindering product separation. (Ghadge and Raheman, 2005; Berchmans and Hirata, 2008; Naik et al., 2008). The problem of soap formation can be addressed by using acid-catalyzed transesterification but the slow reaction rate makes it a less attractive option (Canakci and Van Gerpen, 1999). Therefore an integrated two-step esterification-transesterification method has received more consideration due to its moderate operating conditions, higher reaction rates and relative flexibility (Zullaikah et al., 2005). In the

esterification step fatty acids are converted to alkyl esters reducing FFA content to an acceptable level for the subsequent transesterification step, thus improving overall product yield. In the present study, the esterification step was investigated using two different reactor configurations, to evaluate the best approach leading to up to standard specification under mild conditions at lower cost.

Objectives

The objectives for this part of the study included selection of suitable homogeneous acid catalyst and determination of suitable operating conditions of mixing, reaction system, and temperature. The selection of operating conditions is guided by need for special process safety and environmental considerations for small to medium scale production processes. Methanol (a flammable, toxic alcohol) and H_2SO_4 (a corrosive, flammable acid) are two hazardous chemicals required to convert vegetable oil into biodiesel. Overexposure to methanol can cause neurological damage and other health problems. Methanol also presents a serious fire risk. The reaction temperature is limited to 60°C to allow operation near atmospheric pressure and sulphuric acid catalyst concentration is limited to 5 wt.% for safety and environmental considerations.

3.2 Experimental Details

3.2.1 Materials and Chemicals

Anhydrous grade methanol (99.9%) was acquired from EMD Millipore Corp (USA). Refined Canola oil used in the experiments was the Saporito Brand marketed by Costco wholesale stores. Anhydrous grade ethyl alcohol was obtained from Commercial Alcohols. Phenolphthalein indicator solution 1% (w/v) in 50% (v/v) Isopropanol was provided by VWR (Canada). Reagent grade sodium hydroxide NaOH (97%), potassium hydroxide KOH (85%), oxalic acid (99.5%), and concentrated sulfuric acid (95-98%) were supplied by Caledon Laboratories Ltd. Oleic acid at 90% FFA was purchased from Alfa Aesar, and CAS grade concentrated hydrochloric acid from Fisher Scientific.

3.2.2 Equipment

All experiments were performed in a one-liter jacketed glass reactor of 140mm height and 100mm inside diameter. It was equipped with a reflux condenser, a 63.5 mm in diameter impeller with three pitched blades (45°) of 5mm width placed concentrically at 36 mm from the bottom, and four baffles (10mm width) equably allocated to provide an effective mixing of reactants and products. A schematic of the experimental set up can be seen in **Figure 3-1**. The vessel was linked to a water bath LAUDA E100 capable of maintaining the reactor temperature at the prefixed value within $\pm 1^\circ\text{C}$, by means of a tubular heater controlled by a modified PID (proportional-integral-derivative) controller. A thermocouple (TRACEABLE provided by VWR) was utilised to oversee the reaction temperature. Also a laser tachometer (MONARCH PLT200) was employed to measure the impeller RPM. Three ports were accessible from the lid of the reactor, one was utilized to attach the condenser to the system, the other one was the inlet of the rod of the impeller, and the third was used to convey the reactants into the vessel and to get intermittent samples for analysis. In addition, the reactor was equipped with a drain valve to empty the contents of the reactor at the end of reaction. Extra equipment employed during experiments comprised: a rotary evaporator Hei-Vap Value manufactured by Heidolph Instruments Germany for vacuum distillation in order to separate water or methanol from the reaction mixture, and separatory funnels.

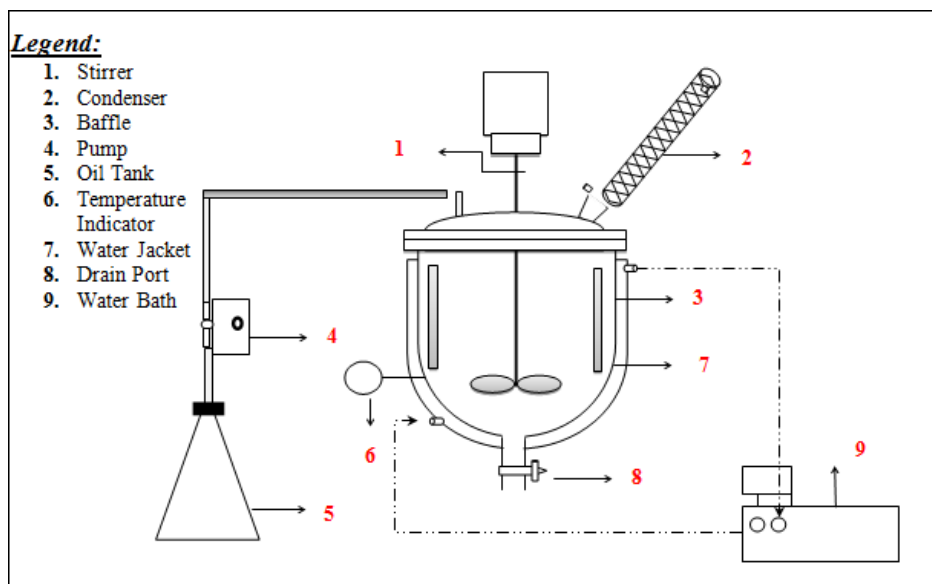


Figure 3-1 Schematic of Experimental setup for homogeneous catalysed esterification

3.2.3 Experimental Procedure

High FFA feedstock was simulated by a model mixture prepared by combining a known amount of oleic acid to refined canola oil. Oleic acid was selected since it is one of the dominant fatty acids present in several vegetable oils such as rapeseed, karanja, soybean and palm oil; as well as in animal fats for instance poultry fat, yellow and brown grease (Lotero et al., 2005). Acidity was fixed to 30mgKOH/g corresponding to 15% FFA content by weight. Methanol was selected as alcohol by reason of its low cost (Demirbas, 2010), large availability and widespread use in the biodiesel industry (Moser, 2011). Methanol excess was used to shift the equilibrium of the reversible reaction toward the direction of ester formation according to Chatelier's principle (Feng et al., 2011). The molar ratio of Methanol to FFA of 20:1 was set for all experiments, based on previous literature investigations (Jeromin et al., 1987; Robles-Medina et al., 2009; Koh, 2011; Santori et al., 2012; Coupard et al., 2014; Konwar et al., 2014; Fu et al., 2015).

For batch mode operation, acidified oil was first added to the reactor where the water circulating inside the jacket provided the heat necessary for the oil to reach the desired temperature. Then, the methanol/sulphuric acid blend was transferred into the reaction system. A mixing speed of 720rpm was set for the experiments to overcome mass transfer limitation (Sendzikiene et al., 2004; Berrios et al., 2007). Reaction was continued for 90 min for all experiments, and intermittent samples were collected as reaction progressed for analysis. Initial experiments were repeated two times, and the

difference between repeat runs was found to be within 2%. This indicated good reproducibility, thus for subsequent experiments no replicates were conducted. The reaction temperature was retained at 60°C that is below the boiling point of methanol (64.7°C) at atmospheric pressure (Sendzikiene et al., 2004) with the purpose of maintaining the methanol in liquid state without the necessity to pressurize the reaction vessel (Canakci and Gerpen, 2001). On the other hand, a set of experiments were performed at temperatures in the sequence of 30-60°C with the intent to investigate the temperature effect, and kinetic parameters of the reaction system.

For the semi-batch mode, the methanol/sulphuric acid blend was mixed at 300rpm and heated to the desired temperature inside the reactor. While in a separate container, the acidified oil (canola oil+ oleic acid) was mixed by mean of magnetic stirrer, and heated to matching temperature. When the set temperature was reached in both sides, a metering pump was used to supplement the acidified oil into the reactor at a constant flow rate of 18ml/min. At this feed rate the reaction was assigned to progress under semi-batch mode for 25minutes. After all AO was fed to the reactor, the reaction continued under batch mode for the remaining 65minutes. In order to investigate the mixing intensity for overcoming the mass transfer limitation the impeller speed was altered over the course of the reaction from 300rpm for the first 15min, 400rpm from 15 to 30min, then 600 rpm for the remaining 60 minutes. As the reaction advanced, intermittent samples were collected at regular intervals to analyze the reaction progress.

Subsequently at the end of reaction, the reaction mix for both modes was shifted to a separatory funnel for overnight decantation in order to ensure complete phases separation. The block flow diagram of the esterification reaction using homogeneous catalyst is shown on **Figure 3-2**.

After decantation the system was biphasic constituted by:

- Top layer composed by water, excess methanol, and most of the catalyst.
- Bottom organic layer principally containing FAME, unreacted TG and FFA.

Vacuum evaporation at 90°C and (-50) kPa pressure was applied to remove traces of water and excess alcohol from the bottom layer. After evaporation, the esterified oil became unclouded, a sign of impurities removal.

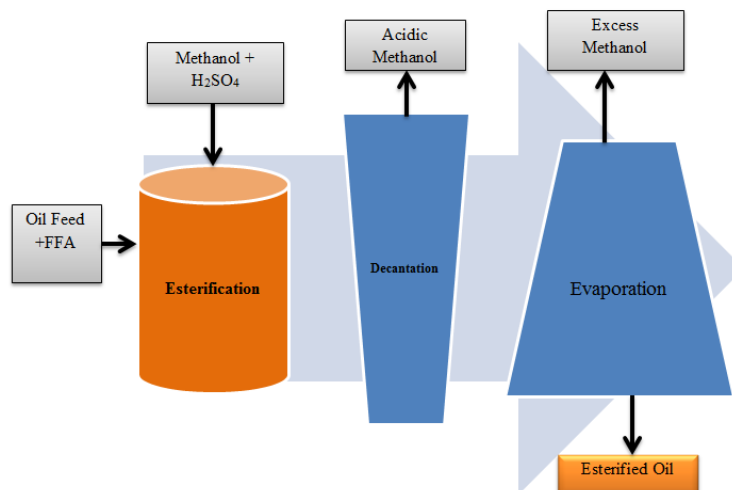


Figure 3-2 Block Flow diagram for homogeneous catalyst Esterification reaction

3.2.3.1 Acid Content Analysis

The samples collected at specific intervals were analysed by a standard acid-base titration procedure to evaluate the FFA content. Prior to titration the sodium hydroxide solution was standardized by means of dehydrated oxalic acid for accurate determination of the solution normality. Depending on the FFA range the alkaline solution concentrations used were approximately 0.012, and 0.031N. The withdrawn samples (about 2g each) were weighed, then washed with distilled water to remove methanol from the organic phase. Soon after, the vials were deposited in a fridge to completely stop the reaction, and allowed to stand for 3-4 hours for further phase separation. Finally, the top layers were removed from the vials using a micropipette and transferred to Erlenmeyer flask for analysis.

The titration procedure pursued in this work is a modified method of the American Oil Chemists Society (A.O.C.S.) Official Method Ca 5a-40 wherein lesser amounts of sample can be utilised as illustrated by (Rukunudin et al., 1998). In this method a weighted amount of the sample was dissolved in a predefined quantity of ethanol, then a few droplets of phenolphthalein as indicator were added, and the titration is then performed by means of the alkaline NaOH solution at pre-set normality varying with the range of FFA content. All glassware was clean and dried with compressed air prior to titrations. The endpoint was reached when a permanent pale pink color was observed and lasted for at least 30 secs, at that moment the volume of NaOH solution

consumed is recorded. The acidity (FFA content) as oleic acid in the sample was calculated by means of the equation 3.1:

$$FFA\% = \frac{V_{NaOH\ used} \times N_{NaOH} \times 282}{Wt_{sample}} \times 100 \quad (3.1)$$

Where:

FFA: Free acidity as oleic acid (%)

V_{NaOH}: Volume of NaOH solution used during titration (ml)

N_{NaOH}: Exact normality of alkaline solution (mol/L)

Wt_{sample}: Weight of titrated sample (g)

282: Molecular weight of oleic acid (g/mol)

Conversion of esterification reaction was calculated as follows:

$$Conversion(\%) = \frac{FFA_i - FFA_t}{FFA_i} \times 100\% \quad (3.2)$$

Where:

FFA_i: Initial FFA content

FFA_t: FFA content at a given time

3.3 Results and discussion

Esterification was carried out with the aim to reduce the FFA content in oil to a standard level (< 1mgKOH/g). In this reaction, a fatty acid molecule reacts with an alcohol molecule to produce a methyl ester and a water molecule in the presence of an acid catalyst as illustrated in **Figure 3-3**.



Figure 3-3 Esterification reaction (Johnson, 2016)

As mentioned earlier, batch and semi- batch modes of mixing were studied. Although, batch mode is common practice in industry, its mixing effects can be limited especially at the beginning of the reaction between two immiscible liquids. In order to overcome the mass transfer limitation, a procedure consisting on gradual feeding of the preheated acidic oil into a blend of methanol and catalyst solution inside the reactor. This technique was formerly proposed by (Pal and Prakash, 2012) for transesterification (methanolysis) of TG. For instance, as oil droplets falls into a pool of methanol and catalyst solution, they easily get spread uniformly through the reaction system. By adjusting the AO feeding rate to 18ml/min, the methanol to FFA molar ratio was amplified specially in the early stages of the reaction with values of: 100:1 at 5min, 50:1 at 10min, 25:1 at 20min, and finally a 20:1 from 25min to 90min.

The role of mixing intensity was examined by adjusting the rpm for semi-batch mode stepwise: 300 in first 15 minutes, 400 for the next 15 minutes and 600 for the remaining 60 minutes. The FFA content in the feed was fixed to 15 wt. % which is the standard for yellow grease (<15% FFA) (Kulkarni and Dalai, 2006; Chai et al., 2014), also this concentration of FFA is representative of the value in most non-edible oils. Additionally, the higher FFA in oil feed was also expected to show clear differentiation between the two methods. H_2SO_4 was chosen as catalyst because it is currently employed for AO pretreatment, at commercial scale due to its demonstrated activity and low cost (Konwar et al., 2014).

3.3.1 Batch Mode of operation

Comparing the graphs for the FFA diminution with time (**Figure 3-4**) and conversion percentage with time progress (**Figure 3-5**) for batch mode at different temperatures, it can be observed that the temperature has positive effect on overall FFA conversion. The conversion rate is slow for temperature below 40°C but increases significantly for higher temperatures. The conversion rate

at lower temperatures could also be affected by higher viscosity of oil which in turn affects the mixing. The viscosity of oil decreases nearly half from about 46 cP at 30°C to 20 cP at 60°C.

The desired conversion of nearly 97% for FFA is reached in about 60 min at 60°C and nearly 70 min at 50°C. However, at lower temperatures, the final conversion remains well below the target. So the recommended operating temperature is 60°C. Also it can be pointed out that at 60°C, conversion stabilize after 60 minutes pointing that equilibrium is almost reached at that time as seen from the values of conversion which are: 97.05% at 90 min, and 96.97% at 60 min.

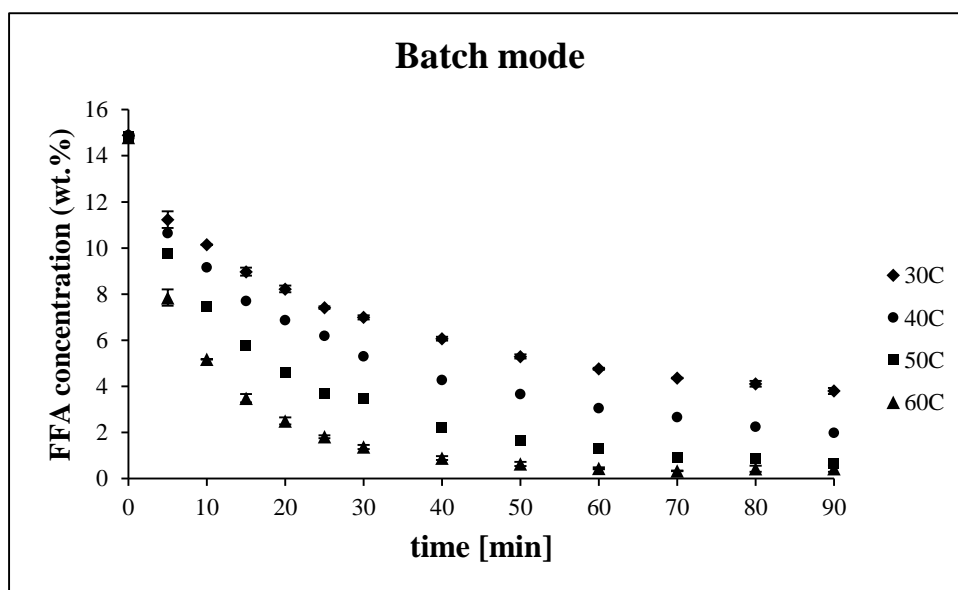


Figure 3-4 FFA% versus. Time for Batch Mode Operation

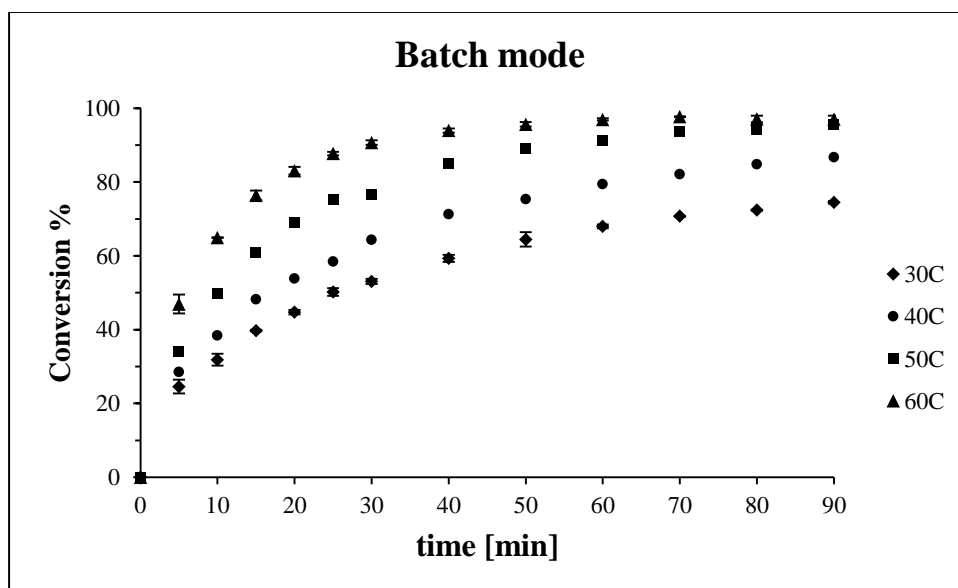


Figure 3-5 Conversion% versus. Time for Batch Mode Operation

3.3.2 Semi-Batch mode of operation

Comparison of FFA diminution with time (**Figure 3-6**) and conversion percentage along with time progress (**Figure 3-7**) show that the temperature change over the selected range has similar effect on overall FFA conversion as was noticed for batch mode. However, in semi-batch the reaction behaved differently, it was observed that in the first 10 minutes a sharp decrease in FFA content achieving 41.25, 48.5, 63.7, and 73.2% conversion at 30, 40, 50, and 60°C respectively.

Between 15 and 25 minutes a plateau was noticed where conversion was nearly constant which can be attributed to the nature of this mode of operation. The reaction system was modeled using appropriate balance equations. The reactor was initially filled with the required amount of alcohol and catalyst and agitation was initiated. The oil feed with FFA content was started at a constant rate. The mass conservation principle applicable to the mass of species (i) for the semi-batch reactor can be stated as:

$$\left\{ \begin{array}{l} \text{Input rate of } i \text{ into} \\ \text{reactor} \end{array} \right\} - \left\{ \begin{array}{l} \text{Output of } i \text{ from} \\ \text{reactor} \end{array} \right\} + \left\{ \begin{array}{l} \text{rate of production of} \\ i \text{ within the reactor} \end{array} \right\} \\ = \left\{ \begin{array}{l} \text{rate of accumulation of } i \\ \text{in the reactor} \end{array} \right\}$$

At the selected feed rate of about 18 ml/min, all the oil feed was pumped in about 27 min and the reactor operated in batch mode subsequent to the end of feeding. At the end of feeding (~27 minutes) the fatty acids concentration starts decreasing gradually as the reaction followed a batch mode after all oil has been added to the reactor. A quick comparison of the conversion level indicates similar final values as with the batch mode.

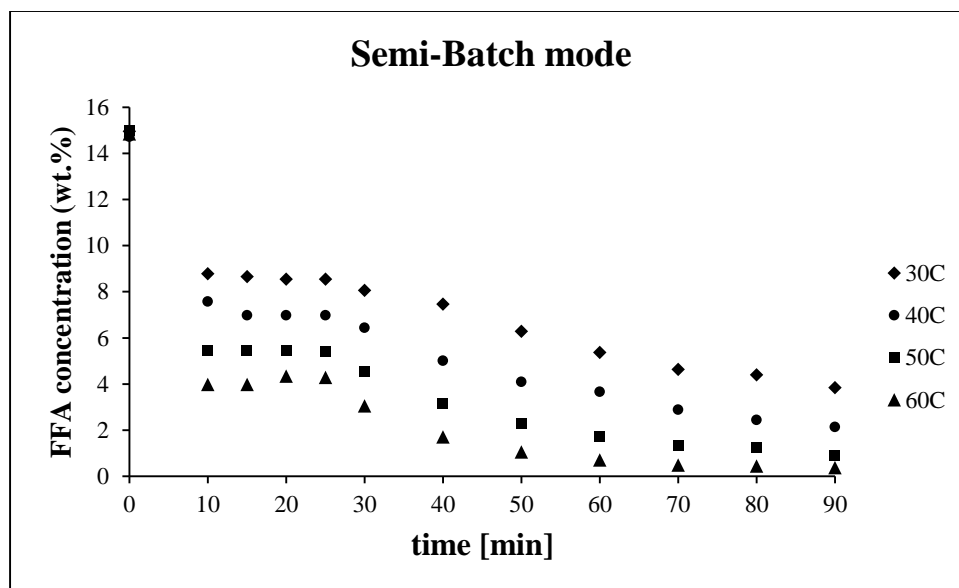


Figure 3-6 FFA% vs. Time for Semi-Batch Mode Operation

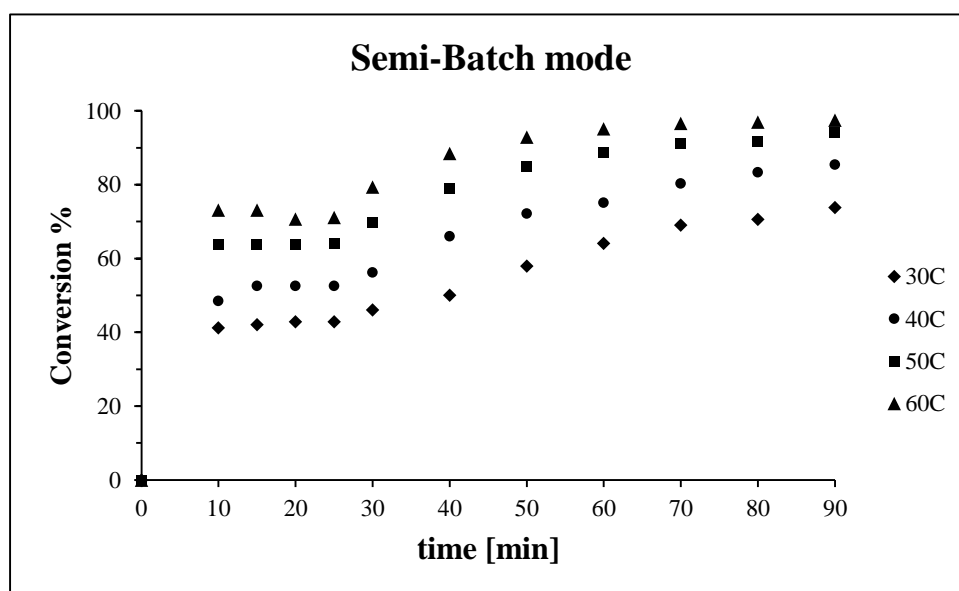


Figure 3-7 Conversion% vs. Time for Semi-Batch Mode

3.3.2.1 Comparison of Batch and Semi-Batch mode of operation

Figure 3-8 compares the change in the FFA concentration with respect to time at all reaction temperatures for both reaction modes. It can be seen that initially FFA concentrations are lower (as expected) with semi-batch compared to batch mode. However, FFA concentration for semi-batch mode increases sharply due to continuous feeding. The FFA concentration levels in semi-

batch cross and go above those in batch mode at higher durations. After reaching a maximum near the end of feeding, the FFA concentrations decrease gradually as the reactor continues to operate in the batch mode. It is also observed that final concentration levels are quite similar for the two modes.

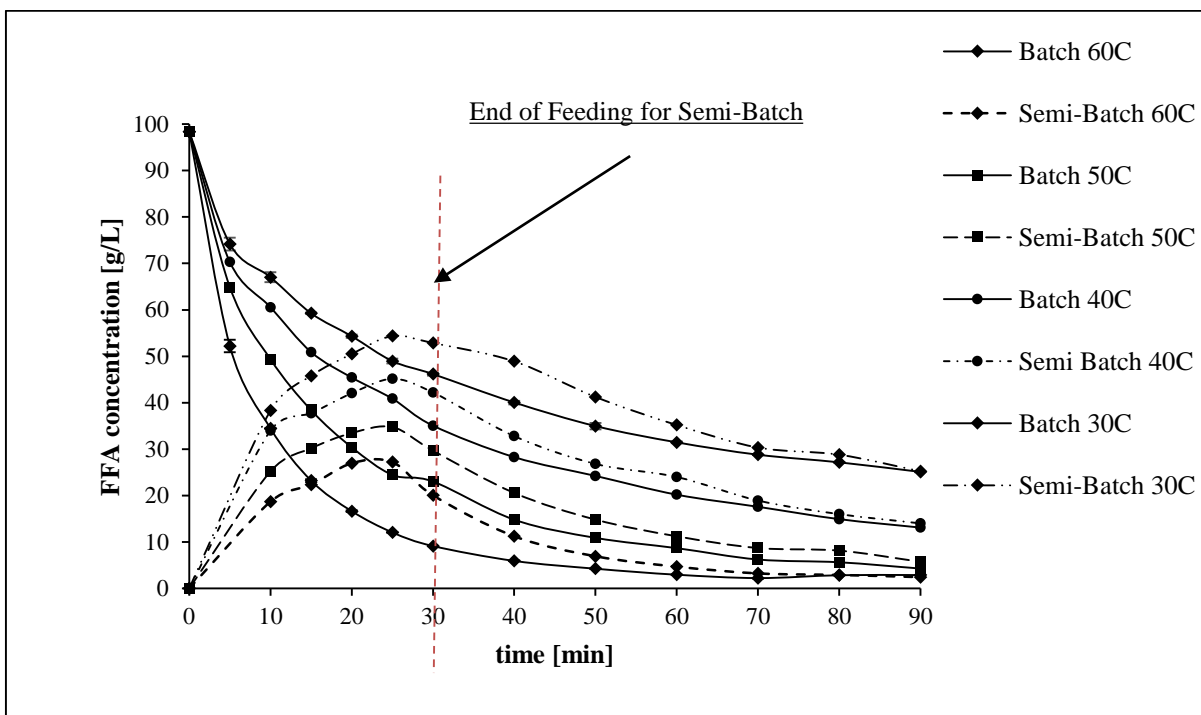


Figure 3-8 FFA Concentration profile [g/L] for Batch and Semi-Batch Mode.

Comparison of FFA conversions with time for the two modes of operations are presented in **Figure 3-9**. It is observed that initial conversion levels are higher with the semi-batch mode, go through a plateau and increase gradually again at the end of gradual feeding. The final conversion levels are quite similar for the two modes.

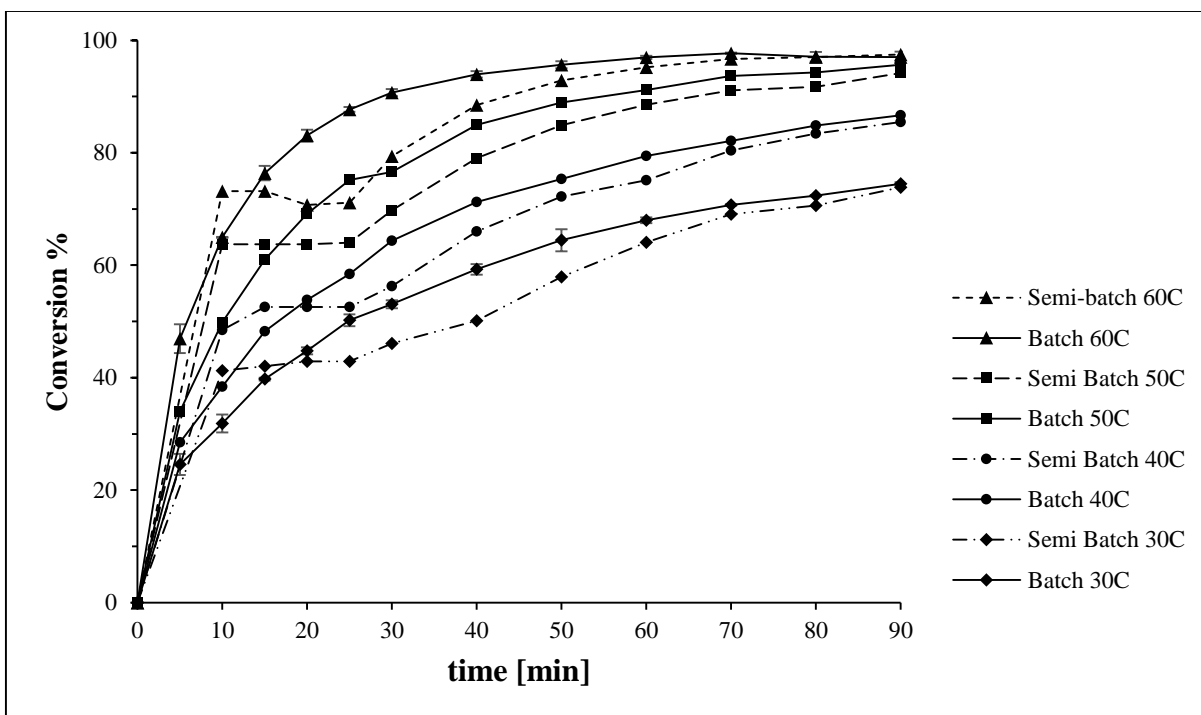


Figure 3-9 FFA Conversion profile [%] for Batch and Semi-Batch Mode

It can therefore be concluded although the two reaction operation modes show different performance at the beginning it becomes insignificant after roughly 30 minutes of reaction. Two curves of conversion of batch and semi-batch modes almost approaches one another showing the same values. The conversion rate at 60°C shows that it is the optimum temperature for the esterification, also as it can be seen from the graph the reaction seems to reach the equilibrium after 60 min for both modes. The final conversion percentages at 90 minutes were 97.50, and 97.05% for semi-batch and batch mode respectively. Taking into account that after 30 min of reaction there is no difference between batch and semi-batch operation mode lets conclude that best parameters for esterification reaction to achieve the highest conversion are 60°C and 60 minutes.

The results of this study contrast with the benefits reported for semi-batch mode of operation for transesterification reaction (methanolysis) in literature studies (Pal, 2011; Pal and Prakash, 2012). It may be pointed out that the two reaction systems (transesterification and esterification) are quite different. A plausible explanation can be that esterification occurs in a single step, while methanolysis follows a three step reaction scheme.

3.4 Mathematical Models

3.4.1 Models for Batch mode

The batch mode experimental data were represented by two models. In first one the reaction was assumed to be pseudo-homogeneous and follows second-order reversible kinetics. On the other hand, the second model assumed the esterification reaction to follow pseudo first-order kinetics, and the apparent reaction order was found to be 1.5.

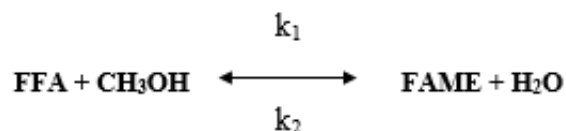
3.4.1.1 First Batch Mode Kinetic Model

In the first model, the mechanism proposed by Su et al. (Su et al., 2008; Su, 2013) was chosen to obtain the kinetic expression. In this approach induced by Aafaqi et al. (Aafaqi et al., 2004) the esterification kinetic model evaluation relies on the following assumptions:

- The rate of the reaction is kinetically controlled
- The rate of auto catalyzed esterification is negligible relative to the catalyzed rate
- The effect of liquid-liquid splitting on the reaction are ignored under intense mixing
- The reaction system is considered as an ideal solution

Under these assumptions, the reaction is assumed to be pseudo-homogeneous and follows second-order reversible kinetics. The second order with respect to FFA was suggested by various authors (Tesser et al., 2009, 2010).

Esterification generic equation is given by:



And the reaction rate of the esterification reaction can be expressed as:

$$r_A = \frac{-dC_{FFA}}{dt} = k_1 \cdot C_{FFA} \cdot C_{MeOH} - k_2 \cdot C_{FAME} \cdot C_{H_2O} \quad (3.3)$$

Where:

k₁: forward reaction rate constant [L.mol⁻¹.min⁻¹]

C_{FFA}: molar concentration of FFAs [mol/L]

C_{MeOH}: molar concentration of methanol [mol/L]

k₂: reverse reaction rate constant [L.mol⁻¹.min⁻¹]

C_{FAME}: molar concentration of fatty acid methyl esters [mol/L]

C_{H₂O}: molar concentration of water [mol/L]

Since the reactants and products concentrations corresponds to FFAs conversion, Eq.3.3 can be further reformulated into the form of Eq.3.4 wherein FFAs conversion is asserted as a dependant variable.

$$\frac{dx}{dt} = k_1 \cdot C_{FFA_i} \cdot \left[(1-x)(\theta-x) - \frac{x^2}{K_e} \right] \quad (3.4)$$

Where:

x: FFAs conversion

k₁: forward reaction rate constant [L.mol⁻¹.min⁻¹]

C_{FFA_i}: initial molar concentration of FFAs [mol/L]

θ: molar ratio of methanol to FFAs

K_e: equilibrium constant

At equilibrium the net rate is equal to zero (dx/dt=0), therefore Eq.3.4 can be rearranged into Eq.3.5 for K_e evaluation:

$$K_e = \frac{k_1}{k_2} = \frac{x_e}{(1-x_e)(\theta-x_e)} \quad (3.5)$$

where **x_e** is FFAs conversion at equilibrium state, it has to be noted that the values of final conversion in experiments were taken as first approximation of equilibrium conversion for the iteration process. Later these values were found to be very close to the calculated equilibrium FFAs conversion values as shown in **Table 3-1**.

Table 3-1 Equilibrium conversion values

Temperature [°C]	Final experiment FFA conversion	Equilibrium conversion
30	0.7448	0.7632
40	0.8667	0.8808
50	0.9565	0.977
60	0.977	0.9922

Once the value of K_e is determined, Eq.3.4 can be further integrated and rearranged as Eq.3.6 (Su et al., 2008).

$$\ln \left[\frac{(-1 - \theta + a_2)x + 2\theta}{(-1 - \theta - a_2)x + 2\theta} \right] = a_2 \cdot k_1 \cdot C_{FFA_i} \cdot t \quad (3.6)$$

Where

θ : molar ratio of methanol to FFA

with:

$$a_2 = [(\theta + 1)^2 - 4a_1\theta]^{1/2} \quad (3.6.a)$$

$$a_1 = 1 - \frac{1}{K_e} \quad (3.6.b)$$

Furthermore, to simplify notation

$$\alpha = \ln \left[\frac{(-1 - \theta + a_2)x + 2\theta}{(-1 - \theta - a_2)x + 2\theta} \right] \quad (3.6.c)$$

$$\beta = \frac{1}{a_2 \cdot C_{FFA_i}} \quad (3.6.d)$$

Then Eq.3.6 reduces to Eq.3.7:

$$\alpha * \beta = k_1 \cdot t \quad (3.7)$$

From the experimental data and determined K_e , the forward reaction rate k_1 can be obtained as the slope of the graph:

$$\alpha * \beta = f(t) \quad (3.7. a)$$

In order to express the variation of FFAs conversion with time, Eq.3.6 can be rearranged into Eq.3.8, as an explicit expression for x:

$$x = \frac{2\theta(e^{a_2 \cdot k_1 \cdot C_{FFA_i} \cdot t} - 1)}{[(-1 - \theta + a_2) - (-1 - \theta + a_2) \cdot e^{a_2 \cdot k_1 \cdot C_{FFA_i} \cdot t}]} \quad (3.8)$$

The determination of the kinetic parameters appearing in Eq. 3.5 and 3.6, conversion at equilibrium x_e and equilibrium constant K_e , was executed by a nonlinear fitting. The parameters were adjusted by a program iteratively until a predefined criterion is satisfied. In our case, the criterion is the minimization of the sum of square errors (SSE) between experimental and calculated FFAs conversion values (Ancheyta et al., 2002):

$$SSE = \sum_{i=1}^{i=n} (y_i - \hat{y}_i)^2 \quad (3.9)$$

The minimization of SSE resulted automatically on the minimization of the root mean square error (RMS), (Tesser et al., 2009) between the calculated and experimental FFAs conversion defined by:

$$RMS = \sqrt{\frac{1}{n} \sum_{i=1}^n (y_i - \hat{y}_i)^2} \quad (3.10)$$

The predictive capability of model was evaluated by the linear correlation coefficient (r^2) defined as the following equation:

$$r^2 = 1 - \frac{\sum_{i=1}^n (y_i - \hat{y}_i)^2}{\sum_{i=1}^n (y_i - \bar{y})^2} \quad (3.11)$$

Where

n: number of samples

y_i: actual experiment data (conversion: x) of the ith sample

\hat{y}_i : model predicted data (conversion: x) of the ith sample

\bar{y}_i : average of all experimental data (conversion: x)

The coefficient r^2 is normalized between 0 and 1, with a high r^2 value validating better correlation between experimental and model predicted value. The plot of experimental FFAs conversion along with model calculated values at different temperatures is shown in **Figure 3-10** where the lines represents the model, also example of calculations are shown in **Appendix-C**. It can be seen from the plot, that the model predicts the experimental data correctly after the first 30minutes. However the data in the first 30minutes are offset, this can be attributed to the effect of viscosity and methanol solubility at this temperature. The high values of r^2 for other temperatures demonstrated that the model predictions were in good agreement with the experimental data this can be confirmed by the model-fitting criterions shown in **Table 3-2**, where r^2 value at all temperatures is roughly 0.95.

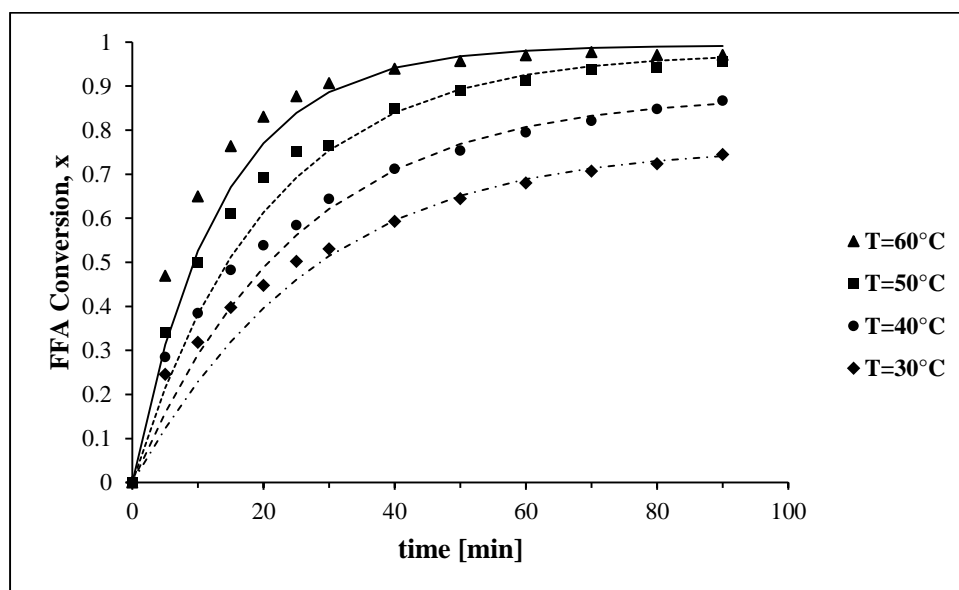


Figure 3-10 FFA conversion vs. time along with the prediction results of the first batch model

Table 3-2 model-fitting statistics for the first batch model

Temperature [°C]	r ²	RMS	SSE
30	0.9414	0.0510	0.0338
40	0.9543	0.0524	0.0356
50	0.9489	0.0614	0.0490
60	0.9426	0.0649	0.0547

3.4.1.2 Estimation of the First Batch Mode model parameter

After determination of the equilibrium constant K_e , the forward rate constant k_1 is determined using equation 3.7.a. The plot of $\alpha.\beta$ against time for all temperature is very close to the origin as shown in **Figure 3-11**. Therefore, the slope of each straight line is used to assess the k_1 values, **Table 3-3** summarizes the rate constants at each temperature.

Table 3-3 estimation of the rate constants for the first batch mode kinetic model

T [K]	K_e	k_1 [L.mol ⁻¹ .min ⁻¹]
303.15	0.1279	0.0038
313.15	0.3403	0.005
323.15	2.176	0.007
333.15	6.6193	0.0109

It has to be noted that the equilibrium rate constant, as well as the equilibrium conversion increased with temperature owing to the endothermic nature of the esterification reaction (Aafaqi et al., 2004).

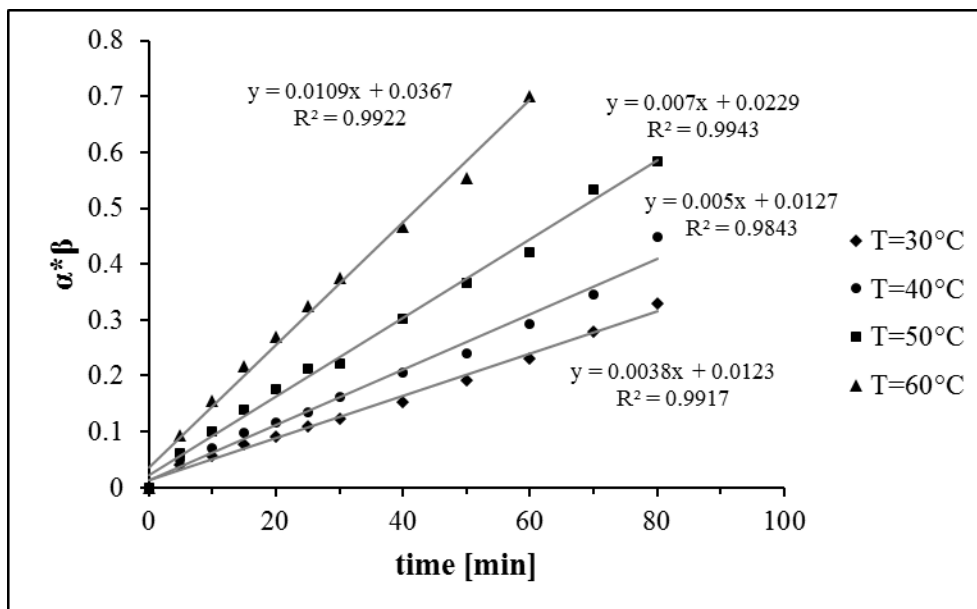


Figure 3-11 Determination of k_1 values for First batch mode model

The temperature dependency of kinetic constant is described by Arrhenius law:

$$k_1 = k_{1,0} \exp\left(\frac{-E_1}{RT}\right) \quad (3.12)$$

$$K_e = K_{e,0} \exp\left(\frac{-\Delta h}{RT}\right) \quad (3.13)$$

Where:

$K_{e,0}$: frequency (pre-exponential) factor for equilibrium rate constant;

$k_{1,0}$: frequency (pre-exponential) factor for forward rate constant;

E_1 : activation energy of forward reaction, [J/mol];

Δh : molar heat of the reaction, [J/mol];

T : temperature, [K];

R : universal gas constant, [8.314 J/mol. K].

In order to find the pre-exponential factor, as well as the activation energy for esterification reaction. The Arrhenius equation is linearized in the following form:

$$\ln k = \ln k_0 - \frac{E}{RT} \quad (3.14)$$

Then $\ln k_1$ and $\ln K_e$ are plotted as a function of reciprocal temperature $(1/RT) * 10^3$, as shown in **Figure 3-12**.

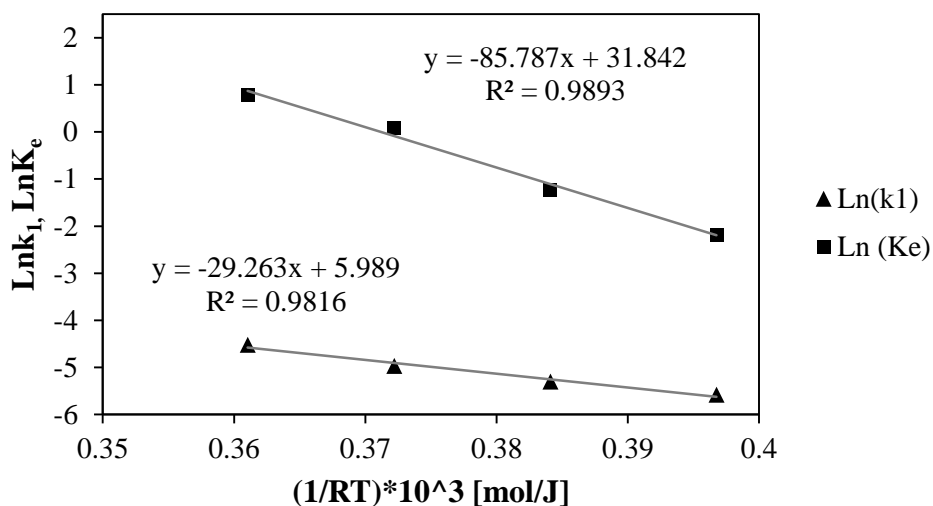


Figure 3-12 Arrhenius Van't Hoff plot for First batch mode model

The results for the first batch mode model are as shown in **Table 3-4**:

Table 3-4 Arrhenius equation parameters for the first batch mode model

<i>Frequency factor: $k_{1,0}$</i>	399.015
<i>Frequency factor: $K_{e,0}$</i>	$6.74 * 10^{13}$
<i>Activation Energy: E_1 [kJ/mol]</i>	29.26
<i>Molar heat of the reaction: Δh [kJ/mol]</i>	85.78

3.4.1.3 Comparison of predicted and experimental data

After determining the kinetic parameters, the goodness- of- fit of the experimental data to the proposed model was evaluated by comparing the experimental conversion values with the ones predicted by the model. The plot generated can be ascertained in **Figure 3-13**, where the slope of the solid line is equal to unity. It was found that 73% of the data were predicted with errors less than 10%. These model prediction error values are comparable with the ones mentioned in literature. For instance (Berrios et al., 2007) obtained 75% reproducibility at 10% error margin, while (Chai et al., 2014) got 90% reproducibility at 15% error margin.

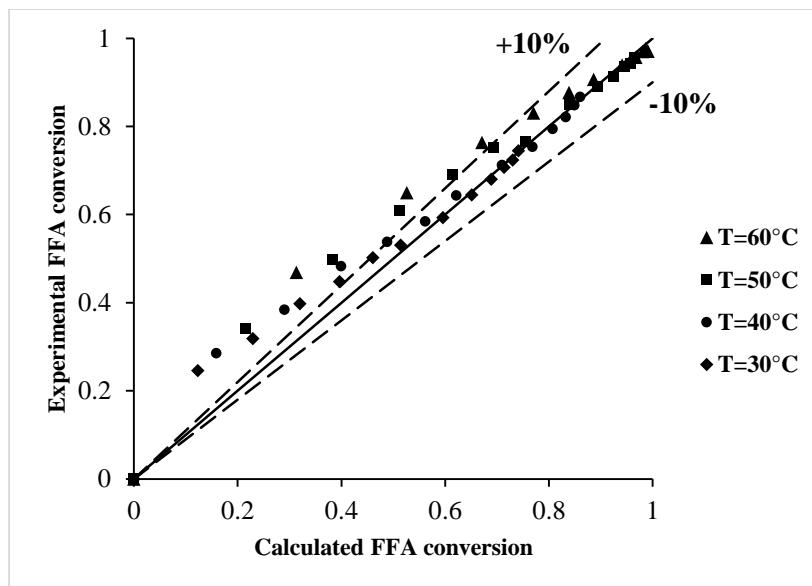


Figure 3-13 Experimental versus. Calculated FFA conversion for the First Batch mode catalyst model

3.4.1.4 Second Batch Mode Kinetic Model

Analogously, to the first model, the second esterification kinetic model evaluation relies on the following assumptions:

- The rate of the reaction is kinetically controlled.
- The rate of the non-catalyzed esterification is negligible relative to the catalyzed reaction.
- The chemical reaction took place in oil phase.
- The mole ratio of methanol/FFA was high enough to maintain a constant methanol concentration through the process.

Under these conditions, the FFA esterification reaction is assumed to be reversible heterogeneous process. Therefore, the forward reaction is pseudo-homogeneous first order and reverse reaction is second order, according to Berrios (Berrios et al., 2007). Rate expression can be written as:

$$-\frac{dC_{FFA}}{dt} = k_1 C_{FFA} - k_2 C_{FAME} C_{water} \quad (3.15)$$

Sendzikiene and Berrios (Sendzikiene et al., 2004; Berrios et al., 2007; Chai et al., 2014) reports that rate of reverse reaction (and k_2 respectively) is negligible comparing to forward reaction.

Hence, second term from equation can be excluded. Especially this is true for initial times of reaction when there is no water yet in reaction mixture, as the components used in the reaction are anhydrous. Furthermore, Sendzikiene noticed that the apparent (observed) kinetic parameters changed during the reaction time. For instance, at 60°C the reaction rate constant changed from 0.0154 to 0.0045[min^{-1}] and reaction order changed from 0.69 to 1.5. Overall reaction rate might be written as homogeneous pseudo-first order to the power n:

$$r_A = -\frac{dC_{FFA}}{dt} = k_1 * (C_{FFA})^n \quad (3.16)$$

Or in finite differences:

$$r_A = -\frac{C_{FFA}^i - C_{FFA}^{i+1}}{t_i - t_{i+1}} = k_1 * (C_{FFA}^i)^n \quad (3.17)$$

Where

n: reaction order

C_{FFA}^i : actual experiment data of FFA concentration for the ith sample

C_{FFA}^{i+1} : actual experiment data of FFA concentration for the (ith+1) sample

k₁: apparent forward reaction rate constant for pseudo-first order

t_i: actual experiment data of time for the ith sample

t_{i+1}: actual experiment data of time for the (ith+1) sample

Since the reactants and products concentrations corresponds to FFAs conversion where:

$$C_{FFA} = C_{FFA_i} * (1 - x) \quad (3.18)$$

Therefore Eq.3.16 can be further reformulated into the form of Eq.3.19 wherein FFAs conversion is asserted as a dependant variable.

$$\frac{dx}{dt} = k_1 * (C_{FFA_i})^{n-1} * (1 - x)^n \quad (3.19)$$

Where:

x: FFAs conversion

k₁: apparent forward reaction rate constant for pseudo-first order

C_{FFA}: molar concentration of FFAs [mol/L]

C_{FFAi}: initial molar concentration of FFAs [mol/L]

n: reaction order

t: time

In order to evaluate the reaction order, the left side of Eq.3.17 was used to plot: $r_A=f(t)$, and obtain a curve fit in the form: $r_A=a*t^b$, the corresponding plots at different temperature are shown in **Figure 3-14**. Then the fitting equation was used to determine the reaction rate at different time. Additionally, it has to be noted that the first point for the fitting equation on each graph from **Figure 3-14** has been taken as the experimental rate calculated by Eq.3.17.

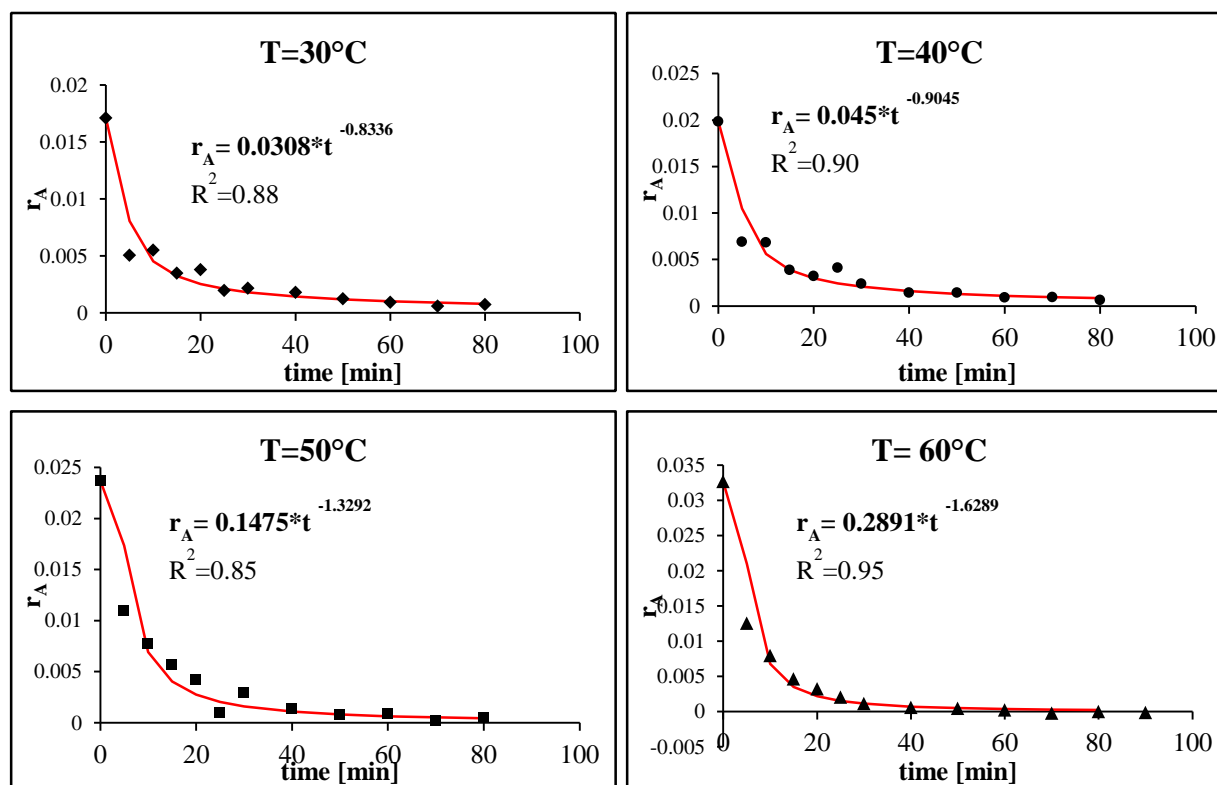


Figure 3-14 Fitting curve for r_A versus. **time** at different temperatures

Subsequently the equation 3.16 was linearized in the form of:

$$\ln(r_A) = \ln(k_1) + n * \ln(C_{FFA}) \quad (3.20)$$

Then by plotting the graph of $\ln(r_A)$ as a function of $\ln(C_{FFA})$ as shown in **Figure 3-15**, the slope of the curve represented the apparent equation order at each temperature. Afterward the average of the reaction order (1.485) as shown in **Table 3-5** was rounded to 1.5, and taken as the overall reaction order.

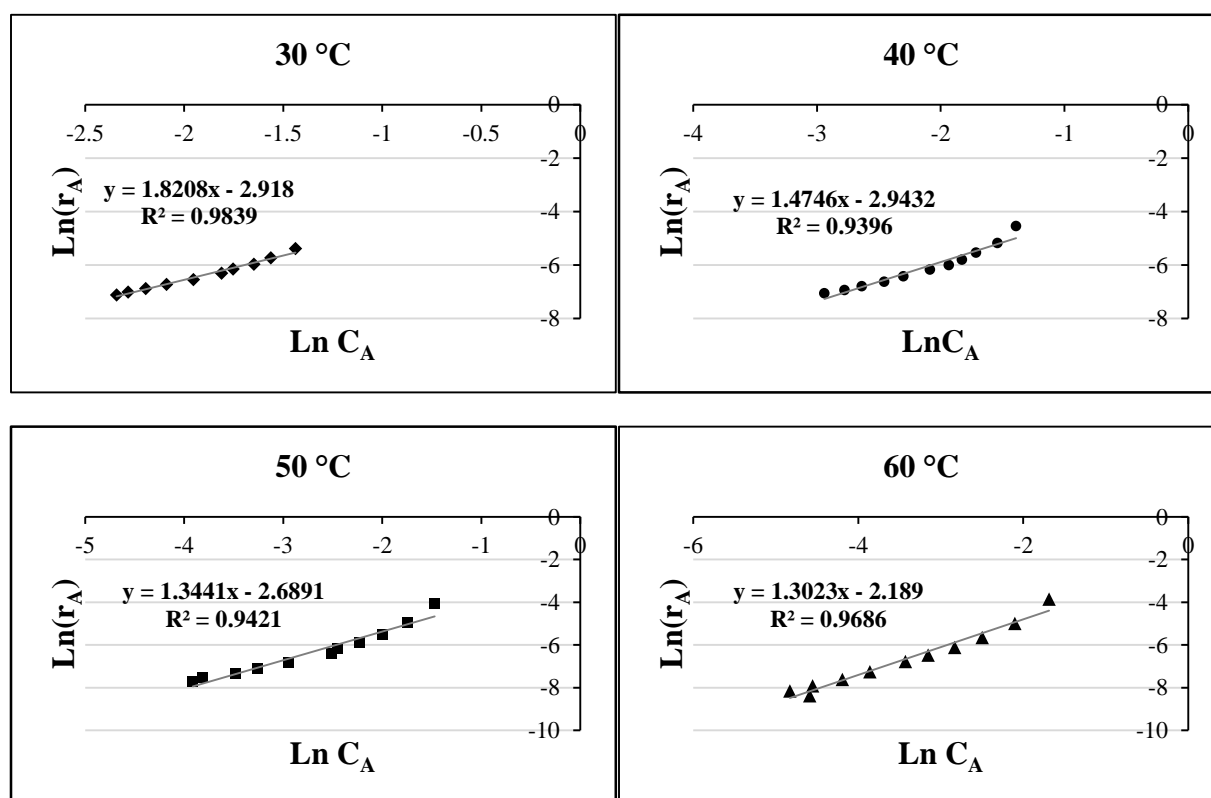


Figure 3-15 Graph of $\ln(r_A)$ versus. $\ln(C_{FFA})$ at different temperatures

Table 3-5 Estimation of the reaction order

T [°C]	n (apparent reaction order)
30	1.8208
40	1.4746
50	1.3441
60	1.3023
Average	1.4854

At this point Eq. 3.16 can be rewritten as (3.16.a):

$$r_A = -\frac{dC_{FFA}}{dt} = k_1 \cdot C_{FFA}^{1.5} \quad (3.16.a)$$

For sake of notation simplification, the FFAs concentration C_{FFA} will be noted as C_A , the FFAs conversion x will be noted as x_A , the FFAs initial concentration C_{FFAi} will be noted as C_{A0} for the following derivation, where equation (3.16.a) will be combined with equation 3.18 to give **Eq.3.16. b**:

$$C_{A0} \cdot \frac{dx_A}{dt} = k_1 \cdot C_{A0}^{1.5} \cdot (1 - x_A)^{1.5} \quad (3.16.b)$$

$$\Rightarrow \int_0^{x_A} \frac{dx_A}{(1 - x_A)^{1.5}} = k_1 \cdot C_{A0}^{0.5} \cdot \int_0^t dt$$

$$\Rightarrow \frac{(1 - x_A)^{-0.5}}{0.5} - \frac{1}{0.5} = k_1 \cdot C_{A0}^{0.5} \cdot t$$

$$\Rightarrow (1 - x_A)^{-1} = \left[1 + \frac{1}{2} \cdot k_1 \cdot C_{A0}^{0.5} \cdot t \right]^2 \quad (3.21)$$

By taking:

$$\alpha = \frac{1}{2} \cdot C_{A0}^{0.5} \quad (3.21.a)$$

The Equation.3.21 after rearrangement becomes:

$$x_A = 1 - \frac{1}{(1 + \alpha \cdot k_1 \cdot t)^2} \quad (3.22)$$

By taking the k_1 as the exponentials of the values obtained from the intercepts of the graphs in **Figure 3-15** as a first approximation. The determination of the kinetic parameter k_1 appearing in **Equation-3.22**, was executed by a nonlinear fitting. The k_1 value was adjusted by a program iteratively until a predefined criterion was satisfied. In our case, the criterion is the minimization of the sum of square errors (SSE) as previously defined in **Equation-3.9** between experimental and calculated FFAs conversion values (Ancheyta et al., 2002):

The minimization of SSE resulted automatically on the minimization of the quadratic mean square error (RMS), (Tesser et al., 2009) between the calculated and experimental FFAs conversion defined by **Equation-3.10**. The predictive capability of model was evaluated by the linear correlation coefficient (r^2) defined by **Equation-3.11**.

The plot of experimental FFAs conversion along with model calculated values at different temperatures is shown in **Figure 3-16** where the lines represents the model where the lines represents the model, also example of calculations are shown in **Appendix-D**. It can be seen from the plot, that the model predicts the experimental data very well except at 30°C where the $r^2=0.9292$, this can be attributed to the effect of viscosity and methanol solubility at this temperature. The high values of r^2 for other temperatures demonstrated that the model predictions were in good agreement with the experimental data, this can be confirmed by the model-fitting criterions shown in **Table 3-6**.

Table 3-6 model-fitting statistics for the second batch model

Temperature [°C]	r^2	RMS	SSE
30	0.9292	0.0560	0.0408
40	0.9794	0.0352	0.0161
50	0.9979	0.0126	0.0020
60	0.9993	0.0070	0.0006

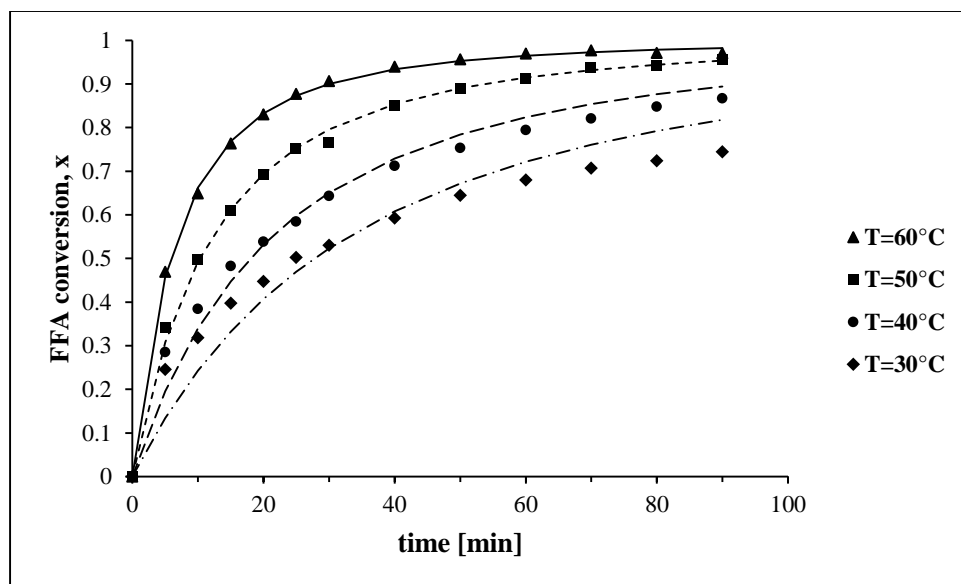


Figure 3-16 conversion vs. time along with the prediction results of the second batch model

3.4.1.5 Estimation of the model parameter

After determination of the forward reaction rate constant k_1 , which is the apparent rate of reaction the true rate constant $k_{1\text{true}}$ is determined using equation 3.23:

$$k_{1app} = k_{1true} * C_{MeOH_i} \quad (3.23)$$

Where:

$k_{1app} = k_1$: apparent forward reaction rate constant for pseudo-first order

k_{1true} : true forward reaction rate constant for second order

C_{MeOH_i} : initial molar concentration of Methanol [mol/L]

Since:

$$C_{MeOH_i} = 20 * C_{FFA_i} \quad (3.23a)$$

Then equation 3.23 becomes:

$$k_{1true} = \frac{k_{1app}}{20 * C_{FFA_i}} \quad (3.24)$$

The values of $k_1 = k_{1app}$ and k_{1true} are presented in **Table 3-7**.

Table 3-7 Values of $k_{1\text{app}}$ and $k_{1\text{true}}$ for the second batch model

$k_{1\text{app}}$	$k_{1\text{true}}$	$\ln k_{1\text{app}}$	$\ln k_{1\text{true}}$	$(1/TR) * 1000$
$[\text{L}^{1/2} \cdot \text{min}^{-1} \cdot \text{mol}^{-1/2}]$	$[\text{L}^{3/2} \cdot \text{min}^{-1} \cdot \text{mol}^{-3/2}]$			$[\text{mol/J}]$
0.05059	0.0073	-2.9840	-4.9246	0.3968
0.07814	0.0112	-2.5493	-4.4899	0.3841
0.13694	0.0197	-1.9882	-3.9288	0.3722
0.24426	0.0351	-1.4095	-3.3501	0.3610

These values were used to generate the graphs for Arrhenius equation (**Eq.3.12**) in the linearized form (**Eq.3.14**). Then plot $\ln k_{1\text{app}}$ and $\ln k_{1\text{true}}$ as a function of reciprocal temperature $(1/RT) * 10^3$, as shown in **Figure 3-17**.

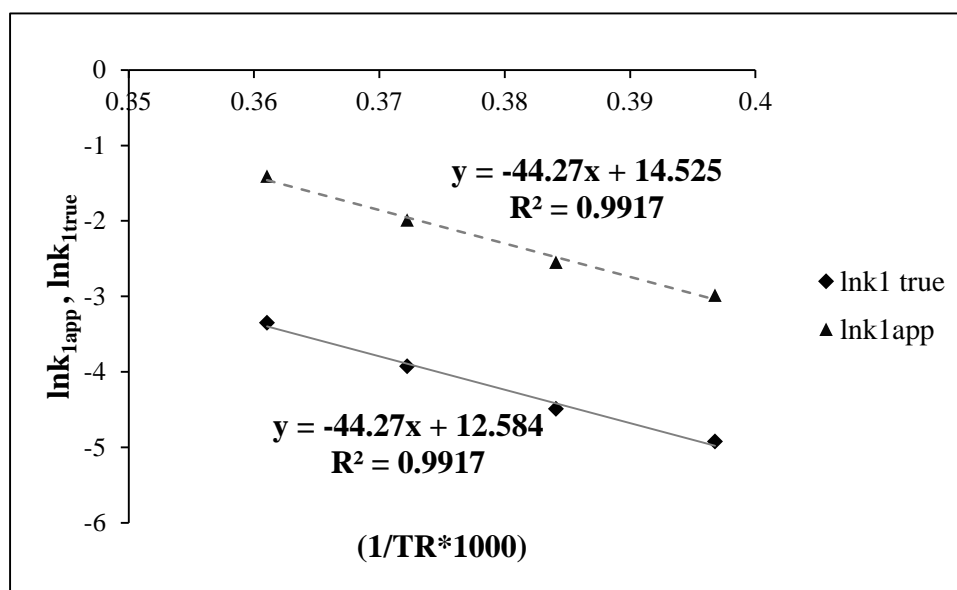


Figure 3-17 Determination of kinetic constants values for Second batch mode model
Consequently, the obtained values for the pre-exponential and activation energy for esterification reaction, are summarized in **Table 3-8**:

Table 3-8 Arrhenius Equation parameters for the second batch mode model

<i>Frequency factor: $k_{1,0\text{app}}$</i>	$2.032 * 10^6$
<i>Frequency factor: $k_{1,0\text{true}}$</i>	$2.91 * 10^5$
<i>Activation Energy: E_1 [kJ/mol]</i>	44.27

3.4.1.6 Comparison of predicted and experimental data

After determining the kinetic parameters, the goodness-of-fit of the experimental data to the proposed model was evaluated by comparing the experimental conversion values with the ones predicted by the model. The plot generated can be ascertained in **Figure 3-18**, where the slope of the solid line is equal to unity. It was found that 90% of the data were predicted with errors less than 10%, this value goes even higher at 95% where the values at 30°C are not considered. These model prediction error values are comparable with the ones mentioned in literature. For instance (Berrios et al., 2007) obtained 75% reproducibility at 10% error margin, while (Chai et al., 2014) got 90% reproducibility at 15% error margin.

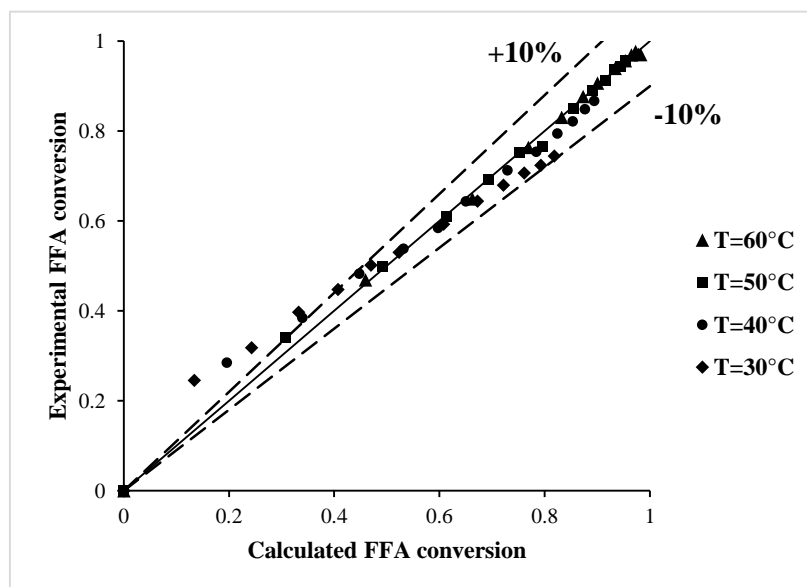


Figure 3-18 Experimental Versus. Calculated FFA conversion for the Second Batch mode catalyst model

3.4.1.7 Comparison with literature

The obtained values of the pre-exponential factor and activation energy obtained from the second batch mode kinetic model were compared with literature articles as shown in **Table 3-9**:

Table 3-9 Comparison of the kinetics parameters obtained by the second batch kinetic model with literature

Literature	Marchetti	Sendzikiene	Berrios	Su	Chai	This study
Reference	(Marchetti et al., 2010)	(Sendzikiene et al., 2004)	(Berrios et al., 2007)	(Su, 2013)	(Chai et al., 2014)	Second Model
Properties						
Acid type	Sulfuric	Sulfuric	Sulfuric	hydrochloric	Sulfuric	Sulfuric
Acid [%]	1.03-5.14	1-5	5 and 10	0.1-1M	5-15	5
Alcohol type	Ethanol	Methanol	Methanol	Methanol	Methanol	Methanol
FFA type	Oleic acid	Oleic acid	Oleic acid	Soybean, enzyme hydrolyzed	Mix, mostly Oleic	Oleic acid
Initial FFA%	10.68	up to 33	2.5-3.5	100	5	15
Alcohol/FFA molar ratio	6.1	-	20-240	10	20-60	20
Oil type	Sunflower	rapeseed	mix	Soybean	Waste cooking oil (WCO)	Canola
Temperature [°C]	35-55	20-60	30-60	30-70	35-65	30-60
Reaction time [min]	250	180	120	350	120	90
Activation energy of the forward reaction [kJ/mol]	23.137	13.3	50.745 at 5% acid conc.	44.86	20.7-45.9	44.27
Pre-exponential factor of the forward reaction	0.058 [L/kg. s]	1.27	$2.869 \cdot 10^6$ [5%]	$2.869 \cdot 10^6$ [L/mol.min]	0.043- $1.79 \cdot 10^5$	$2.03 \cdot 10^6$
Activation energy of the backward reaction	-	-	31.007[5%]	-		
Pre-exponential factor of the backward reaction	-	-	37.068[5%]	-		

3.4.2 Model for Semi-Batch mode

As stated previously the semi-batch mode didn't procure significant advantage in term of conversion compared to batch. Nevertheless, an attempt has been made to model this system as the batch mode is considered to be a special case of semi-batch.

The reaction system was modeled taking into account that the reactor volume varies with time. Also the concentration of FFA is varying as a function of feed rate and esterification reaction rate during this phase prior to batch made after the end of feeding. The reactor was initially filled with the required amount of methanol and catalyst.

The mass balance for FFA inside the reactor can be expressed as follow:

$$\begin{aligned} &(\textit{input rate into reactor}) - (\textit{output rate from reactor}) + \\ &(\textit{rate of production within the reactor}) = (\textit{rate of accumulation inside the reactor}) \end{aligned}$$

The above equation can be expressed in term of FFA mass as follows:

$$Q \cdot C_f - 0 + rV_R = \frac{dm_{FFA}}{dt} \quad (3.25)$$

Where:

C_f: FFA concentration in the feed [g/L]

C_{FFA}: FFA concentration at any time [g/L]

Q: feed rate [L/min]

V_R: Volume of the reactor at any time [L]

m_{FFA}: mass of FFA [g]

r: reaction rate [g/L.min]

t: time

Since:

$$V_R = V_0 + Q \cdot t \quad (3.26)$$

And:

$$m_{FFA} = (V_0 + Q \cdot t) * C_{FFA} \quad (3.27)$$

Equation 3.26 can be written:

$$Q \cdot C_f + r(V_0 + Q \cdot t) = \frac{d[(V_0 + Q \cdot t) * C_{FFA}]}{dt} \quad (3.28)$$

$$\Rightarrow Q \cdot C_f + r(V_0 + Q \cdot t) = V_0 \frac{dC_{FFA}}{dt} + Q \cdot C_{FFA} + Q \cdot t \cdot \frac{dC_{FFA}}{dt} \quad (3.28.a)$$

After arrangement Equation 3.28 becomes:

$$r = k_1 \cdot C_{FFA}^{1.5} = \frac{dC_{FFA}}{dt} + Q \cdot \frac{(C_{FFA} - C_f)}{(V_0 + Q \cdot t)} \quad (3.29)$$

Where:

V₀: Reactor volume at t=0, [L]

C_{FFA}: FFA concentration at any time [g/L]

k₁: forward rate of reaction

Q: feed rate [L/min]

r: reaction rate [g/L.min]

t: time

Also the conversion of FFA at any time is given by:

$$x_{FFA}(t) = \frac{\text{mass of FFA fed } (t) - \text{mass of FFA inside reactor } (t)}{\text{mass of FFA fed } (t)}$$

Therefore:

$$C_{FFA}(t) = \frac{Q \cdot C_f \cdot t \cdot (1 - x_{FFA})}{(V_0 + Q \cdot t)} \quad (3.30)$$

The **Equation-3.29** is an initial value problem with $C_{FFA}=0$ at $t=0$. The equation is stiff as the concentration is a function of both reaction rate and pump feed into reactor. We were unable to solve corresponding least square problem with any available solver in Maple in order to estimate kinetic parameters using data for the entire experimental run.

The kinetic constants obtained in the second batch model were applied to **Equation-3.29** only for the time when feed of FFA to reactor was over. This is equivalent to batch mode in **Equation-3.22**. The obtained solution is shown in **Figure 3-19**. We can see a close match between experimental and calculated data point to the right of a dashed line. Therefore, we can assure with confidence the adequacy of found kinetic parameters.

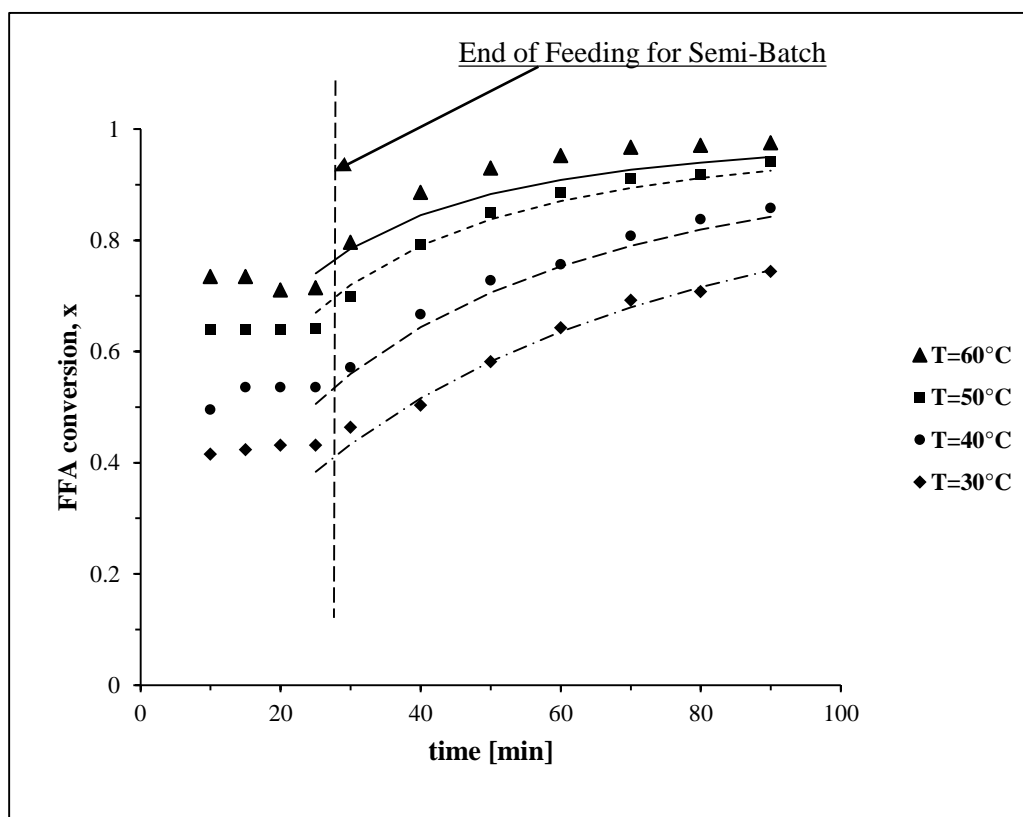


Figure 3-19 FFA conversion versus time for semi-batch mode.

3.5 Conclusions

Effects of temperature, reaction time and mixing modes were investigated for esterification reaction using methanol and homogeneous catalyst H_2SO_4 , to convert FFA in feedstock to methylesters. The results show that temperature of 60°C and reaction time of 60 minutes can provide close to 97% conversion of FFA, corresponding to 0.45wt.% that is up to standard concentration. At lower temperatures reaction time required for similar conversion is significantly higher which can lead to unacceptably lower production rates and lower yields.

The conversion obtained with semi-batch mode of operation is similar compared to batch. This contrasts with the benefits obtained from this mode of operation for transesterification (methanolysis) found previously by (Pal, 2011; Pal and Prakash, 2012). A plausible explanation can be that esterification occurs in a single step, while methanolysis follows a three step reaction scheme.

Two kinetic models have been proposed to predict the experimental data, and estimates of kinetic parameters for the esterification reaction are presented.

References

Aafaqi, R.; Mohamed, A. R.; Bhatia, S. Kinetics of Esterification of Palmitic Acid with Isopropanol Using P-Toluene Sulfonic Acid and Zinc Ethanoate Supported over Silica Gel as Catalysts. *J. Chem. Technol. Biotechnol.* **2004**, *79* (10), 1127–1134.

Ancheyta, J.; Angeles, M. J.; Macias, M. J.; Marroquin, G.; Morales, R. Changes in Apparent Reaction Order and Activation Energy in the Hydrodesulfurization of Real Feedstocks. *Energy and Fuels* **2002**, *16* (1), 189–193.

Atadashi, I. M.; Aroua, M. K.; Abdul Aziz, a. R.; Sulaiman, N. M. N. Production of Biodiesel Using High Free Fatty Acid Feedstocks. *Renew. Sustain. Energy Rev.* **2012**, *16* (5), 3275–3285.

Berchmans, H. J.; Hirata, S. Biodiesel Production from Crude Jatropha Curcas L. Seed Oil with a High Content of Free Fatty Acids. *Bioresour. Technol.* **2008**, *99* (6), 1716–1721.

Berrios, M.; Siles, J.; Martin, M.; Martin, A. A Kinetic Study of the Esterification of Free Fatty Acids (FFA) in Sunflower Oil. *Fuel* **2007**, *86* (15), 2383–2388.

Canakci, M.; Van Gerpen, J. Biodiesel Production Via Acid Catalysis. *Trans. ASAE (American Soc. Agric. Eng.* **1999**, *42* (1984), 1203–1210.

Canakci, M.; Gerpen, J. Van. Biodiesel Production from Oils and Fats with High Free Fatty Acids. *Trans. ASAE* **2001**, *44* (6), 1429–1436.

Chai, M.; Tu, Q.; Lu, M.; Yang, Y. J. Esterification Pretreatment of Free Fatty Acid in Biodiesel Production , from Laboratory to Industry. *Fuel Process. Technol.* **2014**, *125*, 106–113.

Coupard, V.; Bournay, L.; Toth, E.; Maury, S. United States Patent:Process for Pretreatment of Vegetable Oils by Heterogeneous Catalysis of the Esterification of Fatty Acids. US9234158 B2, 2014.

Demirbas, A. Biodiesel for Future Transportation Energy Needs. *Energy Sources, Part A Recover. Util. Environ. Eff.* **2010**, *32* (September 2013), 1490–1508.

Feng, Y.; Zhang, A.; Li, J.; He, B. A Continuous Process for Biodiesel Production in a Fixed Bed Reactor Packed with Cation-Exchange Resin as Heterogeneous Catalyst. *Bioresour. Technol.* **2011**, *102* (3), 3607–3609.

Fu, J.; Chen, L.; Lv, P.; Yang, L.; Yuan, Z. Free Fatty Acids Esterification for Biodiesel Production Using Self-Synthesized Macroporous Cation Exchange Resin as Solid Acid Catalyst. *Fuel* **2015**, *154*, 1–8.

Van Gerpen, J. Biodiesel Processing and Production. *Fuel Process. Technol.* **2005**, *86*, 1097–1107.

Ghadge, S. V.; Raheman, H. Biodiesel Production from Mahua (*Madhuca Indica*) Oil Having High Free Fatty Acids. *Biomass and Bioenergy* **2005**, *28* (6), 601–605.

Jeromin, L.; Peukert, E.; Wollmann, G. United States Patent: Process for the Pre-Esterification of Free Fatty Acids in Fats and Oils. 4,698,186, 1987.

Johnson, M. esterification reaction <http://davyprotech.com/what-we-do/licensed-processes-and-core-technologies/licensed-processes/biodiesel/specification/>.

Koh, A. Two-Step Biodiesel Production Using Supercritical Methanol and Ethanol, University of Iowa, 2011.

Konwar, L. J.; Das, R.; Thakur, A. J.; Salminen, E.; Mäki-Arvela, P.; Kumar, N.; Mikkola, J. P.; Deka, D. Biodiesel Production from Acid Oils Using Sulfonated Carbon Catalyst Derived from Oil-Cake Waste. *J. Mol. Catal. A Chem.* **2014**, *388–389* (September), 167–176.

Kulkarni, M. G.; Dalai, A. K. Waste Cooking Oil - An Economical Source for Biodiesel: A Review. *Ind. Eng. Chem. Res.* **2006**, *45*, 2901–2913.

Leung, D. Y. C.; Wu, X.; Leung, M. K. H. A Review on Biodiesel Production Using Catalyzed Transesterification. *Appl. Energy* **2010**, *87* (4), 1083–1095.

Lotero, E.; Liu, Y.; Lopez, D. E.; Suwannakarn, K.; Bruce, D. a.; Goodwin, J. G. Synthesis of Biodiesel via Acid Catalysis. *Ind. Eng. Chem. Res.* **2005**, *44* (14), 5353–5363.

Ma, F.; Hanna, M. A. Biodiesel Production : A Review. **1999**, *70*, 1–15.

Marchetti, J. M.; Pedernera, M. N.; Schbib, N. S. Production of Biodiesel from Acid Oil Using Sulfuric Acid as Catalyst: Kinetics Study. *Int. J. Low-Carbon Technol.* **2010**, *6* (1), 38–43.

Meher, L.; Vidyasagar, D.; Naik, S. Technical Aspects of Biodiesel Production by Transesterification—a Review. *Renew. Sustain. Energy Rev.* **2006**, *10* (3), 248–268.

Moser, B. Biodiesel Production, Properties, and Feedstocks. *Biofuels* **2011**, No. March, 285–347.

Naik, M.; Meher, L. C.; Naik, S. N.; Das, L. M. Production of Biodiesel from High Free Fatty Acid Karanja (*Pongamia Pinnata*) Oil. *Biomass and Bioenergy* **2008**, *32* (4), 354–357.

Pal, K. Investigations of Transesterification of Canola Oil with Methanol and Ethanol for a New Efficient Method of Biodiesel Production. PhD Thesis, University of Western Ontario, 2011.

Pal, K. D.; Prakash, A. New Cost-Effective Method for Conversion of Vegetable Oil to Biodiesel. *Bioresour. Technol.* **2012**, *121*, 13–18.

Robles-Medina, A.; González-Moreno, P. A.; Esteban-Cerdán, L.; Molina-Grima, E. Biocatalysis: Towards Ever Greener Biodiesel Production. *Biotechnol. Adv.* **2009**, *27* (4), 398–408.

Rukunudin, I. H.; White, P. J.; Bern, C. J.; Bailey, T. B. A Modified Method for Determining Free Fatty Acids from Small Soybean Oil Sample Sizes. *J. Am. Oil Chem. Soc.* **1998**, *75* (5), 563–568.

Santori, G.; Di Nicola, G.; Moglie, M.; Polonara, F. A Review Analyzing the Industrial Biodiesel Production Practice Starting from Vegetable Oil Refining. *Appl. Energy* **2012**, *92*, 109–132.

Sawangkeaw, R.; Bunyakiat, K.; Ngamprasertsith, S. A Review of Laboratory-Scale Research on Lipid Conversion to Biodiesel with Supercritical Methanol (2001-2009). *J. Supercrit. Fluids* **2010**, *55* (1), 1–13.

Sendzikiene, E.; Makareviciene, V.; Janulis, P.; Kitrys, S. Kinetics of Free Fatty Acids Esterification with Methanol in the Production of Biodiesel Fuel. *Eur. J. Lipid Sci. Technol.* **2004**, *106* (12), 831–836.

Su, C.-H. Kinetic Study of Free Fatty Acid Esterification Reaction Catalyzed by Recoverable and Reusable Hydrochloric Acid. *Bioresour. Technol.* **2013**, *130*, 522–528.

Su, C.-H.; Fu, C.-C.; Gomes, J.; Chu, I.-M.; Wu, W.-T. A Heterogeneous Acid-Catalyzed Process for Biodiesel Production from Enzyme Hydrolyzed Fatty Acids. *AIChE J.* **2008**, *54* (No.1), 327–336.

Tesser, R.; Casale, L.; Verde, D.; Di Serio, M.; Santacesaria, E. Kinetics of Free Fatty Acids Esterification: Batch and Loop Reactor Modeling. *Chem. Eng. J.* **2009**, *154* (1–3), 25–33.

Tesser, R.; Casale, L.; Verde, D.; Di Serio, M.; Santacesaria, E. Kinetics and Modeling of Fatty Acids Esterification on Acid Exchange Resins. *Chem. Eng. J.* **2010**, *157* (2–3), 539–550.

Zullaikah, S.; Lai, C.-C.; Vali, S. R.; Ju, Y.-H. A Two-Step Acid-Catalyzed Process for the Production of Biodiesel from Rice Bran Oil. *Bioresour. Technol.* **2005**, *96* (17), 1889–1896.

CHAPTER 4

4 Esterification Reaction using Heterogeneous catalyst

4.1 Introduction

Biodiesel is a nonpetroleum-based fuel that consists of alkyl esters derived from either the transesterification of triglycerides (TGs) or the esterification of free fatty acids (FFAs) with low molecular weight alcohols. It can be used as an alternative in diesel fuel or fuel blends as it has similar flow and combustion properties to petroleum based diesel (Kinast, 2003). As a point of comparison, pure biodiesel (B100) releases about 90% of the energy that normal diesel does, and hence, its expected engine performance is nearly the same in terms of engine torque and horsepower. Biodiesel has many advantages over petroleum based diesel. It is bio-degradable, non-toxic, and has a higher flash point than petroleum based diesel. Low emission profile, oxygen content of 10-11% add to the significant advantages of using biodiesel (Lotero et al., 2005). Biodiesel is an environmentally friendly fuel since it provides a solution to recycle carbon dioxide and it does not contribute to global warming.

However, cost of producing biodiesel is not economically competitive with petroleum-based fuel mostly due to high cost of feedstock which are often edible-grade refined oils. Economic feasibility of biodiesel could be improved if low cost feedstock such as waste cooking oil (WCO), animal fats, and non-edible oils are used for production. However these low cost feedstock have high free fatty acid (FFA) which reacts with base to produce soap and water inhibiting typical alkaline transesterification (Bournay et al., 2005; Coupard et al., 2014, 2016; Lee et al., 2014; Boz et al., 2015) The soap formation creates a difficult problem of product separation, and catalyst consumption which ultimately reduce biodiesel yield.

In order to avoid this problem high FFA feedstock is pretreated by esterification of FFA to reduce their concentration in the transesterification inlet stream to a standard level below 0.5% (w/w) (Melero et al., 2009). Esterification offers an efficient approach for fatty acids removal and at the same time it leads to improved product yield.

As presented in **Figure 4-1**, free fatty acids (FFAs) reacts with methanol in presence of acid catalyst to produce methyl ester (biodiesel) and water. Then the pretreated oil can be transesterified with an alkali catalyst to convert the triglycerides to methylesters.



Figure 4-1 Esterification reaction to produce biodiesel (Johnson, 2016)

An economic assessment of different biodiesel production processes (homogeneous alkali and acid catalysts, heterogeneous acid catalyst, and supercritical) has been undergone by (West et al., 2008). The study revealed that heterogeneous solid acid catalyzed process is advantageous over others. As it requires the lowest total capital investment and manufacturing costs, and had the only positive after tax rate-of-return.

Other advantages from the use of heterogeneous catalyst for a two-step esterification-transesterification mechanism would be the ease of separation, reusability, fewer inputs into the reaction stream resulting on less wastes, as no soap would be formed. On the other hand heterogeneous catalysts yield of methylesters is lower compared to homogeneous catalysts (Ullah et al., 2015). Additionally, they are prone to deactivation due to many reasons such as, poisoning, leaching and coking.

A unique heterogeneous commercial process is based on Esterfip-H technology developed by the French Institute of Petroleum (IFP) (Bournay et al., 2005; Michel Bloch, 2006). In this continuous process, the transesterification reaction is carried out in two fixed bed reactors by a completely heterogeneous catalyst that consists of a mixed oxide of zinc and aluminium (zinc aluminate oxide). The process operate at 180-220°C and 62 bar corresponding to the vapor pressure of methanol at this temperature range (Santacesaria et al., 2012; Omberg, 2015). Biodiesel yield obtained is around 100% and purity higher than 99%. However, the raw material must have very low FFA (< 0.25%) and water (< 1000ppm) content as the catalysts used is alkaline in nature and higher concentration of FFA or water in feedstock would lead to soap formation as discussed earlier (Hillion et al., 2007).

The development of the Esterfip-H process has triggered the aspiration to find new heterogeneous catalysts that are more efficient, moisture resistant, and eventually able to promote simultaneously the esterification of FFA along with transesterification of triglycerides.

Consequently, to the aforementioned reasons, and due to the increasing awareness of the economic and environmental costs of alkali catalyzed chemical processes. A growing interest for heterogeneous catalysis has created an prospect for the use of solid acid catalysts in esterification. In this study, a search for suitable heterogeneous catalyst to carry out the esterification reaction has been conducted. The selection criteria were stability, selectivity and activity at low temperature and pressure (mild conditions: 60°C, 1atm). These operating conditions are typical for small to medium scale biodiesel production facilities, using homogeneous catalyst. To accomplish this objective, four preselected heterogeneous catalysts have been evaluated based on the above-mentioned criteria at different operating conditions.

The ultimate goal was to find the key catalyst able to unlock the vast potential in term of energy offered by the low cost, high FFA content feedstock.

Objectives

The objectives for this part of the study included selection of suitable heterogeneous acid catalyst and determination of suitable operating conditions of mixing, catalyst loading, reaction time, and temperature for the reaction system. The catalyst stability has also been tested under different reaction conditions. The selection of operating conditions is guided by need for special process safety and environmental considerations. Since methanol (a flammable, toxic alcohol) presents a serious fire risk, moreover overexposure to methanol can cause neurological damage and other health problems. The reaction temperature is limited to 60°C to allow operation near atmospheric pressure. These conditions are typical for small to medium scale production facilities operating with homogeneous type catalysts. Furthermore, the introduction of heterogeneous catalyst without changing operating conditions for actual plants will imply significant cost reductions in term of ease of process. Finally, the introduction of heterogeneous catalyst has direct environmental impact, considering that the washing step in homogeneous process generating large amount of wastewater would be completely eliminated.

4.2 Experimental Details

4.2.1 Materials and Chemicals

Refined Canola oil used in the experiments was the Saporito Brand marketed by Costco wholesale stores. Anhydrous grade methanol (99.9%) was acquired from EMD Millipore Corp (USA). Anhydrous grade ethyl alcohol was obtained from Commercial Alcohols. Anhydrous reagent grade diethyl ether (99%), dichloromethane, and 1 % (w/v) phenolphthalein indicator solution in 50 % (v/v) Isopropanol was provided by VWR (Canada). Reagent grade sodium hydroxide (97%), potassium hydroxide (85%), oxalic acid (99.5%), concentrated sulfuric acid (95-98%), acetone (99.5%), and hexane (98.5%) were supplied by Caledon Laboratories Ltd. Oleic acid at 90% FFA was procured by Alfa Aesar, and CAS grade concentrated hydrochloric acid by Fisher Scientific. Chlorosulfonic acid (99%), and high purity (davisil grade 633) silica gel with pore size of 60 Å along with 35-60 and 200-425 mesh particles size were supplied by Sigma-Aldrich (Canada). Heterogeneous catalyst Amberlyst 15 was acquired from VWR (Canada), while Amberlyst BD20 was ordered from Dow Chemicals. In addition, Silica sulfuric acid (SSA) based on sulfuric, and Chlorosulfonic acid were synthesized in laboratory.

4.2.2 Silica Sulfuric Acid preparation

Silica sulfuric acid (SSA) is prepared by acid impregnation method. Two distinct catalysts are prepared using Sulfuric and Chlorosulfonic acid as active species.

4.2.2.1 Method 1: preparation of SSA using Sulfuric acid (SSA1)

In this method adapted from (Maleki et al., 2012), concentrated sulfuric acid (3ml) was added to a slurry of silica gel (10g) in dry diethyl ether (50ml). The mixture was shaken for 6min, followed by solvent drying under reduced pressure for 30 minutes at room temperature. The resulting white solid $\text{H}_2\text{SO}_4\text{-SiO}_2$ (SSA1 catalyst) was then heated at 130°C for 3h, then stored in desiccator, using blue indicating calcium sulfate CaSO_4 as desiccant. These catalysts are easy to handle, can be stored indefinitely, and re-activated as needed by oven heating for 12h (Riego et al., 1996). Two size of silica gel (60Å pore size, 35-60 mesh, and 200-425 mesh particle) were dried overnight at 130°C prior to be used in catalyst preparation. This resulted into two distinct catalysts of this type,

the first referred to as SSA1-35 based on the 35-60 mesh particle size, while the second referred to as SSA1-200 was built upon the 200-425 mesh particle size. SSA1-200 was synthesized in order to compare the catalyst activity at increased surface area.

4.2.2.2 Method 2: preparation of SSA using Chlorosulfonic acid (SSA2)

In this method adapted from (Shah et al., 2014a, 2014b) according to the method reported by (Zolfigol, 2001) with some modification, Zolfigol method was also mentioned by (Dabiri et al., 2008). In this technique a 500ml suction flask containing a gas outlet is equipped with a constant-pressure dropping funnel holding Chlorosulfonic acid (23.3g, 0.2mol). The suction flask was charged with a suspension of silica gel (60g) in dichloromethane (200ml). Chlorosulfonic acid was added dropwise over 30 min at room temperature through the constant-pressure dropping funnel. The gas outlet tube carried out the HCl gas that evolved immediately from the reaction vessel into a glass container retaining an NaOH solution to absorb it. Furthermore, to complete the removal of HCl gas the resultant mixture was stirred for 30 min at room temperature. The solvent was evaporated under reduced pressure accompanied by heating. A white-grey solid (SSA2) of 73.56g was obtained and stored in a desiccator. Similarly, to the first method of catalyst preparation, two size of silica gel (60Å pore size, 35-60 mesh, and 200-425 mesh particle) were dried overnight at 140°C prior to be used in catalyst preparation. This resulted into two distinct catalysts of this type, the first referred to as SSA2-35 based on the 35-60 mesh particle size, while the second referred to as SSA2-200 was built upon the 200-425 mesh particle size. SSA2-200 was synthesized in order to compare the catalyst activity at increased surface area. It can be noticed that that the reaction is easy and clean without any work-up (Zolfigol, 2001) because HCl gas is evolved from the reaction immediately as shown in the reaction scheme on **Figure 4-2**.

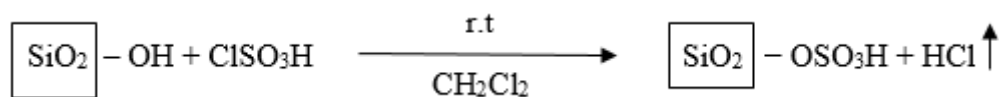


Figure 4-2 Scheme of SSA2 synthesis

4.2.3 Resin Catalysts Drying and Activation:

The resin catalysts received from the supplier were mostly wet and required drying procedure for activation. Water slurry drying method was used for Amberlyst BD20 catalyst (received in fully swollen with water form). In order to prepare the quantity required for several experiments, 50g of wet resin were mixed with 300ml of distilled water for 10 min, then water was removed by filtration repeating the same procedure for a total of 250 gram of raw catalyst. After filtration the wet catalyst weighed around 400g, this quantity was oven dried for 24 hours at 105°C resulting on a dried catalyst weighting 68.6g. This corresponded to a water content reduction of 72.56% ($[(250-68.6)/250] * 100\%$).

For Amberlyst 15, since the catalyst was received in dry form it was simply oven dried for 34 hours at 105°C. The initial quantity was 100g that yielded 53.55g after drying, corresponding to a 46.45% moisture reduction. As shown in **Figure 4-3**, at same reaction conditions the activity of prepared solid catalyst is improved compared to non activated ones for both resins. For instance, the conversion of BD20 improved from 18.4 to 59.6%, while the conversion of A-15 rose from 14.53 to 47.14% before and after preparation respectively. The SEM photography for BD20 and A-15 before and after preparation are presented in **Figure 4-4**, it can be observed that the two catalyst contrasts in morphology as BD20 is non porous as opposite to the porous catalyst A-15.

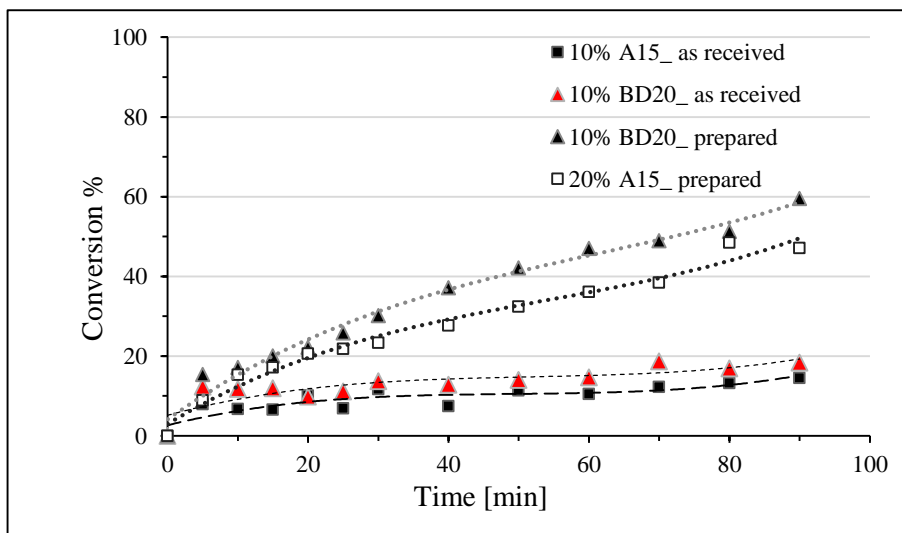


Figure 4-3 Comparison between prepared and as received resin catalysts. Reaction conditions: FFA=15%, Methanol/FFA=20:1, catalyst loading 10wt% (except prepared Amberlyst 15=20wt.%), Reaction time:90min, Temperature= 60°C.

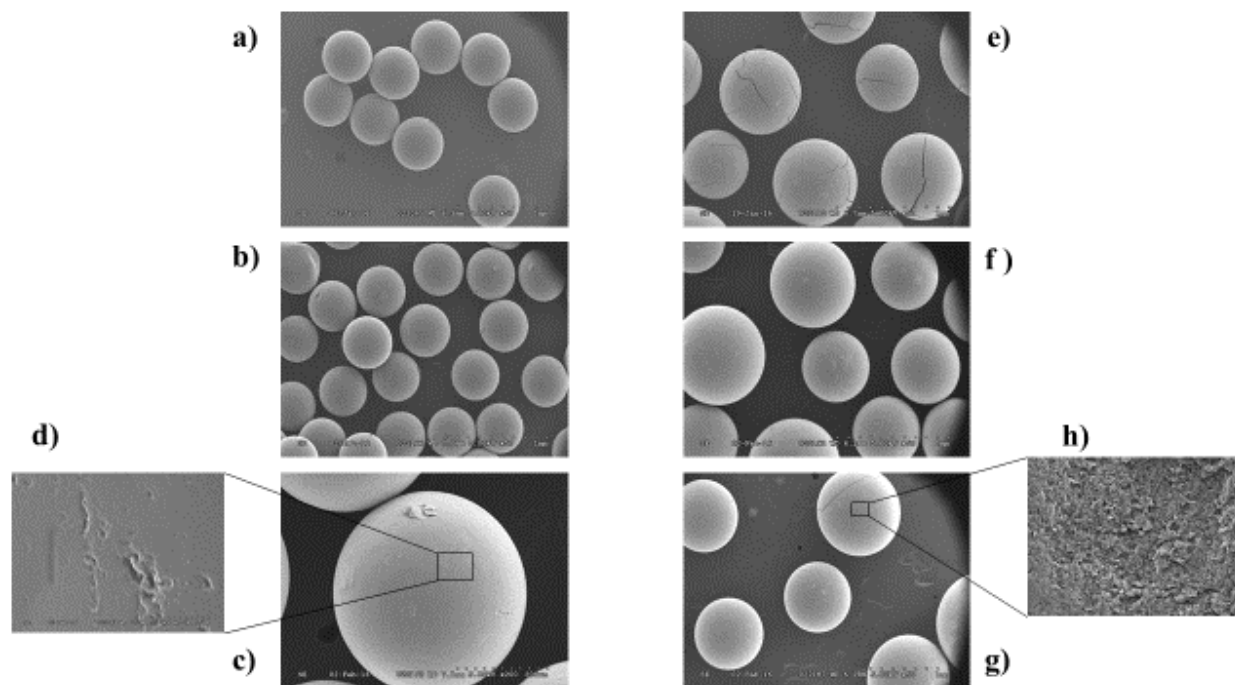


Figure 4-4 SEM images of cation exchange resins: (a) Amberlyst BD20 as received, (b) Amberlyst BD20 prepared, (c) Amberlyst BD20 prepared higher magnifications, (d) Amberlyst BD20 prepared surface view, (e) Amberlyst-15 as received, (f) Amberlyst-15 prepared, (g) Amberlyst-15 prepared at different view (h) Amberlyst-15 prepared surface view.

4.2.4 Equipment

All experiments were performed in a one-liter jacketed glass reactor of 140mm height and 100mm inside diameter. It was equipped with a reflux condenser, a 63.5 mm in diameter impeller with three pitched blades (45°) of 5mm width placed concentrically at 36 mm from the bottom, and four baffles (10mm width) evenly allocated to provide an effective mixing of reactants and products. A schematic of the experimental set up can be seen in **Figure 4-5**. The vessel was linked to a water bath LAUDA E100 capable of maintaining the reactor temperature at the prefixed value within $\pm 1^\circ\text{C}$, by means of a tubular heater controlled by a modified PID (proportional-integral-derivative) controller. A thermocouple (TRACEABLE provided by VWR) was utilised to oversee the reaction temperature. Also a laser tachometer (MONARCH PLT200) was employed to measure the impeller RPM. Three ports were accessible from the lid of the reactor, one was utilized to attach

the condenser to the system, the other one was the inlet of the rod of the impeller, and the third was used to convey the reactants into the vessel and to get intermittent samples for analysis. In addition, the reactor was equipped with a drain valve to empty the contents of the reactor at the end of reaction. Extra equipment employed during experiments comprised: a rotary evaporator Hei-Vap Value manufactured by Heidolph Instruments Germany, a constant-pressure dropping funnel, a vacuum filtration setup, and separatory funnels.

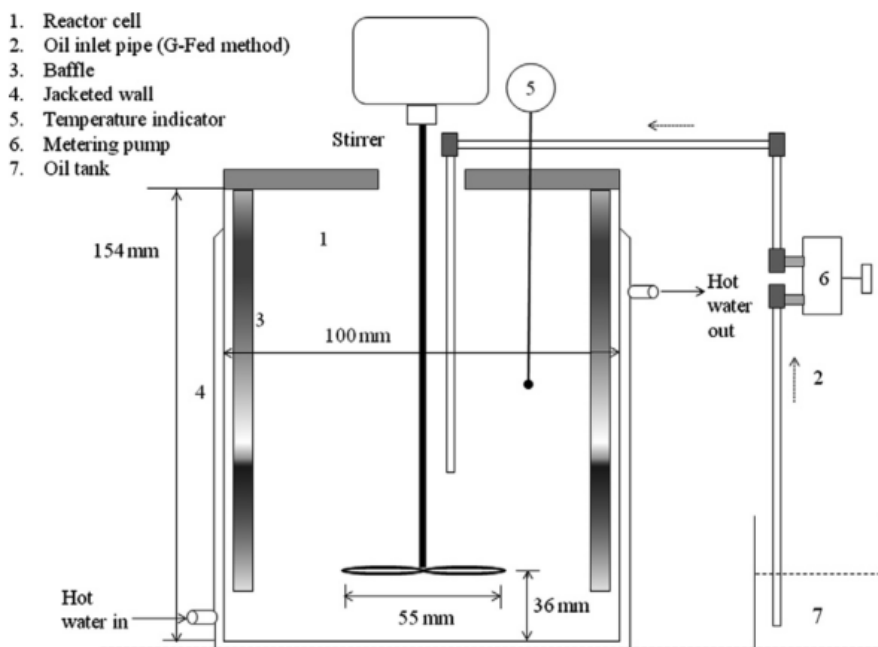


Figure 4-5 Schematic of Experimental Set up used to experiment heterogeneous catalyst (Pal and Prakash, 2012)

4.2.4.1 Brunauer–Emmett–Teller (BET)

The BET (Brunauer–Emmett–Teller) method in ASAP 2010 (Micrometrics, Canada) was used to determine the catalysts surface area. The BET surface area is determined by the physical adsorption/desorption of an inert gas, mostly nitrogen at 77K on a solid surface (Park et al., 2010) that leads to an adsorption isotherm also referred to as BET isotherm. The quantity of gas adsorbed at a particular pressure allows to estimate the catalyst surface area, pore diameter, and pores volume.

4.2.4.2 Scanning Electron Microscopy (SEM)

High resolution images of the catalysts surface were generated using the scanning electron microscopy (SEM) technique. The SEM is a type of electron microscope where highly magnified images of the sample are produced by scanning it with a stream of electrons. As a result of the interaction between the sample atoms and electrons a signal is generated that contains information about its composition and surface topography, **Figure 4-6** shows a schematic of the functioning mechanism for the SEM.

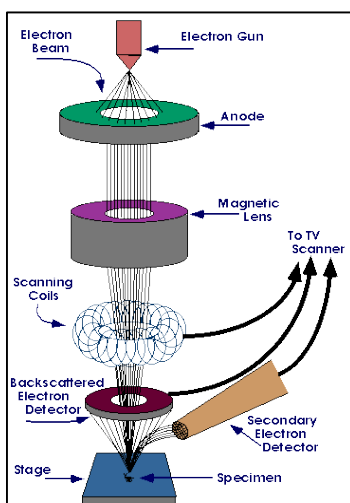


Figure 4-6 Schematic of an SEM (Purdue University - Scanning Electron Microscope)

In this study, catalysts samples were prepared by water removal, then made conductive by application of a thin layer of gold coating before being analyzed using a Hitachi S-2600 SEM equipment.

4.2.5 Experimental Procedure

High FFA feedstock was simulated by a model mixture prepared by combining a known amount of oleic acid to refined canola oil. Oleic acid was selected since it is one of the dominant fatty acids present in several vegetable oils such as rapeseed, karanja, soybean and palm oil; as well as in animal fats for instance poultry fat, yellow and brown grease (Lotero et al., 2005). Acidity was fixed to 30mgKOH/g corresponding to 15% FFA content by weight. Methanol was selected as alcohol by reason of its low cost (Demirbas, 2010), large availability and widespread use in the biodiesel industry (Moser, 2011). Also due to the fact that methanol is significantly more active

compared to ethanol for esterification reaction at 60°C (Pisarello et al., 2010). Methanol excess was used to shift the equilibrium of the reversible reaction toward the direction of ester formation according to Chatelier's principle (Feng et al., 2011). The molar ratio Methanol to FFA of 20:1 was set for all experiments, based on previous literature investigations (Jeromin et al., 1987; Robles-Medina et al., 2009; Koh, 2011; Santori et al., 2012; Coupard et al., 2014; Konwar et al., 2014; Fu et al., 2015). Acidified oil was first added to the reactor operating under batch mode, where the water circulating inside the jacket provided the heat necessary for the oil to reach the desired temperature. Then, the methanol/solid catalyst mixture was transferred into the reaction system. A mixing speed of 720rpm was set for the majority of experiments (Sendzikiene et al., 2004; Berrios et al., 2007; Pappu et al., 2013). In addition, several experiments were conducted at mixing speed fixed at 200 up to 900 rpm in order to study the mixing effect on overcoming mass transfer limitation. Reaction was continued for 90 min for most experiments, yet to study the effect of reaction time extended runs were performed for preselected duration in the range of 120-240 min, and intermittent samples were collected as reaction progressed for analysis. Initial experiments were repeated 4 times, and standard deviation was found to be within 4%. This indicated good reproducibility, therefore for subsequent experiments no replicates were conducted. The reaction temperature was retained at 60°C that is below the boiling point of methanol (64.7 °C) at atmospheric pressure (Sendzikiene et al., 2004) with the purpose of maintaining the methanol in liquid state without the necessity to pressurize the reaction vessel (Canakci and Gerpen, 2001). On the other hand, a set of experiments were performed at temperatures in the sequence of 30-60 °C with the intent to investigate the temperature effect on the reaction system. The block flow diagram of the esterification reaction using heterogeneous catalyst is shown on **Figure 4-7**.

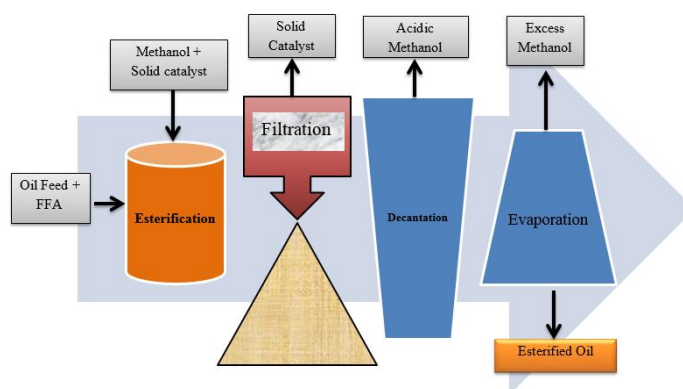


Figure 4-7 Block flow diagram for esterification reaction using heterogeneous catalyst

After esterification, the agitation was stopped and the reaction mixture was filtered to remove the solid catalyst. Then, transferred to a separatory funnel for overnight decantation in order to ensure complete phases separation (see **Figure 4-8**). After decantation the system was biphasic comprising: a top layer constituted by excess methanol and water; in addition to a bottom phase (organic layer) mainly composed of unreacted TG, FAME, and the remaining FFA. Vacuum evaporation at 90°C and (-50) kPa pressure was applied to remove traces of water and excess alcohol from the bottom layer. After evaporation the esterified oil became unclouded, a sign of removal of impurities. (see **Figure 4-9**).

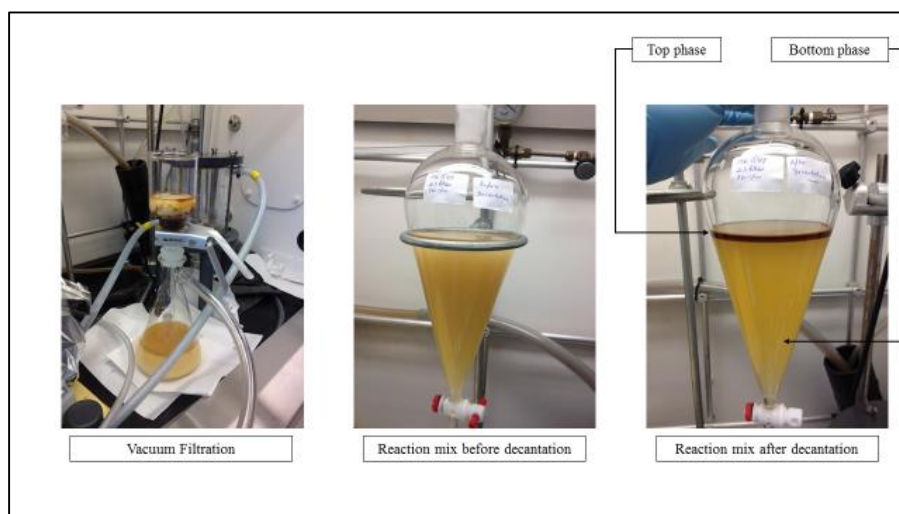


Figure 4-8 Filtration and Decantation

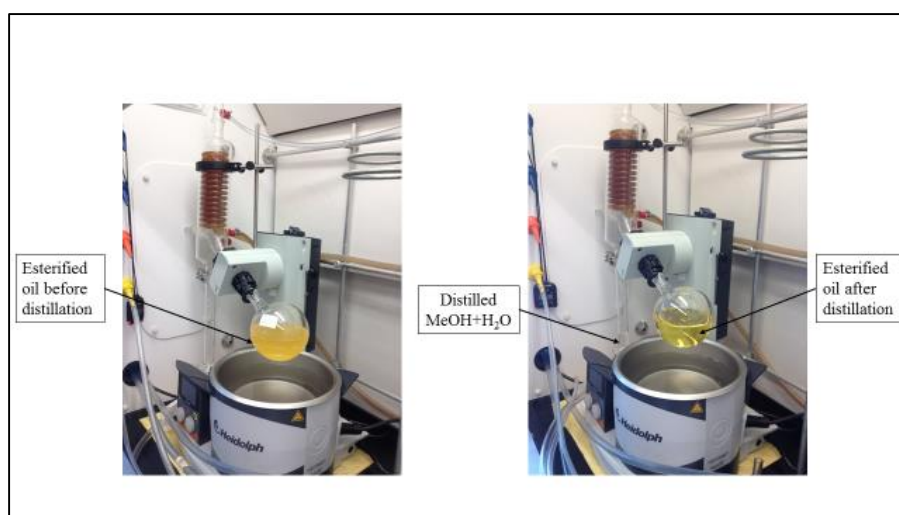


Figure 4-9 Vacuum distillation setting

4.2.5.1 Acid Content Analysis

The samples collected at specific intervals were analysed by a standard acid-base titration procedure to evaluate the FFA content. Prior to titration the sodium hydroxide solution was standardized by means of dehydrated oxalic acid for accurate determination of the solution normality. Depending on the FFA range the alkaline solution concentrations used were approximately 0.012, and 0.031N. The withdrawn samples (about 2g/ea.) were weighted, then washed with distilled water with aim to remove the methanol from the organic phase. Soon after, the vials were deposited in the fridge to completely stop the reaction, and allowed to stand for 3-4 hours for further phase separation. Finally, the top layers were removed from the vials using a micropipette and transferred to Erlenmeyer flask for analysis.

The titration procedure pursued in this work is a modified method of the American Oil Chemists Society (A.O.C.S.) Official Method Ca 5a-40 wherein lesser amounts of sample can be utilised as illustrated by (Rukunudin et al., 1998). In this method a weighted amount of the sample was dissolved in a predefined quantity of ethanol, then a few droplets of phenolphthalein as indicator were added, and the titration is then performed by means of the alkaline NaOH solution at pre-set normality varying with the range of FFA content. All glassware was clean and dried with compressed air prior to titrations. The endpoint was reached when a permanent pale pink color was observed and lasted for at least 30 secs, at that moment the volume of NaOH solution consumed is recorded. The acidity (FFA content) as oleic acid in the sample was calculated by means of the following equation (**Eq.4.1**):

$$\text{FFA}\% = \frac{V_{\text{NaOH used}} \times N_{\text{NaOH}} \times 282}{Wt_{\text{sample}}} \times 100 \quad (4.1)$$

Where:

FFA: Free acidity as oleic acid (%)

V_{NaOH}: Volume of NaOH solution used during titration (ml)

N_{NaOH}: Exact normality of alkaline solution (mol/L)

Wt_{sample}: Weight of titrated sample (g)

282: Molecular weight of oleic acid (g/mol)

Conversion of esterification reaction was calculated as follows:

$$\text{Conversion}(\%) = \frac{\text{FFA}_i - \text{FFA}_t}{\text{FFA}_i} \times 100\% \quad (4.2)$$

Where:

FFA_i: Initial FFA content

FFA_t: FFA content at a given time

4.3 Results and discussion

The introduction of a pre-treatment esterification stage into an integrated two-step biodiesel production process is of primordial importance for high FFA feedstock. This pre-treatment prevents undesirable side reactions (see **Figure 4-10**) leading to high soap concentration through reaction of FFAs with the alkaline catalyst in the main transesterification reaction stage. Additionally, the soap instigates downstream processing problems at the product separation stage by way of emulsion formation (Luque et al., 2010; Park et al., 2010), and gel formation (Atadashi et al., 2012a). Furthermore, soaps formation consumes and deactivates the alkali catalyst resulting on an exceedingly difficult biodiesel purification process (Atadashi et al., 2013).

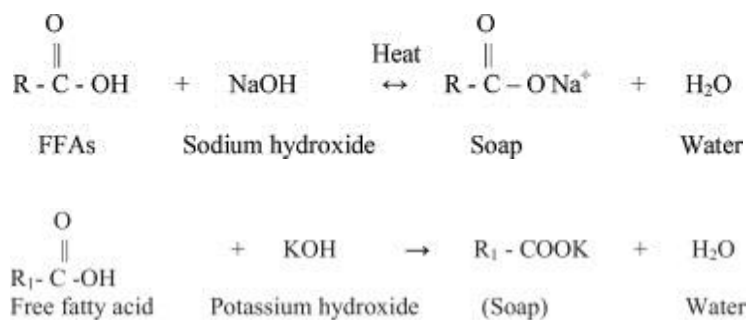


Figure 4-10 Saponification from FFAs. (Atadashi et al., 2012a, 2013).

Esterification was carried out with the postulation that the solid acid catalyst should reduce the acid value of the mixture to an acceptable level below 1mg KOH/g corresponding to 0.5% FFA content by weight (Berrios et al., 2007; ASTM D664, 2011; Santori et al., 2012). In this reaction, a mole-to-mole basis reaction takes place between FFA and alcohol molecules in the presence of an acid catalyst, this generates a methyl ester and a water molecule as illustrated in **Figure 4-11**.

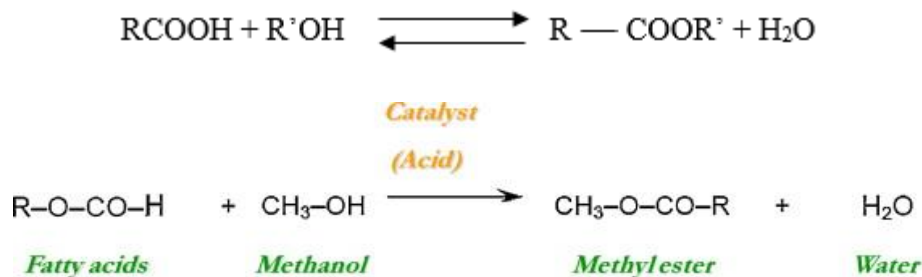


Figure 4-11 Esterification Reaction (Borges and Díaz, 2012)

In order to identify catalyst with suitable characteristics (i.e. high activity and low deactivation) for biodiesel synthesis, this study compared the catalytic activity of a selected number of solid catalysts in the esterification of oleic acid with methanol. These include supported sulfuric acid on Silica (SSA1), supported sulfonic acid on Silica (SSA2), macroreticular copolymer styrene-DVB (divinylbenzene) (Amberlyst-15), and gel type resin, Amberlyst BD20. **Table 4-1** shows the characteristics for the resin catalysts. The reaction results using these catalysts were compared to those using H_2SO_4 as homogeneous catalyst.

4.3.1 Catalytic screening tests

Preliminary catalysts screening has been performed to evaluate their performance in term of conversion and stability.

4.3.1.1 Silica supported catalysts

At first silica supported solid catalysts were investigated for their activity, rate of deactivation and effect of particle size. The results of oleic acid conversions obtained with the virgin catalysts are plotted in **Figure 4-12**. From this plot, a comparable activity can be observed for catalysts SSA1-35 and SS1-200 at 95.04 and 93.85% respectively. The increased surface area for SS1-200 didn't influence the conversion compared to SSA1-35, from the graph it can be seen that their activity is very similar along both curves. The curve for SSA2-35 is slightly under SSA1-200 with a final conversion of 90.46%. On the basis of these preliminary screening results, a more detailed study was performed on the silica supported catalysts to investigate their activity and stability after recycle runs.

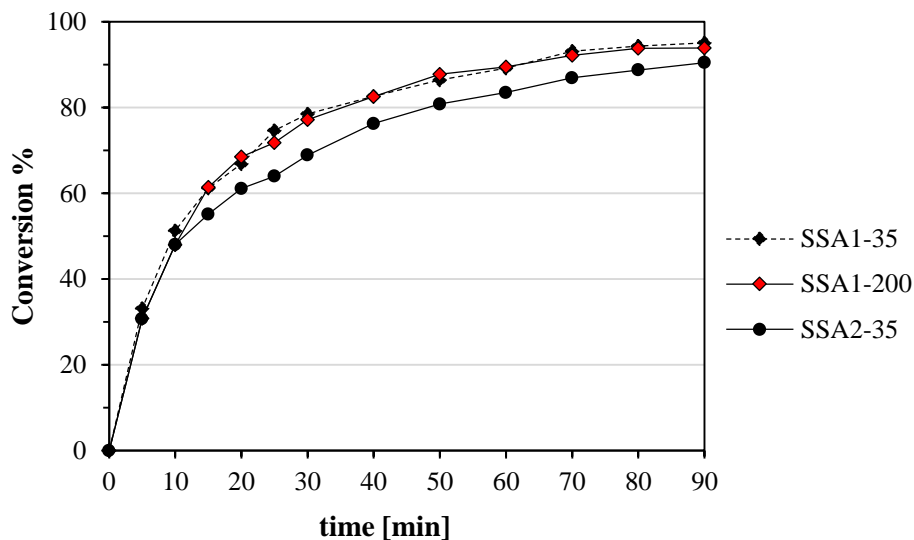
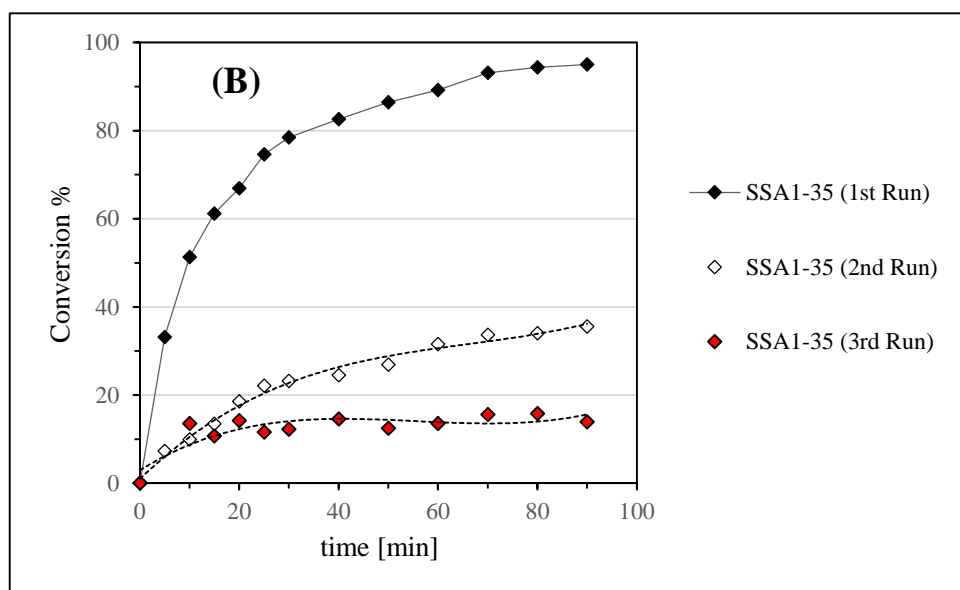
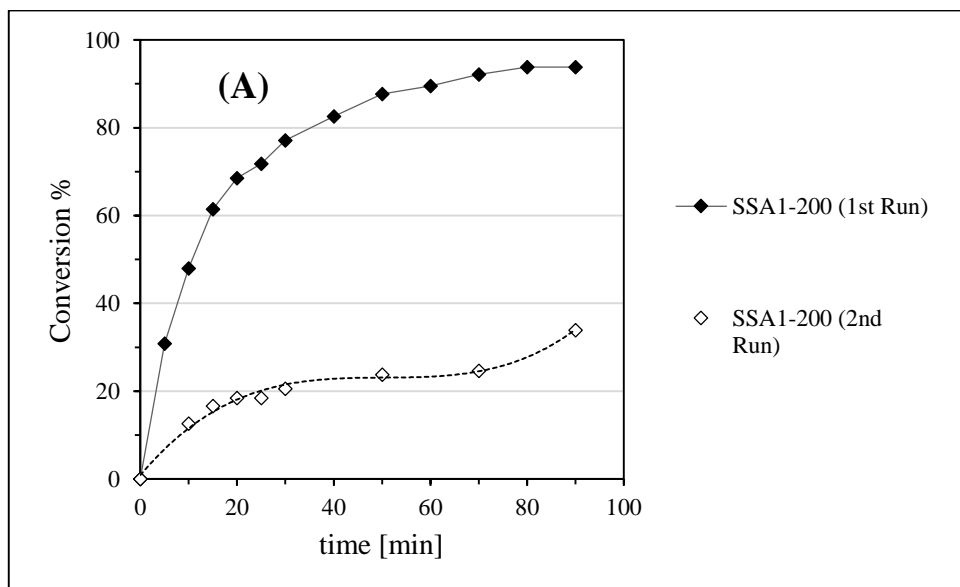


Figure 4-12 Experimental batch runs for catalytic screening. Reaction conditions: FFA = 15 wt.% based on reaction mix, catalyst concentration 10wt.% based on FFA weight; molar ratio of methanol to FFA= 20:1, temperature= 60 °C; agitation speed=720 rpm; reaction time=90min.

4.3.1.2 SSA catalysts deactivation tests

From the results of the deactivation tests for the SSA catalysts shown in **Figure 4-13 A, B, C, D**, it is clear that the activity of this type of catalyst decrease precipitously. Most probably the activity loss is due to the weak bonding between the silica and the two different acids by means of physisorption (Corma and Garcia, 2006). Both methods used for physisorption (adsorption by physical forces) of the soluble catalysts on the silica surface proved to be inefficient to immobilize either H_2SO_4 or HSO_3Cl . Furthermore, the high polarity of the esterification reaction media drove the acid leaching (desorption) from the silica support and their migration into the liquid phase resulting on homogeneous type reaction.



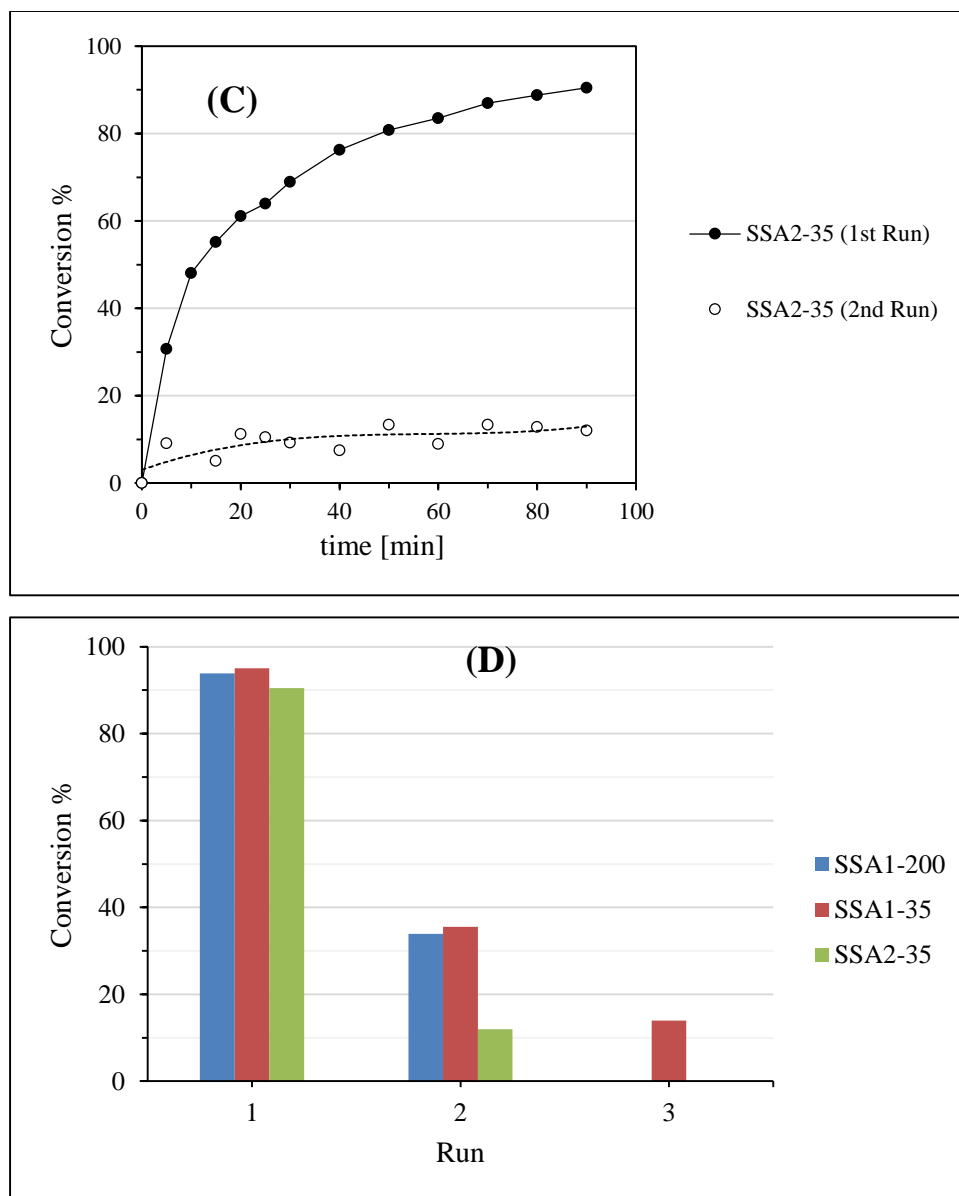


Figure 4-13 Experimental batch runs for the catalytic activity of the SSA catalysts. **(A)** SSA1-200 deactivation test. **(B)** SSA1-35 deactivation test. **(C)** SSA2-35 deactivation test. **(D)** Summary of %conversion attained by individual silica supported catalyst after each run. Reaction conditions: FFA = 15 wt.% based on reaction mix, catalyst concentration 10wt.% based on FFA weight; molar ratio of methanol to FFA= 20:1, temperature= 60 °C; agitation speed=720 rpm; reaction time =90min.

These results are generally in agreement with other literature studies where similar SSA catalysts have been tested, as regeneration is necessary for these type of catalysts (Shah et al., 2014a, 2014b, 2015). Attempts have been made in literature studies to reduce the deactivation rate by developing functionalized silica catalysts to improve the bonding of sulfonic group to silica sites by covalent

anchoring. For example, (Corma and Garcia, 2006) mentioned the different schemes to anchor SO_3H to the mesoporous silica MCM-41, the resulting strong acid catalyst MCM-41/ SO_3H can be considered as the inorganic equivalent of polystyrenes polymers bearing phenylenesulfonic groups such as Amberlyst. As a consequence of these ascertainments, it was decided to deviate from SSA type catalyst and perform more detailed study on the ionic exchange resin catalysts which have shown promise given the strong bonding of acidic group to the resin molecules (Knothe et al., 2010; Kotrba, 2010; Atadashi et al., 2013).

4.3.1.3 Resin catalysts

The two resin catalysts selected for testing are Amberlyst 15 (extensively studied in the literature) and on Amberlyst BD20, more recent, and claimed to be more active and selective. The results of the catalytic activity tests for the ion exchange resins catalysts, presented in **Figure 4-14**, where the two catalysts were compared based on FFA conversion achieved at 90minutes reaction time. The conversions attained were 79.4 and 47.17 % for Amberlyst BD20 and Amberlyst-15 respectively. For this reaction time BD20 displayed nearly a double amount of activity than Amberlyst-15. The role of reaction time was further investigated by increasing the reaction time to 240 minutes. It can be seen in **Figure 4-15** that the FFA conversion increased to nearly 97 and 74% for BD20 and Amb-15 respectively. Although the difference in conversion between the two catalysts decreased, nevertheless BD20 continued to display the higher activity.

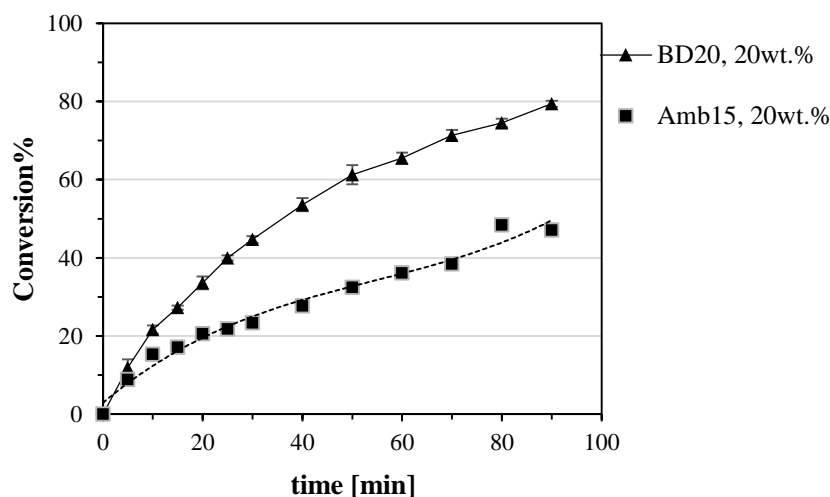


Figure 4-14 Experimental batch runs for the catalytic activity of the ion exchange resins catalysts. Reaction conditions: FFA = 15 wt.% based on reaction mix, catalyst concentration 20wt.% based on FFA weight; molar ratio of methanol to FFA= 20:1, temperature= 60 °

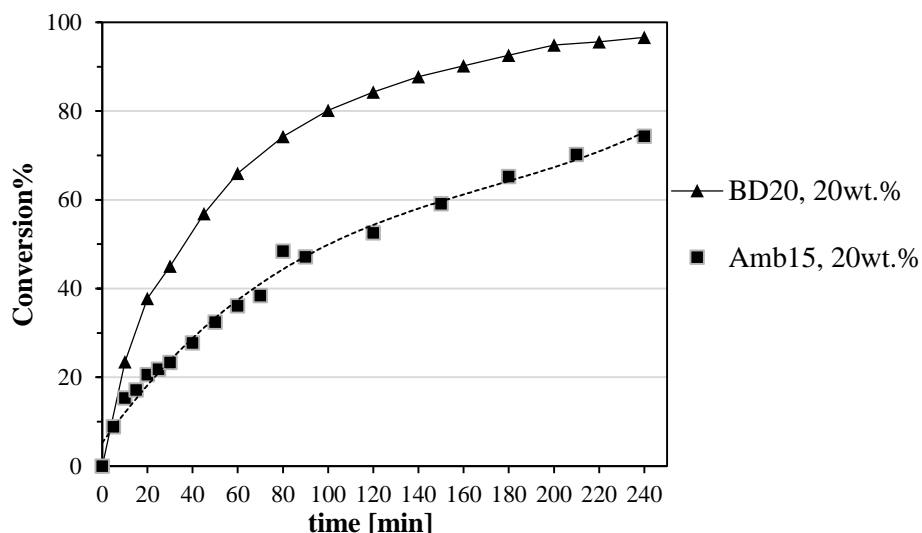


Figure 4-15 Experimental batch runs for the catalytic activity of the ion exchange resins catalysts. Reaction conditions: FFA = 15 wt.% based on reaction mix, catalyst concentration 20wt.% based on FFA weight; molar ratio of methanol to FFA= 20:1, temperature= 60 °C; agitation speed=720 rpm; reaction time =240min.

The difference in activities between the two catalysts were compared based on their catalyst particle properties listed in **Table 4-1**. While the BET surface area, pore size and particle sizes were measured in this study, the concentration of acid sites were obtained from literature sources

Table 4-1 Properties of Ion Exchange Resin Catalysts

Properties	Amberlyst 15	Amberlyst BD20
Type	Macroreticular copolymer	Gel ^{c, e}
Matrix	styrene-DVB ^a	styrene-DVB ^e
Acid Site Density [mole H ⁺ /kg], [eq/kg]	4.7 ^{a, c, d}	5.1 ^{c, d}
Cross-linking degree [%]	20-25 ^a	-
BET Surface Area [m ² /g]	53 ^c	<0.1 ^{c, d}
Average Pore Diameter [nm]	30 ^c	Non-porous
Maximum Operating T [°C]	120 ^c	105 ^b
Functional groups	Sulphonic ^a	-

^a (Tesser et al., 2010), ^b (Dow Chemical), ^c (Pappu et al., 2013), ^d (Park et al., 2010), ^e (Fu et al., 2016)

It can be seen that BD 20 has higher density of acid sites and it is essentially non porous. These two properties seem to be contributing to its superior performance (higher activity). While, high acid site concentration directly contributes to catalyst activity, the absence of pores enhances the reaction rate by avoiding diffusional slow down.

The BET results for BD20 showed that this gel-type resin is essentially nonporous which explains the limited surface area, while Amberlyst-15 is more porous. This is further observed with increased magnification which revealed that Amberlyst-15 has many inner pores in contrast with BD20 as shown in **Figure 4-16**. The active sites on BD20 are thus concentrated in the surface whereas Amberlyst-15 has fewer acid sites on the surface and more inside the inner pores. (Fu et al., 2015) pointed out that at temperatures ranging from 70-80°C, the acid sites at the out surface of gel-type resins are more accessible to reactants than in the pores of the macroporous resin due to low swelling of the macroporous resins at these temperatures range. This statement is more effective at the temperature set for our experiments (60°C) due to less accentuate swelling of the macroporous resin Amberlyst-15. Furthermore, the water produced in the esterification reaction could be absorbed into the pores of Amberlyst-15 stopping the hydrophobic oil to access this sites which results on less activity for this catalyst. On the contrary Amberlyst BD20 did not grant an opening for water to adsorb on the surface, therefore its activity was conserved despite the existence of water.

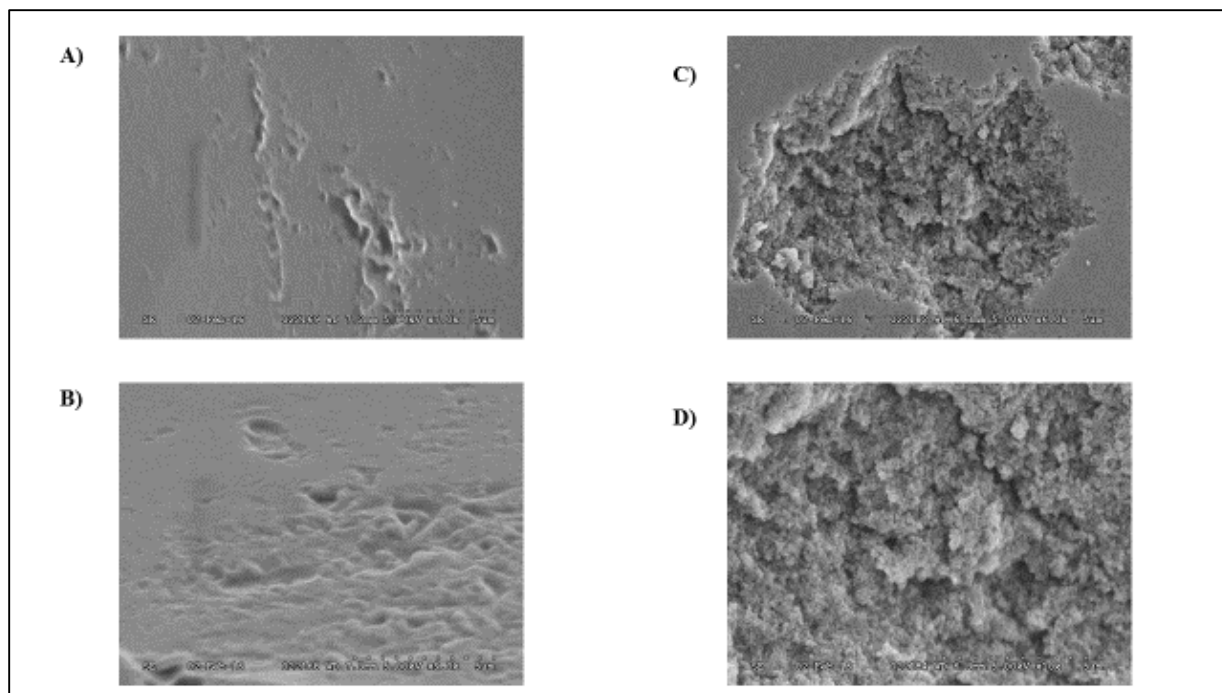


Figure 4-16 SEM Images of catalysts: (A) Amberlyst BD20 outer surface (B) Amberlyst BD20 inner surface, (C) Amberlyst-15 outer surface, (D) Amberlyst-15 inner surface.

Following the afore mentioned preliminary screening experiments results for the four preselected catalysts, a more detailed study has been performed on Amberlyst BD20 as selected catalyst.

4.3.2 Selected Resin Catalysts Study

After preliminary screening, the selected catalyst Amberlyst BD20 has been assessed by means of a series of tests. The objective was to evaluate its performance in terms of: catalyst reusability, as well as the mixing, catalyst loading, temperature, and reaction time effects on the esterification reaction.

4.3.2.1 Reusability test

The first series of tests were conducted to study the BD20 deactivation rate by recycling the used catalyst from one run to next. The results obtained at two catalyst concentrations (10 and 20 wt.%) presented in **Figure 4-17** show good catalyst stability with little loss of activity.

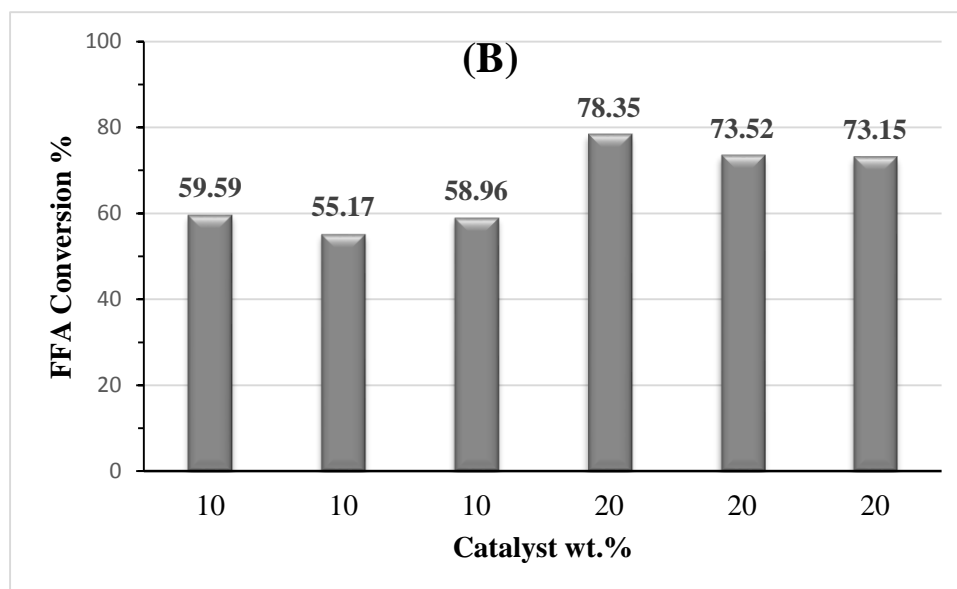
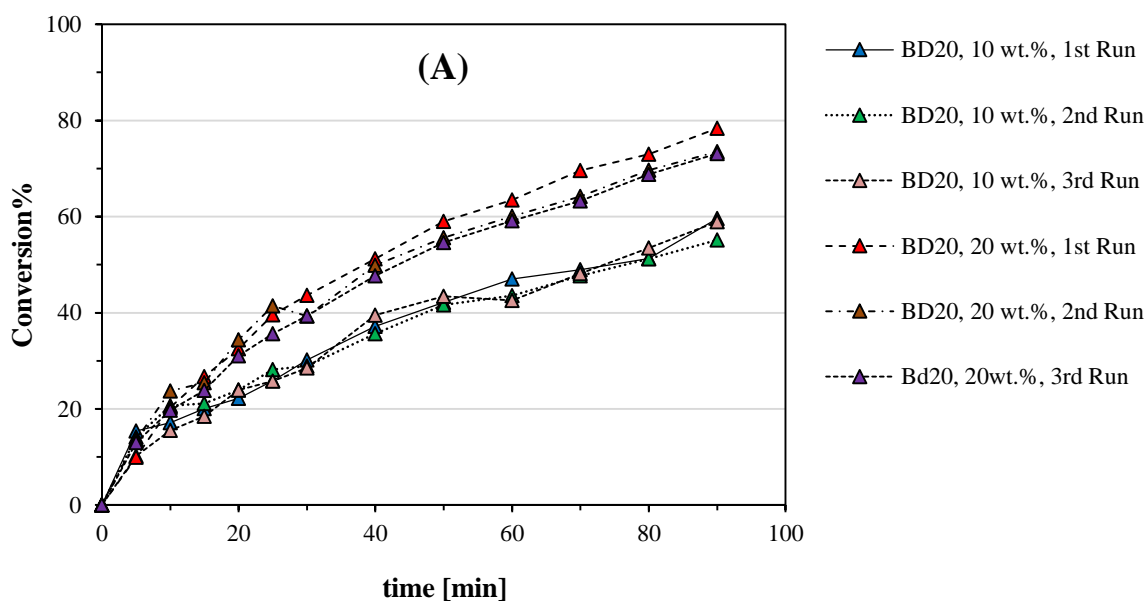


Figure 4-17 (A) and (B) catalyst reusability test for Amberlyst BD20. Reaction conditions: FFA = 15 wt.% based on reaction mix, molar ratio of methanol to FFA= 20:1, agitation speed=720 rpm; reaction time = 90min

In contrast with inorganic metal catalyst for which the leaching is the main cause for deactivation, the resin catalysts deactivation is predominantly due to the deposit of organic substances contained in the feedstock (Lee and Saka, 2010). Although the feedstock used in this study was pure canola oil and oleic acid, we noticed a small deposit on the BD20 surface after reaction. The deposits consisted on white points revealed in the SEM photography as shown in **Figure 4-18**.

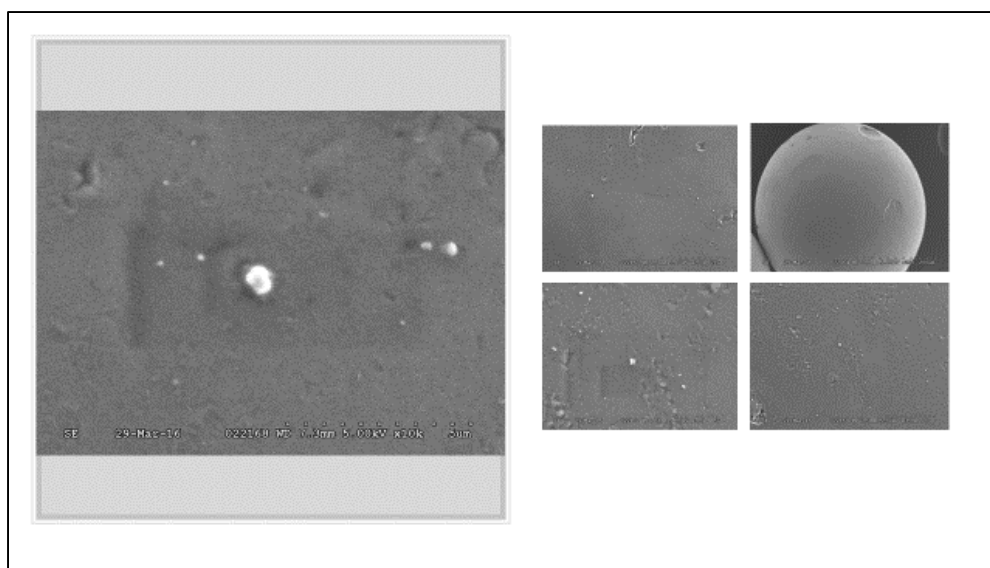


Figure 4-18 Organic deposit on BD20

Since subsequently to the filtration step after reaction, the catalyst was washed with acetone and hexane and oven dried prior to reusability tests. These steps weren't sufficient for the removal of all polar and non-polar impurities such as di- and monoglycerides bonded to oleic acid group (Shibasaki-Kitakawa et al., 2007). This resulted in the slight decrease in catalyst activity. More efficient regeneration procedures such as washing with acidic solution. As well as pretreatment by feedstock desalting would be helpful for sustaining a high catalytic activity of acidic ion-exchange resins for continuous operation, as mentioned in a variety of literature studies (Marchetti and Errazu, 2008; Lee and Saka, 2010).

4.3.2.2 Mixing effect

Next the effects of any external mass transfer resistance were investigated by varying the agitation intensity from 200 to 900 RPM. The results presented in **Figure 4-19 A, B** show no effect of RPM on FFA conversion. This indicates absence of external mass transfer resistance in the system. Also the operation at low RPM would prevent the catalyst depletion due to attrition. Moreover, use of low RPM allowable by this catalyst constitute a way for decreasing energy costs.

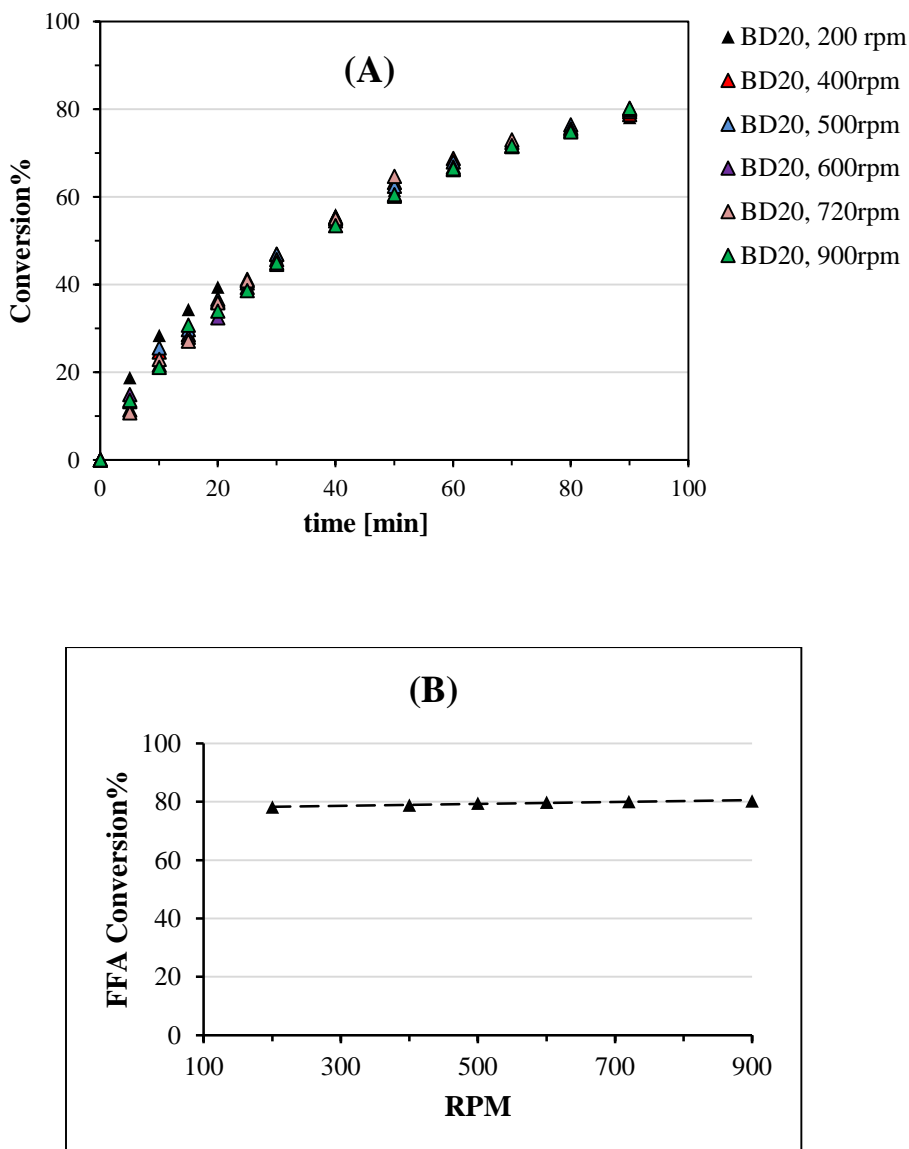


Figure 4-19 (A) and (B) Experimental batch runs for the catalytic activity of Amberlyst BD20 at different RPM. Reaction conditions: FFA = 15 wt.% based on reaction mix, catalyst concentration 20wt.% based on FFA weight; molar ratio of methanol to FFA= 20:1, temperature= 60 °C; reaction time = 90min.

4.3.2.3 Catalyst Loading Effect

Effect of catalyst loading on FFA conversion is presented in **Figure 4-20**. It can be seen that there is significant increase in conversion from 5 wt.% to 20 wt.% catalyst loading. There is no significant increase from 20 to 30 wt.% catalyst loading indicating that optimum catalyst loading may be around 20 wt.%

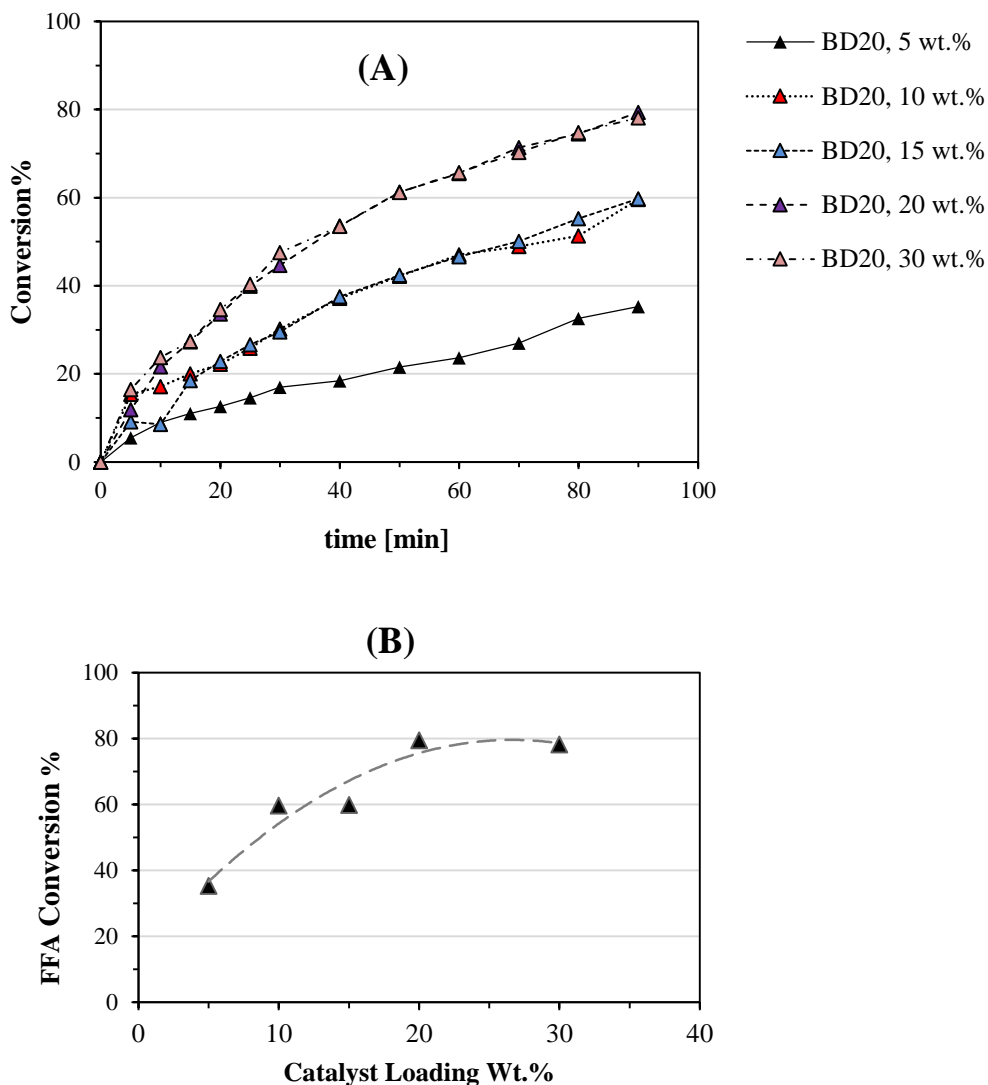


Figure 4-20 (A) and (B) Experimental batch runs for the catalytic activity of Amberlyst BD20 at different catalyst loading. Reaction conditions: FFA = 15 wt.% based on reaction mix, molar ratio of methanol to FFA= 20:1, agitation speed=720 rpm, temperature= 60 ° C; reaction time = 90min.

4.3.2.4 Temperature Effect

The effects of temperature were measured in the range of 30 to 60°C. As shown in **Figure 4-21A**, the conversion increased steadily with increase in temperature. The plot of conversion vs. temperature in **Figure 4-21B** shows the possibility of higher conversion as the temperature is increased further. These results have been used in subsequent section to obtain activation energy for the reaction system.

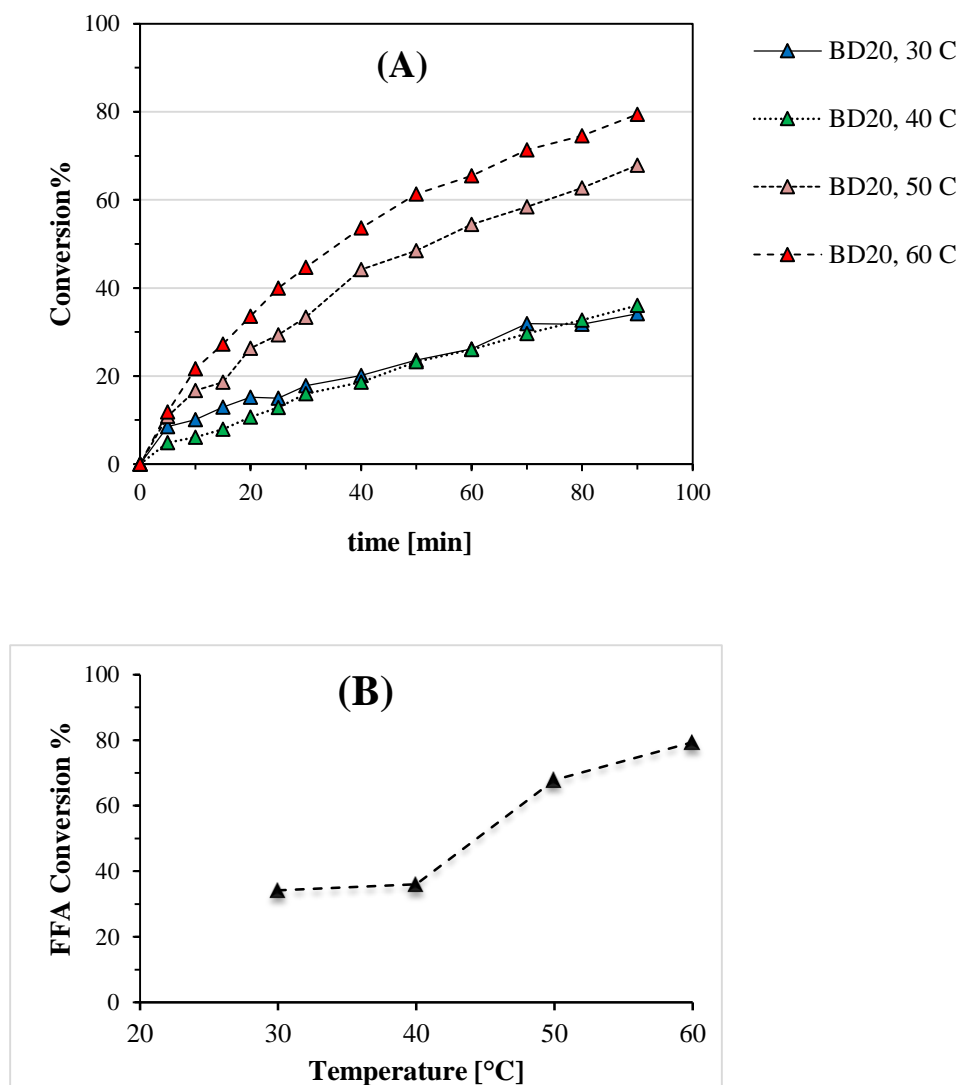


Figure 4-21 (A) and (B) Experimental batch runs for the catalytic activity of Amberlyst BD20 with respect to temperature. Reaction conditions: FFA = 15 wt.% based on reaction mix, catalyst concentration 20wt.% based on FFA weight; molar ratio of methanol to FFA= 20:1, agitation speed=720 rpm; reaction time = 90min.

4.3.2.5 Reaction time effect

The reaction time effect was explored to achieve high conversion of FFA (>96%). Under the conditions used in the study. As shown in **Figure 4-22** it took nearly four hours to reach this level of conversion. The conversion is expected to be higher with less reaction time for greater temperature conditions (Dow Chemical) but will imply the use of pressurized equipment. Since the up-to-standard conversion was achieved at 240min, it can be considered as reasonable trade-off.

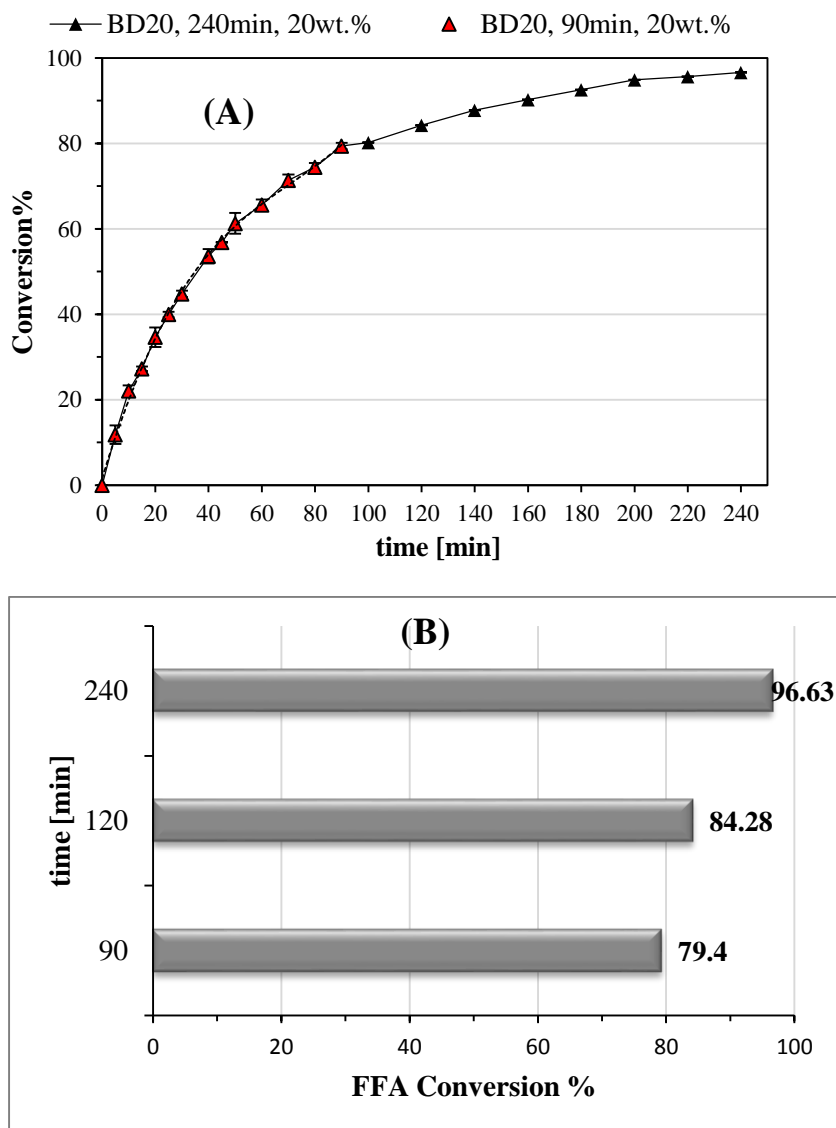


Figure 4-22 (A) and (B) Experimental batch runs for the catalytic activity of Amberlyst BD20 with respect to time. Reaction conditions: FFA = 15 wt.% based on reaction mix, catalyst concentration 20wt.% based on FFA weight; molar ratio of methanol to FFA= 20:1, agitation speed=720 rpm; temperature= 60 °C.

4.4 Kinetic Models for Heterogeneous Catalyst

By analogy to the homogeneous catalyst models, the batch mode experimental data using heterogeneous catalyst were represented by two models. In the first one the reaction was assumed to be pseudo-homogeneous and follows second-order reversible kinetics. On the other hand, the second model assumed the esterification reaction to follow pseudo first-order kinetics, and the apparent reaction order was pondered from the homogeneous second batch model to be 1.5.

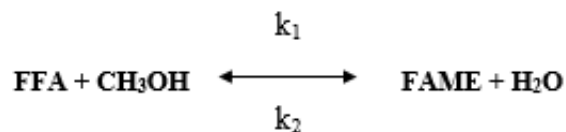
4.4.1 First Heterogeneous Catalyst Kinetic Model

In the first heterogeneous model, the mechanism proposed by Su et al. (Su et al., 2008; Su, 2013) was chosen to obtain the kinetic expression. In this approach induced by Aafaqi et al. (Aafaqi et al., 2004) the esterification reaction is considered to be pseudo-homogeneous, this approach has been used by numerous authors (Tesser et al., 2005, 2009; Pal, 2011; Pappu et al., 2013; Shah et al., 2015). The kinetic model evaluation relies on the following assumptions (Su et al., 2008; Shah et al., 2015):

- a) The rate of the reaction is kinetically controlled.
- b) The rate of auto catalyzed esterification is negligible proportionally to the catalyzed reaction.
- c) The partitioning phenomenon due to the swelling ratio of the polymeric resin is neglected.
- d) The internal and external mass resistances are ignored.
- e) The reaction system is considered as an ideal solution

Under these assumptions, the reaction is assessed to be elementary second order, therefore follows second-order reversible kinetics, the second order with respect to FFA was suggested by various authors (Tesser et al., 2009, 2010).

Esterification generic equation is given by:



Thus, the reaction rate of the esterification reaction can be expressed as:

$$r_A = \frac{-dC_{FFA}}{dt} = k_1 \cdot C_{FFA} \cdot C_{MeOH} - k_2 \cdot C_{FAME} \cdot C_{H_2O} \quad (4.3)$$

Where:

k₁: forward reaction rate constant

C_{FFA}: molar concentration of FFAs [mol/L]

C_{MeOH}: molar concentration of methanol [mol/L]

k₂: reverse reaction rate constant

C_{FAME}: molar concentration of fatty acid methyl esters [mol/L]

C_{H₂O}: molar concentration of water [mol/L]

Since the reactants and products concentrations corresponds to FFAs conversion, Eq.4.3 can be further reformulated into the form of Eq.4.4 wherein FFAs conversion is asserted as a dependant variable.

$$\frac{dx}{dt} = k_1 \cdot C_{FFA_i} \cdot \left[(1-x)(\theta-x) - \frac{x^2}{K_e} \right] \quad (4.4)$$

Where:

x: FFAs conversion

k₁: forward reaction rate constant

C_{FFA_i}: initial molar concentration of FFAs [mol/L]

θ: molar ratio of methanol to FFAs

K_e: equilibrium constant

At equilibrium the net rate is equal to zero (dx/dt=0), therefore Eq.4.4 can be rearranged into Eq.4.5 for K_e evaluation:

$$K_e = \frac{k_1}{k_2} = \frac{x_e}{(1-x_e)(\theta-x_e)} \quad (4.5)$$

where **x_e** is FFAs conversion at equilibrium state, it has to be noted that the values of final conversion in experiments were taken as first approximation of equilibrium conversion for the

iteration process. Later these values were found to be very close to the calculated equilibrium FFAs conversion values as shown in **Table 4-2**

Table 4-2 Equilibrium conversion values

<i>Temperature</i> [°C]	<i>Final experiment</i> <i>FFA conversion</i>	<i>Equilibrium</i> <i>conversion</i>
30	0.3114	0.3472
40	0.3603	0.4081
50	0.6783	0.7228
60	0.9662	0.9643

Once the value of K_e is established, Eq.4.4 can be further integrated and rearranged as Eq.4.6 (Su et al., 2008).

$$\ln \left[\frac{(-1 - \theta + a_2)x + 2\theta}{(-1 - \theta - a_2)x + 2\theta} \right] = a_2 \cdot k_1 \cdot C_{FFA_i} \cdot t \quad (4.6)$$

where

$$a_2 = [(\theta + 1)^2 - 4a_1\theta]^{1/2} \quad (4.6.a)$$

$$a_1 = 1 - \frac{1}{K_e} \quad (4.6.b)$$

Furthermore, to simplify notation

$$\alpha = \ln \left[\frac{(-1 - \theta + a_2)x + 2\theta}{(-1 - \theta - a_2)x + 2\theta} \right] \quad (4.6.c)$$

$$\beta = \frac{1}{a_2 \cdot C_{FFA_i}} \quad (4.6.d)$$

Then Eq.4.6 reduces to Eq.4.7:

$$\alpha * \beta = k_1 \cdot t \quad (4.7)$$

From the experimental data and determined K_e , the forward reaction rate k_1 can be obtained as the slope of the graph:

$$\alpha * \beta = f(t) \quad (4.7. a)$$

In order to express the variation of FFAs conversion with time, Eq.4.6 can be rearranged into Eq.4.8, as an explicit expression for x:

$$x = \frac{2\theta(e^{a_2 \cdot k_1 \cdot C_{FFA_i} \cdot t} - 1)}{[(-1 - \theta + a_2) - (-1 - \theta + a_2) \cdot e^{a_2 \cdot k_1 \cdot C_{FFA_i} \cdot t}]} \quad (4.8)$$

The determination of the kinetic parameters appearing in Eq. 4.5 and 4.6, conversion at equilibrium x_e and equilibrium constant K_e , was executed by a nonlinear fitting. The parameters were adjusted by a program iteratively until a predefined criterion is satisfied. In our case, the criterion is the minimization of the sum of square errors (SSE) between experimental and calculated FFAs conversion values (Ancheyta et al., 2002):

$$SSE = \sum_{i=1}^{i=n} (y_i - \hat{y}_i)^2 \quad (4.9)$$

The minimization of SSE resulted automatically on the minimization of the root mean square error (RMS), (Tesser et al., 2009) between the calculated and experimental FFAs conversion defined by:

$$RMS = \sqrt{\frac{1}{n} \sum_{i=1}^n (y_i - \hat{y}_i)^2} \quad (4.10)$$

The predictive capability of model was evaluated by the linear correlation coefficient (r^2) defined as the following equation:

$$r^2 = 1 - \frac{\sum_{i=1}^n (y_i - \hat{y}_i)^2}{\sum_{i=1}^n (y_i - \bar{y})^2} \quad (4.11)$$

Where

n: number of samples

y_i: actual experiment data (conversion: x) of the ith sample

\hat{y}_i : model predicted data (conversion: x) of the ith sample

\bar{y}_i : average of all experimental data (conversion: x)

The coefficient r^2 is normalized between 0 and 1, with a high r^2 value validating better correlation between experimental and model predicted value. The plot of experimental FFAs conversion along with model calculated values at different temperatures is shown in **Figure 4-23** where the lines represents the model, also example of calculations are shown in **Appendix-E**. It can be seen from the plot, that the model predicts the experimental data accurately, this can be confirmed by the model-fitting criterions with high r^2 values ranging from 0.94-0.99 as shown in **Table 4-3**.

Table 4-3 Model-fitting statistics for the first heterogeneous catalyst model

Temperature [°C]	r^2	RMS	SSE
30	0.9458	0.0228	0.0067
40	0.9865	0.0128	0.0021
50	0.9900	0.0207	0.0055
60	0.9948	0.0206	0.0093

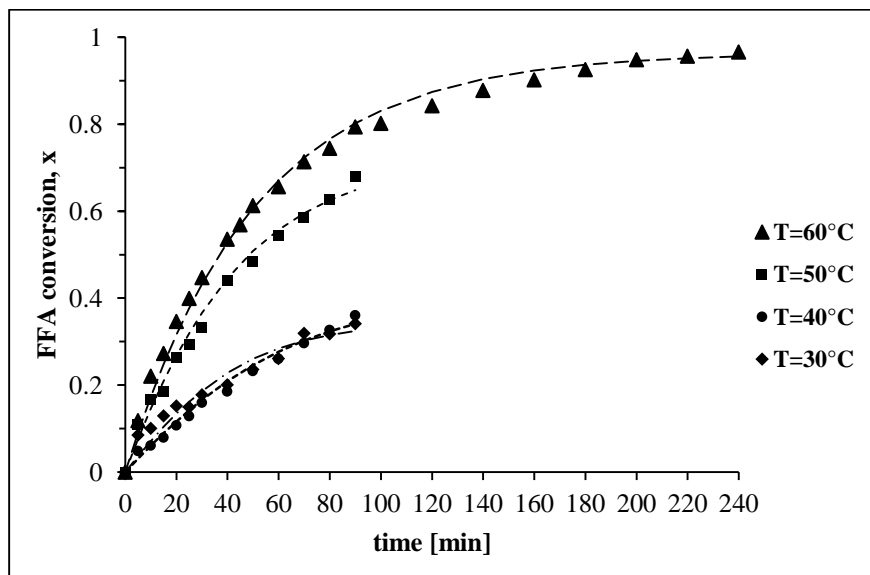


Figure 4-23 FFA conversion vs. time along with the prediction results of the first heterogeneous catalyst model

4.4.1.1 Estimation of the model parameter

After determination of the equilibrium constant K_e , the forward rate constant k_1 is determined using equation 4.7.a. The plot of $\alpha.\beta$ against time for all temperature is very close to the origin as shown in **Figure 4-24**, therefore the slope of each straight line is used to evaluate the k_1 value.

Table 4-4 summarizes the rate constants at each temperature.

Table 4-4 Rate constants for heterogeneous catalyst first model

T [K]	K_e	k_1 [L.mol ⁻¹ .min ⁻¹]
303.15	0.0094	0.0011
313.15	0.0144	0.0009
323.15	0.0978	0.0023
333.15	1.3695	0.0027

It has to be noted that the equilibrium rate constant, as well as the equilibrium conversion increased with temperature owing to the endothermic nature of the esterification reaction (Aafaqi et al., 2004).

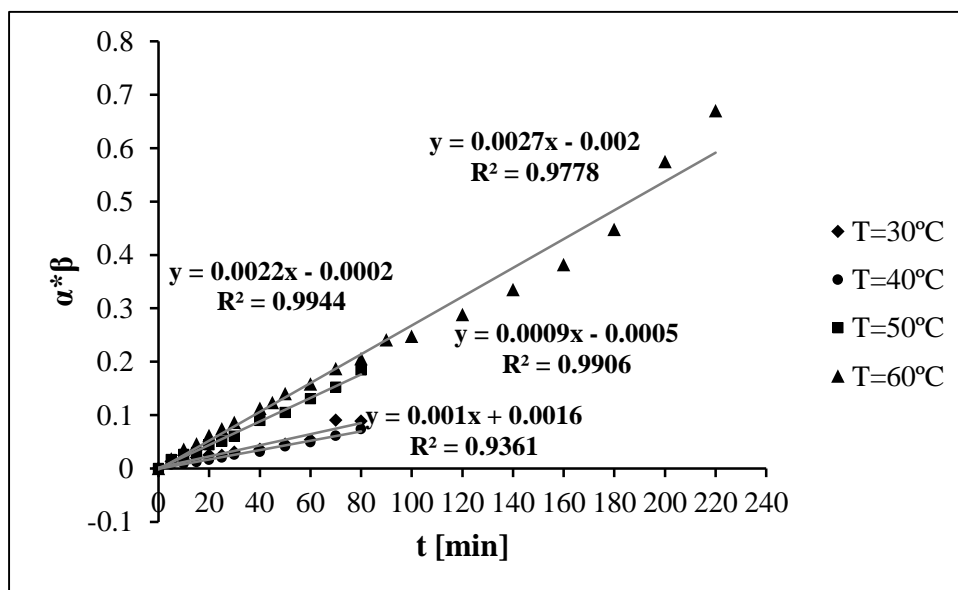


Figure 4-24 Determination of k_1 values for the first heterogeneous catalyst model

The temperature dependency of kinetic constant is described by Arrhenius law:

$$k_1 = k_{1,0} \exp\left(\frac{-E_1}{RT}\right) \quad (4.12)$$

$$K_e = K_{e,0} \exp\left(\frac{-\Delta h}{RT}\right) \quad (4.13)$$

Where:

$K_{e,0}$: frequency (pre-exponential) factor for equilibrium rate constant;

$k_{1,0}$: frequency (pre-exponential) factor for forward rate constant;

E_1 : activation energy of forward reaction, [J/mol];

Δh : molar heat of the reaction, [J/mol];

T : temperature, [K];

R : universal gas constant, [8.314 J/mol. K].

In order to find the pre-exponential factor, as well as the activation energy for esterification reaction. The Arrhenius equation is linearized in the following form:

$$\ln k = \ln k_0 - \frac{E}{RT} \quad (4.14)$$

The plot of $\ln k_1$ and $\ln K_e$ as a function of reciprocal temperature $(1/RT) \cdot 10^3$, are shown in

Figure 4-25:

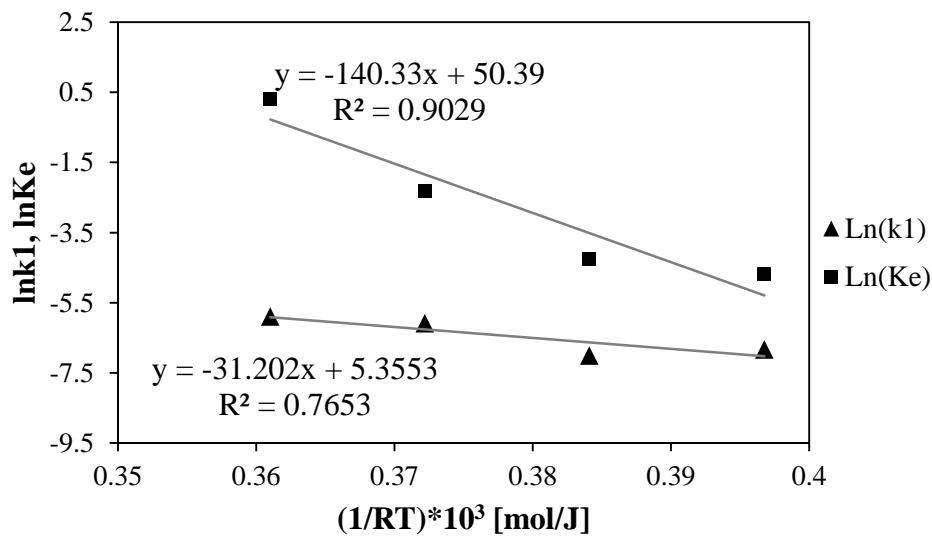


Figure 4-25 Arrhenius Van't Hoff plot for the first heterogeneous catalyst model

The results for the first heterogeneous model are as shown in **Table 4-5**:

Table 4-5 Arrhenius equation parameters for the first heterogeneous model

<i>Frequency factor: $k_{1,0}$</i>	211.72
<i>Frequency factor: $K_{e,0}$</i>	$7.65 \cdot 10^{21}$
<i>Activation Energy: E_1 [kJ/mol]</i>	31.20
<i>Molar heat of the reaction: Δh [kJ/mol]</i>	140.33

4.4.1.2 Comparison of predicted and experimental data

After determining the k_1 values for Equations 4.4 and 4.8, the goodness-of-fit of the experimental data to the proposed model was evaluated by comparing the experimental conversion values with the ones predicted by the model. The plot generated can be ascertained in **Figure 4-26**, where the slope of the solid line is equal to unity. It was found that 78% of the data were predicted with errors less than 10%, this value goes higher at 85% where the values at 30°C are not considered. These model prediction error values are comparable with the ones mentioned in literature. For instance (Berrios et al., 2007) obtained 75% reproducibility at 10% error margin, while (Chai et al., 2014) got 90% reproducibility at 15% error margin.

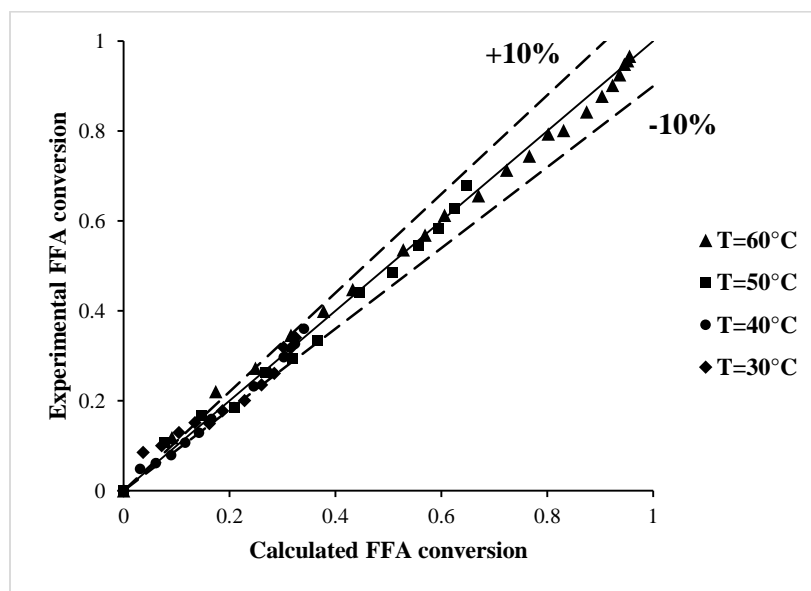


Figure 4-26 Experimental versus. calculated FFA conversion for the first heterogeneous catalyst model

4.4.2 Second Heterogeneous Catalyst Kinetic Model

Analogously, to the first model for heterogeneous catalyst, the second esterification kinetic model evaluation relies on the following assumptions:

- a) The rate of the reaction is kinetically controlled.
- b) The rate of the non-catalyzed esterification is negligible relative to the catalyzed reaction.
- c) The chemical reaction took place in oil phase.
- d) The mole ratio of methanol/FFA was high enough to maintain a constant methanol concentration through the process.
- e) The partitioning phenomenon due to the swelling ratio of the polymeric resin is neglected.

Under these conditions, the FFA esterification reaction is assumed to be reversible heterogeneous process. Therefore, the forward reaction is pseudo-homogeneous first order and reverse reaction is second order, according to Berrios (Berrios et al., 2007). Rate expression can be written as:

$$-\frac{dC_{FFA}}{dt} = k_1 C_{FFA} - k_2 C_{FAME} C_{water} \quad (4.15)$$

Sendzikiene and Berrios (Sendzikiene et al., 2004; Berrios et al., 2007; Chai et al., 2014) reports that rate of reverse reaction (and k_2 respectively) is negligible comparing to forward reaction. Hence, second term from equation can be excluded. Especially this is true for initial times of reaction when there is no water yet in reaction mixture, as the components used in the reaction are anhydrous. Furthermore Sendzikiene noticed that the apparent (observed) kinetic parameters changed during the reaction time. For instance, at 60°C the reaction rate constant changed from 0.0154 to 0.0045[min^{-1}] and reaction order changed from 0.69 to 1.5. Overall reaction rate might be written as homogeneous pseudo-first order to the power n :

$$r_A = -\frac{dC_{FFA}}{dt} = k_1 * (C_{FFA})^n \quad (4.16)$$

Or in finite differences:

$$r_A = -\frac{C_{FFA}^i - C_{FFA}^{i+1}}{t_i - t_{i+1}} = k_1 * (C_{FFA}^i)^n \quad (4.17)$$

Where

n: reaction order

C_{FFA}^i : actual experiment data of FFA concentration for the *i*th sample

C_{FFA}^{i+1} : actual experiment data of FFA concentration for the (*i*+1) sample

k₁: apparent forward reaction rate constant for pseudo-first order

t_i: actual experiment data of time for the *i*th sample

t_{i+1}: actual experiment data of time for the (*i*+1) sample

Since the reactants and products concentrations corresponds to FFAs conversion where:

$$C_{FFA} = C_{FFA_i} * (1 - x) \quad (4.18)$$

Therefore Eq.4.16 can be further reformulated into the form of Eq.4.19 wherein FFAs conversion is asserted as a dependant variable.

$$\frac{dx}{dt} = k_1 \cdot (C_{FFA_i})^{n-1} * (1 - x)^n \quad (4.19)$$

Where:

x: FFAs conversion

k₁: apparent forward reaction rate constant for pseudo-first order

C_{FFA}: molar concentration of FFAs [mol/L]

C_{FFA_i}: initial molar concentration of FFAs [mol/L]

n: reaction order

t: time

The reaction order for the second homogeneous batch model was considered in the assessment for this model. Therefore, Eq. 4.16 can be rewritten as:

$$r_A = -\frac{dC_{FFA}}{dt} = k_1 \cdot C_{FFA}^{1.5} \quad (4.16.a)$$

For sake of notation simplification, the FFAs concentration C_{FFA} will be noted as C_A , the FFAs conversion \mathbf{x} will be noted as \mathbf{x}_A , the FFAs initial concentration C_{FFAi} will be noted as C_{A0} for the following derivation, where equation (4.16.a) will be combined with equation 4.18 to give:

$$\begin{aligned}
 C_{A0} \cdot \frac{dx_A}{dt} &= k_1 \cdot C_{A0}^{1.5} \cdot (1 - x_A)^{1.5} & (4.16.b) \\
 \Rightarrow \int_0^{x_A} \frac{dx_A}{(1 - x_A)^{1.5}} &= k_1 \cdot C_{A0}^{0.5} \cdot \int_0^t dt \\
 \Rightarrow \frac{(1 - x_A)^{-0.5}}{0.5} - \frac{1}{0.5} &= k_1 \cdot C_{A0}^{0.5} \cdot t \\
 \Rightarrow (1 - x_A)^{-1} &= \left[1 + \frac{1}{2} \cdot k_1 \cdot C_{A0}^{0.5} \cdot t \right]^2 & (4.20)
 \end{aligned}$$

By taking:

$$\alpha = \frac{1}{2} \cdot C_{A0}^{0.5} \quad (4.20.a)$$

The Eq.4.20 after rearrangement becomes:

$$x_A = 1 - \frac{1}{(1 + \alpha \cdot k_1 \cdot t)^2} \quad (4.21)$$

By taking the values of k_1 obtained from the second model in case of homogeneous catalyst kinetic model as a first approximation. The determination of the kinetic parameter k_1 appearing in Eq. 4.21, was executed by a nonlinear fitting. The k_1 value was adjusted by a program iteratively until a predefined criterion was satisfied. In our case, the criterion is the minimization of the sum of square errors (SSE) as previously defined in **Equation 4.9** between experimental and calculated FFAs conversion values (Ancheyta et al., 2002):

The minimization of SSE resulted automatically on the minimization of the quadratic mean square error (RMS), (Tesser et al., 2009) between the calculated and experimental FFAs conversion defined by **Equation 4.10**. The predictive capability of model was evaluated by the linear correlation coefficient (r^2) defined by **Equation 4.11**.

The plot of experimental FFAs conversion along with model calculated values at different temperatures is shown in **Figure 4-27** where the lines represents the model, also example of calculations are shown in **Appendix-F**. It can be seen from the plot, that the model predicts the experimental data accurately except at 30°C where the $r^2=0.9019$, this can be attributed to the effect of viscosity and methanol solubility at this temperature. The high values of r^2 for other temperatures demonstrated that the model predictions were in good agreement with the experimental data, this can be confirmed by the model-fitting criteria shown in **Table 4-6**.

Table 4-6 model-fitting statistics for the second batch model

Temperature [°C]	r^2	RMS	SSE
30	0.9019	0.0307	0.0122
40	0.9951	0.0077	0.0007
50	0.9947	0.0151	0.0029
60	0.9967	0.0164	0.0059

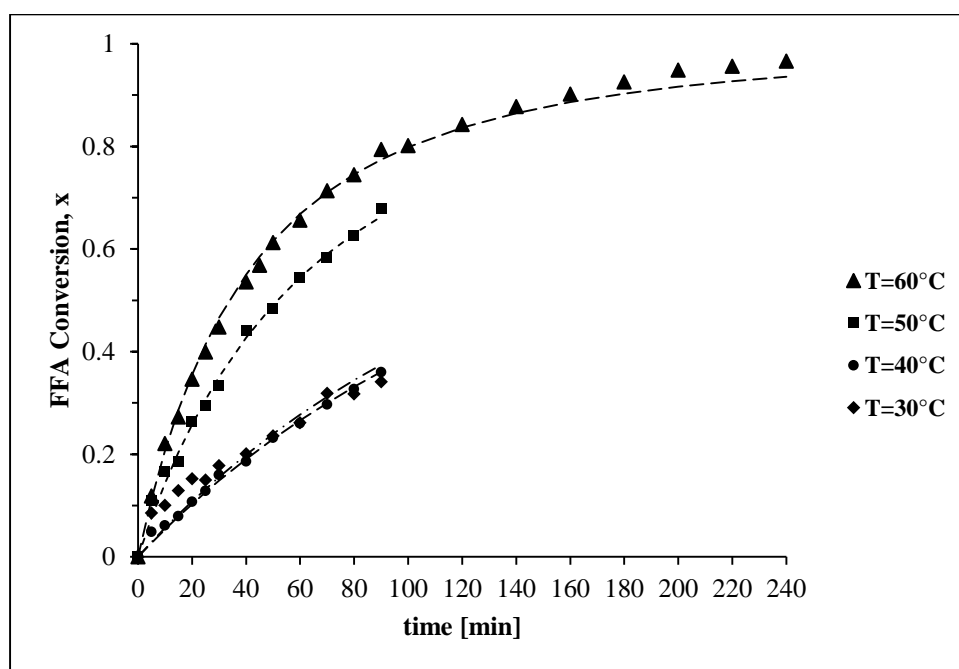


Figure 4-27 conversion vs. time along with the prediction results of the second heterogeneous catalyst model

4.4.2.1 Estimation of the model parameter

After determination of the forward reaction rate constant k_1 , which is the apparent rate of reaction the true rate constant $k_{1\text{true}}$ is determined using Equation 4.22:

$$k_{1app} = k_{1true} * C_{MeOH_i} \quad (4.22)$$

Where:

k_{1app} = k_1 : apparent forward reaction rate constant for pseudo-first order

k_{1true} : true forward reaction rate constant for second order

C_{MeOH_i} : initial molar concentration of Methanol [mol/L]

Since:

$$C_{MeOH_i} = 20 * C_{FFA_i} \quad (4.22a)$$

Then equation 4.22 becomes:

$$k_{1true} = \frac{k_{1app}}{20 * C_{FFA_i}} \quad (4.23)$$

The values of $k_1 = k_{1app}$ and k_{1true} are shown in Table 4-7.

Table 4-7 Values of k_{1app} and k_{1true} for the second heterogeneous catalyst model

k_{1app}	k_{1true}	$\ln k_{1app}$	$\ln k_{1true}$	$(1/TR) * 1000$
$[L^{1/2} \cdot \text{min}^{-1} \cdot \text{mol}^{-1/2}]$	$[L^{3/2} \cdot \text{min}^{-1} \cdot \text{mol}^{-3/2}]$			$[\text{mol/J}]$
0.00992	0.0014	-4.6127	-6.5587	0.3968
0.00942	0.0013	-4.6647	-6.6120	0.3841
0.02716	0.0038	-3.6059	-5.5506	0.3722
0.04148	0.0059	-3.1824	-5.1259	0.3610

These values were used to generate the graphs for Arrhenius equation (Eq.4.12) in the linearized form (Eq.4.14). Then plot $\ln k_{1app}$ and $\ln k_{1true}$ as a function of reciprocal temperature $(1/RT) * 10^3$, as shown in Figure 4-28.

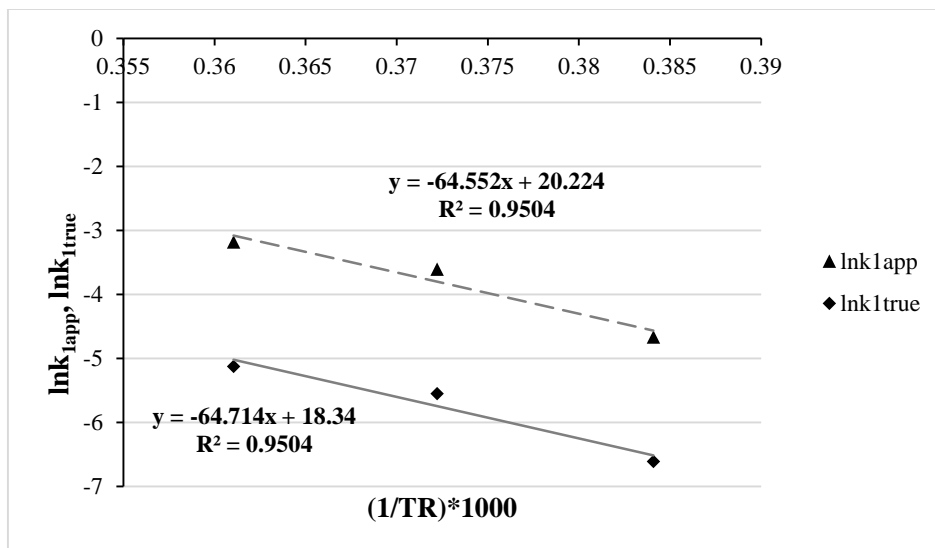


Figure 4-28 Determination of kinetic constants values for Second Heterogeneous Catalyst model

Consequently, the obtained values for the pre-exponential and activation energy for esterification reaction, are summarized in **Table 4-8**:

Table 4-8 Arrhenius Equation parameters for the second Heterogeneous Catalyst Model

<i>Frequency factor: $k_{1,0app}$</i>	6.07 * 10⁸
<i>Frequency factor: $k_{1,0true}$</i>	9.22*10⁷
<i>Activation Energy: E_1 [kJ/mol]</i>	64.71

4.4.2.2 Comparison of predicted and experimental data

After determining the kinetic parameters, the goodness-of-fit of the experimental data to the proposed model was evaluated by comparing the experimental conversion values with the ones predicted by the model. The plot generated can be ascertained in **Figure 4-29**, where the slope of the solid line is equal to unity. It was found that 84% of the data were predicted with errors less than 10%, this value goes higher at 91% where the values at 30°C are not considered. These model prediction error values are comparable with the ones mentioned in literature. For instance (Berrios et al., 2007) obtained 75% reproducibility at 10% error margin, while (Chai et al., 2014) got 90% reproducibility at 15% error margin.

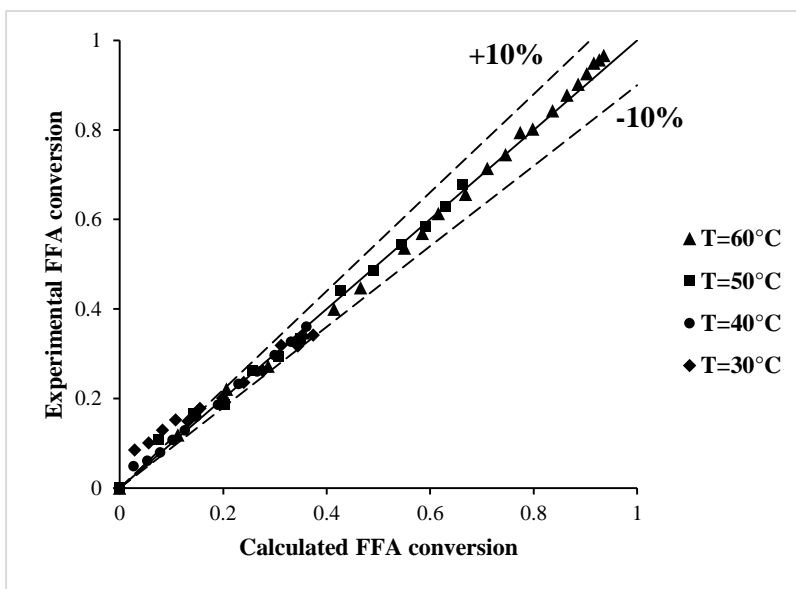


Figure 4-29 Experimental versus. Calculated FFA conversion for the Second heterogeneous catalyst model

4.4.2.3 Comparison with literature

The obtained values of the pre-exponential factor and activation energy obtained from the second heterogeneous catalyst kinetic model were compared with literature papers as shown in **Table 4-9**:

Table 4-9 Comparison of the kinetics parameters obtained by the second heterogeneous catalyst kinetic model with literature

Literature	Tesser	Tesser	Aafaqi	Pappu	Su	This study
Reference	(Tesser et al., 2005)	(Tesser et al., 2010)	(Aafaqi et al., 2004)	(Pappu et al., 2013)	(Su et al., 2008)	
Properties						
Catalyst	Relite CFS	Amberlyst 15, Relite CFS	ZnA/SG	Amberlyst 70	Dowex 88	Amberlyst BD20
Catalyst loading [% to FFA]	5.15-8.8	1.04-9.58	1-5[g/dm ³]	0-3 [kgcat/kgsoIn]	0-53.6	20
Alcohol type	Methanol	Methanol	Isopropanol	various	Methanol	Methanol
FFA type	Oleic acid	Oleins, Oleic acid	Palmitic acid	Butyric acid	Soybean, enzyme hydrolyzed	Oleic acid
Initial FFA%	47-58	47-92.9	up to 33	2.5-3.5	100	15
Alcohol/FFA molar ratio	8.8-10.69	6.5-8	5	6-15	1-20	20
Oil type	Sunflower	Soybean	-	-	Soybean	Canola
Temperature [°C]	50-100	80-120	100-170	100-150	60-80	30-60
RPM	1500	1500	500	550		
Reaction time [min]	200-5000	330	250	120	1800	90
Activation energy of the forward reaction [kJ/mol]	58.57	Amberlyst15:73.05 Relite CFS: 53.42	36.02	41.7	59.44	64.71
Pre-exponential factor of the forward reaction	12.93		11937	113[kgsol/kgcat.sec]	2.869*10 ⁶ [L/mol.min]	9.22*10 ⁷

4.5 Conclusions

Esterification reaction using four different type of heterogeneous catalyst was investigated with the aim to select suitable catalyst able to reduce the FFA concentration in the feedstock into standard level (<0.5 wt.%) prior to alkaline catalysed transesterification at mild reaction conditions (60°C, 1atm). The intended end user for the selected catalyst would be small to medium scale biodiesel plant. After initial screening it was found that the two silica supported acid catalysts (SSA) despite their high initial activity, deactivated rapidly due to active species leaching into the reaction media. On the other hand, the resin catalysts displayed stability in term of deactivation while maintaining high level of conversion. Further assessment of the resin catalysts indicated that Amberlyst BD20 demonstrated better performance (higher activity) than Amberlyst 15 due to high acid site concentration, and the absence of pores resulting on enhanced reaction rate by avoiding diffusional slow down. Therefore, it was selected for a more detailed study, where the effects of catalyst loading (5-30 wt.%), temperature (30-60°C), reaction time (90-240min), and mixing speed (200-900 rpm) were investigated.

The results show that at temperature of 60°C and reaction time of 240 minutes can provide close to 97% conversion of FFA, corresponding to 0.45wt.% that is up to standard concentration. This value of FFA conversion is similar to the value obtained for homogeneous H₂SO₄. The trade-off of increasing the reaction time compared to homogeneous catalyst is well justified, due to inherent advantages for the process in term cost and ease of separation of the catalyst after reaction. Consequently, this catalyst is recommended for further testing for commercial application.

Two kinetic models have been proposed to predict the experimental data. Both models predicted accurately the experimental data with correlation coefficient (r^2) values at 60°C of 0.9948 and 0.9968 for the first and second model respectively. The first model follows second-order reversible kinetics, while the second follows pseudo-homogeneous of order 1.5. Surprisingly the second model predicted 84% of the data with errors less than 10%, while the value was 78% for the first model. These values go even higher when considering the temperature range between 40 to 60°C with values of 91 and 85% for the second and first model respectively. Estimates of kinetic parameters for the esterification reaction are presented.

References

Aafaqi, R.; Mohamed, A. R.; Bhatia, S. Kinetics of Esterification of Palmitic Acid with Isopropanol Using P-Toluene Sulfonic Acid and Zinc Ethanoate Supported over Silica Gel as Catalysts. *J. Chem. Technol. Biotechnol.* **2004**, *79* (10), 1127–1134.

Ancheyta, J.; Angeles, M. J.; Macias, M. J.; Marroquin, G.; Morales, R. Changes in Apparent Reaction Order and Activation Energy in the Hydrodesulfurization of Real Feedstocks. *Energy and Fuels* **2002**, *16* (1), 189–193.

ASTM D664. *Standard Test Method for Acid Number of Petroleum Products by Potentiometric Titration*; USA, 2011; pp 1–10.

Atadashi, I. M.; Aroua, M. K.; Abdul Aziz, a. R.; Sulaiman, N. M. N. Production of Biodiesel Using High Free Fatty Acid Feedstocks. *Renew. Sustain. Energy Rev.* **2012**, *16* (5), 3275–3285.

Atadashi, I. M.; Aroua, M. K.; Abdul Aziz, A. R.; Sulaiman, N. M. N. The Effects of Catalysts in Biodiesel Production: A Review. *J. Ind. Eng. Chem.* **2013**, *19* (1), 14–26.

Berrios, M.; Siles, J.; Martin, M.; Martin, A. A Kinetic Study of the Esterification of Free Fatty Acids (FFA) in Sunflower Oil. *Fuel* **2007**, *86* (15), 2383–2388.

Borges, M. E.; Díaz, L. Recent Developments on Heterogeneous Catalysts for Biodiesel Production by Oil Esterification and Transesterification Reactions: A Review. *Renew. Sustain. Energy Rev.* **2012**, *16* (5), 2839–2849.

Bournay, L.; Casanave, D.; Delfort, B.; Hillion, G.; Chodorge, J. a. New Heterogeneous Process for Biodiesel Production: A Way to Improve the Quality and the Value of the Crude Glycerin Produced by Biodiesel Plants. *Catal. Today* **2005**, *106* (1–4), 190–192.

Boz, N.; Degirmenbasi, N.; Kalyon, D. M. Esterification and Transesterification of Waste Cooking Oil over Amberlyst 15 and Modified Amberlyst 15 Catalysts. *Appl. Catal. B Environ.* **2015**, *165*, 723–730.

Canakci, M.; Gerpen, J. Van. Biodiesel Production from Oils and Fats with High Free Fatty Acids. *Trans. ASAE* **2001**, *44* (6), 1429–1436.

Chai, M.; Tu, Q.; Lu, M.; Yang, Y. J. Esterification Pretreatment of Free Fatty Acid in Biodiesel Production , from Laboratory to Industry. *Fuel Process. Technol.* **2014**, *125*, 106–113.

Corma, A.; Garcia, H. Silica-Bound Homogenous Catalysts as Recoverable and Reusable Catalysts in Organic Synthesis. *Adv. Synth. Catal.* **2006**, *348* (12–13), 1391–1412.

Coupard, V.; Bournay, L.; Toth, E.; Maury, S. United States Patent:Process for Pretreatment of Vegetable Oils by Heterogeneous Catalysis of the Esterification of Fatty Acids. US9234158 B2, 2014.

Coupard, V.; Bournay, L.; Toth, E.; Maury, S. Process for Pretreatment of Vegetable Oils by Heterogeneous Catalyst of the Esterification of Fatty Acids. US Patent. US 9,234,158, 2016.

Dabiri, M.; Salehi, P.; Baghbanzadeh, M.; Zolfigol, M. A.; Agheb, M.; Heydari, S. Silica Sulfuric Acid: An Efficient Reusable Heterogeneous Catalyst for the Synthesis of 2,3-Dihydroquinazolin-4(1H)-Ones in Water and under Solvent-Free Conditions. *Catal. Commun.* **2008**, *9* (5), 785–788.

Demirbas, A. Biodiesel for Future Transportation Energy Needs. *Energy Sources, Part A Recover. Util. Environ. Eff.* **2010**, *32* (September 2013), 1490–1508.

Dow Chemical, C. Specifically-Designed AMBERLYST™ BD20 Catalyst Leads to Effective and Efficient Conversion of FFAs to FAME. Dow Chemical Company pp 1–3.

Feng, Y.; Zhang, A.; Li, J.; He, B. A Continuous Process for Biodiesel Production in a Fixed Bed Reactor Packed with Cation-Exchange Resin as Heterogeneous Catalyst. *Bioresour. Technol.* **2011**, *102* (3), 3607–3609.

Fu, J.; Chen, L.; Lv, P.; Yang, L.; Yuan, Z. Free Fatty Acids Esterification for Biodiesel Production Using Self-Synthesized Macroporous Cation Exchange Resin as Solid Acid Catalyst. *Fuel* **2015**, *154*, 1–8.

Fu, J.; Li, Z.; Xing, S.; Wang, Z.; Miao, C.; Lv, P.; Yuan, Z. Cation Exchange Resin Catalysed Biodiesel Production from Used Cooking Oil (UCO): Investigation of Impurities Effect. *Fuel* **2016**.

Hillion, G.; Delfort, B.; Durand, I. Method for Producing Biofuels, Transforming Triglycerides into at Least Two Biofuel Families: FATTY ACID MONOESTERS and ETHERS And/or SOLUBLE GLYCEROL ACETALS. US 2007/0283619 A1, 2007.

Jeromin, L.; Peukert, E.; Wollmann, G. United States Patent: Process for the Pre-Esterification of Free Fatty Acids in Fats and Oils. 4,698,186, 1987.

Johnson, M. esterification reaction <http://davyprotech.com/what-we-do/licensed-processes-and-core-technologies/licensed-processes/biodiesel/specification/>.

Kinast, J. a. *Production of Biodiesels from Multiple Feedstocks and Properties of Biodiesels and Biodiesel/diesel Blends. Final Report. Report 1 in a Series of 6. Subcontractor Report.*; Golden, Colorado, 2003.

Knothe, G.; Krahl, J.; Van Gerpen, J. *The Biodiesel Handbook, 2nd Edition.*, 2nd Editio.; AOCS Press: Urbana, Illinois, 2010.

Koh, A. Two-Step Biodiesel Production Using Supercritical Methanol and Ethanol, University of Iowa, 2011.

Konwar, L. J.; Das, R.; Thakur, A. J.; Salminen, E.; Mäki-Arvela, P.; Kumar, N.; Mikkola, J. P.; Deka, D. Biodiesel Production from Acid Oils Using Sulfonated Carbon Catalyst Derived from Oil-Cake Waste. *J. Mol. Catal. A Chem.* **2014**, 388–389 (September), 167–176.

Kotrba, R. Bayer, Dow Join Biodiesel Forces. *Focus Catal.* **2010**, 2010 (4), 3.

Lee, A. F.; Bennett, J. A.; Manayil, J. C.; Wilson, K. Heterogeneous Catalysis for Sustainable Biodiesel Production via Esterification and Transesterification. *Chem. Soc. Rev.* **2014**, 43 (22), 7887–7916.

Lee, J. S.; Saka, S. Biodiesel Production by Heterogeneous Catalysts and Supercritical Technologies. *Bioresour. Technol.* **2010**, *101* (19), 7191–7200.

Lotero, E.; Liu, Y.; Lopez, D. E.; Suwannakarn, K.; Bruce, D. a.; Goodwin, J. G. Synthesis of Biodiesel via Acid Catalysis. *Ind. Eng. Chem. Res.* **2005**, *44* (14), 5353–5363.

Luque, R.; Lovett, J. C.; Datta, B.; Clancy, J.; Campelo, J. M.; Romero, A. A. Biodiesel as Feasible Petrol Fuel Replacement: A Multidisciplinary Overview. *Energy Environ. Sci.* **2010**, *3* (11), 1706–1721.

Maleki, B.; Keshvari Shirvan, H.; Taimazi, F.; Akbarzadeh, E. Sulfuric Acid Immobilized on Silica Gel as Highly Efficient and Heterogeneous Catalyst for the One-Pot Synthesis of 2,4,5-Triaryl-1H-Imidazoles. *Int. J. Org. Chem.* **2012**, *2* (1), 93–99.

Marchetti, J. M.; Errazu, A. F. Comparison of Different Heterogeneous Catalysts and Different Alcohols for the Esterification Reaction of Oleic Acid. *Fuel* **2008**, *87* (15–16), 3477–3480.

Melero, J. A.; Iglesias, J.; Morales, G. Heterogeneous Acid Catalysts for Biodiesel Production: Current Status and Future Challenges. *Green Chem.* **2009**, *11* (9), 1285–1308.

Michel Bloch. Improved Glycerin Quality via Solid Catalyst Transesterification : The Esterfip-H Process. In *European Biofuels Forum; Bio-Oil International Conference*, Ed.; 2006; pp 1–20.

Moser, B. Biodiesel Production, Properties, and Feedstocks. *Biofuels* **2011**, No. March, 285–347.

Omberg. Small-Scale Biodiesel Production Based on a Heterogenous Technology- Masters Thesis, Norwegian University of Life Sciences, 2015.

Pal, K. Investigations of Transesterification of Canola Oil with Methanol and Ethanol for a New Efficient Method of Biodiesel Production. PhD Thesis, University of Western Ontario, 2011.

Pal, K. D.; Prakash, A. New Cost-Effective Method for Conversion of Vegetable Oil to Biodiesel. *Bioresour. Technol.* **2012**, *121*, 13–18.

Pappu, V. K. S.; Kanyi, V.; Santhanakrishnan, A.; Lira, C. T.; Miller, D. J. Butyric Acid Esterification Kinetics over Amberlyst Solid Acid Catalysts: The Effect of Alcohol Carbon Chain Length. *Bioresour. Technol.* **2013**, *130*, 793–797.

Park, J.-Y.; Kim, D.-K.; Lee, J.-S. Esterification of Free Fatty Acids Using Water-Tolerable Amberlyst as a Heterogeneous Catalyst. *Bioresour. Technol.* **2010**, *101 Suppl* (1), S62-5.

Pisarello, M. L.; Dalla Costa, B.; Mendow, G.; Querini, C. a. Esterification with Ethanol to Produce Biodiesel from High Acidity Raw Materials: Kinetic Studies and Analysis of Secondary Reactions. *Fuel Process. Technol.* **2010**, *91* (9), 1005–1014.

Riego, J. M.; Sedin, Z.; Zaldívar, J. M.; Marziano, N. C.; Tortato, C. Sulfuric Acid on Silica-Gel: An Inexpensive Catalyst for Aromatic Nitration. *Tetrahedron Lett.* **1996**, *37* (4), 513–516.

Robles-Medina, A.; González-Moreno, P. A.; Esteban-Cerdán, L.; Molina-Grima, E. Biocatalysis: Towards Ever Greener Biodiesel Production. *Biotechnol. Adv.* **2009**, *27* (4), 398–408.

Rukunudin, I. H.; White, P. J.; Bern, C. J.; Bailey, T. B. A Modified Method for Determining Free Fatty Acids from Small Soybean Oil Sample Sizes. *J. Am. Oil Chem. Soc.* **1998**, *75* (5), 563–568.

Santacesaria, E.; Vicente, G. M.; Di Serio, M.; Tesser, R. Main Technologies in Biodiesel Production: State of the Art and Future Challenges. *Catal. Today* **2012**, *195* (1), 2–13.

Santori, G.; Di Nicola, G.; Moglie, M.; Polonara, F. A Review Analyzing the Industrial Biodiesel Production Practice Starting from Vegetable Oil Refining. *Appl. Energy* **2012**, *92*, 109–132.

Sendzikiene, E.; Makareviciene, V.; Janulis, P.; Kitrys, S. Kinetics of Free Fatty Acids Esterification with Methanol in the Production of Biodiesel Fuel. *Eur. J. Lipid Sci. Technol.* **2004**, *106* (12), 831–836.

Shah, K.; Parikh, J.; Dholakiya, B.; Maheria, K. Fatty Acid Methyl Ester Production from Acid Oil Using Silica Sulfuric Acid: Process Optimization and Reaction Kinetics. *Chem. Pap.* **2014a**, *68* (4), 472–483.

Shah, K. A.; Parikh, J. K.; Maheria, K. C. Optimization Studies and Chemical Kinetics of Silica Sulfuric Acid-Catalyzed Biodiesel Synthesis from Waste Cooking Oil. *Bioenergy Res.* **2014b**, *7* (1), 206–216.

Shah, K. A.; Parikh, J. K.; Maheria, K. C. Use of Sulfonic Acid-Functionalized Silica as Catalyst for Esterification of Free Fatty Acids (FFA) in Acid Oil for Biodiesel Production: An Optimization Study. *Res. Chem. Intermed.* **2015**, *41* (2), 1035–1051.

Shibasaki-Kitakawa, N.; Honda, H.; Kuribayashi, H.; Toda, T.; Fukumura, T.; Yonemoto, T. Biodiesel Production Using Anionic Ion-Exchange Resin as Heterogeneous Catalyst. *Bioresour. Technol.* **2007**, *98* (2), 416–421.

Su, C.-H. Kinetic Study of Free Fatty Acid Esterification Reaction Catalyzed by Recoverable and Reusable Hydrochloric Acid. *Bioresour. Technol.* **2013**, *130*, 522–528.

Su, C.-H.; Fu, C.-C.; Gomes, J.; Chu, I.-M.; Wu, W.-T. A Heterogeneous Acid-Catalyzed Process for Biodiesel Production from Enzyme Hydrolyzed Fatty Acids. *AIChE J.* **2008**, *54* (No.1), 327–336.

Tesser, R.; Di Serio, M.; Guida, M.; Nastasi, M.; Santacesaria, E. Kinetics of Oleic Acid Esterification with Methanol in the Presence of Triglycerides. *Ind. Eng. Chem. Res.* **2005**, *44* (21), 7978–7982.

Tesser, R.; Casale, L.; Verde, D.; Di Serio, M.; Santacesaria, E. Kinetics of Free Fatty Acids Esterification: Batch and Loop Reactor Modeling. *Chem. Eng. J.* **2009**, *154* (1–3), 25–33.

Tesser, R.; Casale, L.; Verde, D.; Di Serio, M.; Santacesaria, E. Kinetics and Modeling of Fatty Acids Esterification on Acid Exchange Resins. *Chem. Eng. J.* **2010**, *157* (2–3), 539–550.

Ullah, F.; Dong, L.; Bano, A.; Peng, Q.; Huang, J. Current Advances in Catalysis toward Sustainable Biodiesel Production. *J. Energy Inst.* **2015**, 1–11.

West, A.; Posarac, D.; Ellis, N. Assessment of Four Biodiesel Production Processes Using HYSYS.Plant. *Bioresour. Technol.* **2008**, *99* (14), 6587–6601.

Zolfigol, M. A. Silica Sulfuric acid/ NaNO_2 as a Novel Heterogeneous System for Production of Thionitrites and Disulfides under Mild Conditions. *Tetrahedron* **2001**, 57, 9509–9511.

Purdue University - Scanning Electron Microscope <https://www.purdue.edu/ehrs/rem/rs/sem.htm>.

CHAPTER 5

5 Conclusions and recommendations

5.1 Summary and conclusions

Both homogeneous and heterogeneous catalysts have been tested for esterification of free fatty acid found in yellow grease and non-edible oily feedstock used for biodiesel production. Applicability and limitations of the catalyst types have been pointed out based on extensive testing. Low cost sulphuric acid, selected as the homogeneous catalyst provides high FFA conversion at mild temperatures, with conversion values reaching 97%. A suitable solid acid catalyst for esterification of FFA has been identified (BD20 from Dow Chemical) based on conversion, durability and deactivation studies. The results show that at temperature of 60°C and reaction time of 240 minutes this catalyst can provide close to 97% conversion of FFA, corresponding to 0.45wt.% that is up to standard concentration. This value of FFA conversion is similar to the value obtained for homogeneous catalyst. The trade-off of increasing the reaction time compared to homogeneous catalyst is well justified, due to inherent advantages for the process in term cost and ease of separation of the catalyst after reaction. The absence of pores in the catalyst structure makes it less prone to deactivation due to deposition of known large molecule by-products during the reaction. Detailed kinetic models for the reaction have been developed and tested for reactor sizing purposes.

5.2 Recommendations for Future Work

- The operating parameters for the recommended solid acid catalyst can be further optimized.
- The system could be tested under different reaction conditions, such as varying the molar ratio of methanol to FFA, using feedstock with various initial water content, and use of feedstock having higher initial FFA content.
- The models proposed in this study can be further validated under different operating conditions.
- This study has used simulated feedstock which may be free of some low level impurities. Further tests with more realistic feedstock are recommended.

- Tests of the recommended solid catalyst could be undergone in continuous fashion to estimate the catalyst lifetime, as well as possible regeneration processes.
- It is expected that operating temperature in the range 80 to 90°C would provide lower process time. However, it will require pressurized operation with a whole set of stringent regulations. Higher temperature may also accelerate deactivation rate which needs to be investigated further.

Appendices

List of Appendices

Appendix A	Esterification reactions mass balance (homogeneous catalyst)
Appendix B	Standard calculations for reaction experimental parameters
Appendix C	Example of calculation for First batch mode kinetic model
Appendix D	Example of calculation for Second batch mode kinetic model
Appendix E	Example of calculation for Heterogeneous Catalyst First kinetic model
Appendix F	Example of calculation for Heterogeneous Catalyst Second kinetic model
Appendix G	Technical properties of Biodiesel
Appendix H	ASTM standards of biodiesel (B100) and petrodiesel fuels (PD)

Appendix-A Esterification reactions mass balance (homogeneous catalyst)**Table 0-1** Esterification reactions mass balance (Homogeneous catalyst)

Run	Mode	<i>Input</i>						<i>Output</i>						
		Temperature	Oil	FFA	MeOH	H ₂ SO ₄	Total	BD/TG	Acidic MeOH	Excess MeOH	Samples	Total	Losses	
		°C	g	g	g	g	g	g	g	g	g	g	g	%
1	SB*	30	390	69	156.17	3.44	618.61	452	118	15	35.29	620.29	-1.68	-0.27
3	SB*	40	390	69	156.19	3.45	618.64	453	115	16	34.91	618.91	-0.27	-0.04
5	SB*	50	390	69	156.16	3.46	618.62	446	113	13	36.6	608.6	10.71	1.62
7	SB*	60	390	69	156.18	3.44	618.62	453	107	13	35.5	608.5	10.12	1.64
2	B**	30	390	69	156.22	3.45	618.67	443	119	10	40.39	612.39	6.28	1.01
4	B**	40	390	69	156.22	3.46	618.68	443	117	9	39.99	608.99	9.69	1.57
6	B**	50	390	69	156.17	3.47	618.64	448	117	14	38.03	617.03	1.61	0.26
8	B**	60	390	69	156.16	3.46	618.62	449	109	14	38.9	610.9	7.72	1.25

**: Batch

*: Semi-batch

Appendix-B Standard calculations for reaction experimental parameters

The esterification reaction calculations were performed based on following criteria:

1. Methanol to FFA molar ratio \equiv 20:1
2. Feedstock: FFA + Oil \equiv oleic acid + TG (canola oil)
3. FFA% based on the weight of the feedstock: 15%
4. Liquid Catalyst % based on the weight of FFA: 5%
5. Solid Catalyst % based on the weight of FFA: 5,10,15,20, and 30 %
6. Safe reactor working volume = 700 ml.

Esterification generic equation: $\text{FFA} + \text{CH}_3\text{OH} \rightleftharpoons \text{FAME} + \text{H}_2\text{O}$

$$\frac{n_{\text{MeOH}}}{n_{\text{FFA}}} = \frac{\frac{m_{\text{MeOH}}}{32.04}}{\frac{m_{\text{FFA}}}{282.46}} = 20 \quad \Rightarrow \quad \frac{m_{\text{MeOH}}}{m_{\text{FFA}}} = 2.2686$$

$$m_{\text{MeOH}} = 2.2686 * m_{\text{FFA}} \quad (1)$$

$$m_{\text{FFA}} = 0.15m_{\text{feed}} = 0.15(m_{\text{Oil}} + m_{\text{FFA}}) \quad \Rightarrow \quad \frac{m_{\text{Oil}}}{m_{\text{FFA}}} = \frac{0.85}{0.15} = 5.6666$$

$$m_{\text{Oil}} = 5.6666 * m_{\text{FFA}} \quad (2)$$

$$\frac{m_{\text{FFA}}}{\rho_{\text{FFA}}} + \frac{m_{\text{Oil}}}{\rho_{\text{Oil}}} + \frac{m_{\text{MeOH}}}{\rho_{\text{MeOH}}} + \frac{m_{\text{cat}}}{\rho_{\text{cat}}} = 700 \quad (3)$$

To account only for the reactants present inside the reactor the term related to the catalyst has been neglected therefore equation (3) becomes:

$$\frac{m_{\text{FFA}}}{0.895} + \frac{m_{\text{Oil}}}{0.92} + \frac{m_{\text{MeOH}}}{0.7918} = 700 \quad (3.1)$$

$$\Rightarrow \frac{m_{\text{FFA}}}{0.895} + \frac{5.6666 * m_{\text{FFA}}}{0.92} + \frac{2.2686 * m_{\text{FFA}}}{0.7918} = 700$$

$$\Rightarrow m_{\text{FFA}} \left(\frac{1}{0.895} + \frac{5.6666}{0.92} + \frac{2.2686}{0.7918} \right) = 700$$

$$m_{\text{FFA}} = 69.02 \text{ g}$$

However, to account for the amount of Oleic acid present in supplier solution (90%) the mass of raw Oleic acid has to be adjusted accordingly, and the effective amount used in experiments is:

$$m_{\text{raw Oleic Acid}} = \frac{69.02}{0.9} = 76.69 \text{ g}$$

$$m_{\text{MeOH}} = 156.58 \text{ g}$$

$$m_{\text{oil}} = 391.10 \text{ g}$$

Depending on the catalyst loading desired for a given experiment, the weight of the catalyst is calculated accordingly as a percentage of FFA. For example, at 10wt.% loading the weight of catalyst will be: $69.02 \times 10\% = 6.902 \text{ g}$. That will translate as $[6.902 / (69.02 + 391.10)] \times 100\%$ in term of loading to the Acidified oil (Oil+FFA), in other words that would be **1.5wt.%**. Furthermore, if we take into consideration the reaction mixture (AO + Methanol) the catalyst weight percentage will represent only $[6.902 / (460.12 + 156.58)] \times 100\%$, which is equivalent to **1.12wt.%**. A summary for the esterification reaction Inputs is provided in **Table 0-2**

Table 0-2 Input requirement for Esterification reaction

<i>Variable</i>	<i>Value</i>	<i>Units</i>
<i>MeOH to FFA molar ratio</i>	20	-
<i>Weight of AO (Acid Oil)</i>	460.12	g
<i>Weight of Canola</i>	391.10	g
<i>Weight of FFA</i>	69.02	g
<i>Weight of Methanol</i>	156.58	g
<i>Weight of Catalyst</i>	Variable	g
<i>MW Canola</i>	882.1	g/mole
<i>MW FFA</i>	282.46	g/mole
<i>MW AO</i>	792.154	g/mole
<i>MW MeOH</i>	32.04	g/mole
<i>Moles of Acid Oil</i>	0.5808	mole
<i>Moles of Canola</i>	0.4433	mole
<i>Moles of FFA</i>	0.2443	mole
<i>Moles of MeOH</i>	4.887	mole
<i>Moles of H₂SO₄*</i>	0.0351	mole
<i>Molar ratio H₂SO₄/FFA*</i>	0.1440	-
<i>Mass ratio H₂SO₄/AO*</i>	0.0074	-
<i>Molar ratio MeOH/AO*</i>	7.1058	-

*: only for homogeneous catalyst

Appendix-C Example of calculation for First batch mode kinetic model

T [°C]	X _{eq}	K _{eq}	a ₁	a ₂	FFA ₀	θ	k ₁
30	0.763	0.128	-6.822	31.412	0.3481	20	0.0038
40	0.881	0.340	-1.939	24.415	0.3481	20	0.005
50	0.977	2.176	0.540	19.944	0.3481	20	0.007
60	0.992	6.619	0.849	19.315	0.3481	20	0.0109

T=60°C

t [min]	X _{FFAexp} ,	X _{FFAcalc} ,	X _{FFAexp} -X _{FFAcalc}	(X _{FFAexp} -X _{FFAcalc}) ²	(X _{FFAexp} -X _{FFAavg}) ²
0	0.0000	0.0000	0.0000	0.0000	0.6255
5	0.4692	0.3135	0.1557	0.0242	0.1035
10	0.6495	0.5260	0.1235	0.0152	0.0200
15	0.7639	0.6711	0.0928	0.0086	0.0007
20	0.8306	0.7706	0.0601	0.0036	0.0016
25	0.8771	0.8390	0.0381	0.0015	0.0074
30	0.9069	0.8862	0.0207	0.0004	0.0135
40	0.9395	0.9414	-0.0019	0.0000	0.0221
50	0.9566	0.9678	-0.0112	0.0001	0.0275
60	0.9697	0.9805	-0.0108	0.0001	0.0320
70	0.9770	0.9866	-0.0095	0.0001	0.0347
80	0.9708	0.9895	-0.0187	0.0003	0.0324
90	0.9705	0.9909	-0.0204	0.0004	0.0323
Average	0.7909		Σ=	0.0547	0.9529

r²= 0.9426

RMS= 0.0649

Appendix-D Example of calculation for Second batch mode kinetic model

T [°C]	k ₁	α	FFA ₀ [mol/L]	Lnk ₁	1/TR*1000 [mol/J]
30	0.0506	0.2950	0.3481	-2.9840	0.3968
40	0.0781	0.2950	0.3481	-2.5493	0.3841
50	0.1369	0.2950	0.3481	-1.9882	0.3722
60	0.2443	0.2950	0.3481	-1.4095	0.3610

Apparent

T=60°C

t [min]	XFFA _{exp}	XFFA _{calc,60C}	XFFA _{exp} -XFFA _{calc}	(XFFA _{exp} -XFFA _{calc}) ²	(XFFA _{exp} -XFFA _{avg}) ²
0	0	0	0	0	0.6255
5	0.4692	0.4596	0.0096	9.26E-05	0.1035
10	0.6495	0.6622	-0.0127	0.00016	0.0200
15	0.7639	0.7691	-0.0052	2.69E-05	0.0007
20	0.8306	0.8322	-0.0016	2.41E-06	0.0016
25	0.8771	0.8726	0.0045	2.039E-05	0.0074
30	0.9069	0.9000	0.0070	4.85E-05	0.0135
40	0.9395	0.9337	0.0058	3.40E-05	0.0221
50	0.9566	0.9528	0.0038	1.42E-05	0.0275
60	0.9697	0.9647	0.0050	2.47E-05	0.0320
70	0.9770	0.9726	0.0044	1.94E-05	0.0347
80	0.9708	0.9781	-0.0074	5.41E-05	0.0324
90	0.9705	0.9822	-0.0117	0.0001	0.0323
AVG	0.7909		Σ=	0.0006	0.9529

r²= 0.9993

RMS= 0.0070

Appendix-E Example of calculation for Heterogeneous Catalyst First kinetic model

T [°C]	X _{eq}	K _{eq}	a ₁	a ₂	FFA ₀ [mol/L]	θ	k ₁
30	0.34725	0.0094	-105.3858	94.1906	0.3500	20	0.00108
40	0.40814	0.0144	-68.6129	77.0067	0.3505	20	0.0009
50	0.72284	0.0978	-9.2254	34.3371	0.3496	20	0.00228
60	0.96433	1.3695	0.2698	20.4796	0.3492	20	0.00275

T=60°C

t [min]	XFFA _{exp}	XFFA _{calc}	XFFA _{exp} -XFFA _{calc}	(XFFA _{exp} -XFFA _{calc}) ²	(XFFA _{exp} -XFFA _{avg}) ²
0	0	0	0	0	0.3851
5	0.11866	0.0913	0.0273	0.0007	0.2519
10	0.22114	0.1739	0.0472	0.0022	0.1596
15	0.27273	0.2486	0.0241	0.0006	0.1210
20	0.34645	0.3162	0.0303	0.0009	0.0752
25	0.39953	0.3773	0.0222	0.0005	0.0489
30	0.44775	0.4327	0.0151	0.0002	0.0299
40	0.53602	0.5281	0.0079	6.24E-05	0.0072
45	0.56863	0.5692	-0.0005	2.91E-07	0.0027
50	0.61291	0.6063	0.0066	4.31E-05	5.92E-05
60	0.65605	0.6705	-0.0144	0.0002	0.0013
70	0.71357	0.7231	-0.0095	9.06E-05	0.0086
80	0.74457	0.7663	-0.0217	0.0005	0.0154
90	0.79404	0.8017	-0.0076	5.84E-05	0.0301
100	0.80176	0.8308	-0.0290	0.0008	0.0328
120	0.84283	0.8742	-0.0314	0.0010	0.0494
140	0.8775	0.9036	-0.0261	0.0007	0.0660
160	0.90214	0.9233	-0.0212	0.0004	0.0793
180	0.92555	0.9367	-0.0111	0.0001	0.0930
200	0.94871	0.9457	0.0031	9.33E-06	0.1077
220	0.95642	0.9517	0.0047	2.19E-05	0.1128
240	0.96627	0.9558	0.0104	0.0001	0.1195
AVG	0.6206		Σ=	0.0093	1.7972

$$r^2 = \mathbf{0.9948}$$

$$\mathbf{RMS = 0.0206}$$

Appendix-F Example of calculation for Heterogeneous Catalyst Second kinetic model

T [°C]	k1	α	FFA0 [mol/L]	Lnk1	1/TR*1000 [mol/J]
30	0.00992	0.2958	0.3500	-5.3879	0.3968
40	0.00942	0.2958	0.3505	-4.6647	0.3841
50	0.02716	0.2958	0.3496	-3.6059	0.3722
60	0.04149	0.2958	0.3492	-3.1824	0.3610

Apparent

T=60°C

t [min]	XFFAexp	XFFAcalc	XFFAexp-XFFAcalc	(XFFAexp-XFFAcalc) ²	(XFFAexp-XFFAavg) ²
0	0	0	0	0	0.3851
5	0.1187	0.1123	0.0064	4.06E-05	0.2519
10	0.2211	0.2067	0.0145	0.0002	0.1596
15	0.2727	0.2868	-0.0140	0.0002	0.1210
20	0.3464	0.3553	-0.0089	7.87E-05	0.0752
25	0.3995	0.4144	-0.0149	0.0002	0.0489
30	0.4478	0.4658	-0.0180	0.0003	0.0299
40	0.5360	0.5501	-0.0141	0.0002	0.0072
45	0.5686	0.5850	-0.0164	0.0003	0.0027
50	0.6129	0.6159	-0.0030	0.0000	5.92E-05
60	0.6561	0.6683	-0.0123	0.0002	0.0013
70	0.7136	0.7107	0.0029	8.46E-06	0.0086
80	0.7446	0.7454	-0.0008	6.75E-07	0.0154
90	0.7940	0.7742	0.0198	0.0004	0.0301
100	0.8018	0.7984	0.0033	1.11E-05	0.0328
120	0.8428	0.8364	0.0064	4.07E-05	0.0494
140	0.8775	0.8647	0.0128	0.0002	0.0660
160	0.9021	0.8861	0.0160	0.0003	0.0793
180	0.9256	0.9029	0.0227	0.0005	0.0930
200	0.9487	0.9162	0.0325	0.0011	0.1077
220	0.9564	0.9270	0.0295	0.0009	0.1128
240	0.9663	0.9358	0.0305	0.0009	0.1195
AVG	0.6206		$\Sigma=$	0.0059	1.7972

$r^2=$ **0.9967**

RMS= **0.0164**

Appendix-G Technical properties of biodiesel (Demirbas, 2010)

Common name	Biodiesel (biodiesel)
Common chemical name	Fatty acid (m)ethyl ester
Chemical formula range	C ₁₄ -C ₂₄ methyl esters or C ₁₅₋₂₅ H ₂₈₋₄₈ O ₂
Kinematic viscosity range [mm ² /s, at 313K]	3.3-5.2
Density range [kg/m ³ , at 288K]	860-894
Boiling point range [K]	>475
Flash point range [K]	420-450
Distillation range [K]	470-600
Vapor pressure [mmHg, at 295K]	<5
Solubility in water	Insoluble in water
Physical appearance	Light to dark yellow, clear liquid
Odor	Light musty/soapy odor
Biodegradability	More biodegradable than petroleum diesel
Reactivity	Stable, but avoid strong oxidizing agents

Appendix-H ASTM standards of biodiesel (B100) and petrodiesel fuels (PD) (Demirbas, 2010)

Property	Test method	ASTM D975 (PD)	ASTM D6751 (B100)
Flash point	D93	325 K min	403K
Water and sediment	D2709	0.05 max vol.%	0.05 max vol.%
Kinematic viscosity (at 313K)	D445	1.3-4.1 mm ² /s	1.9-6.0 mm ² /s
Sulfated ash	D874	-	0.02 max wt.%
Ash	D482	0.01 max wt.%	-
Sulfur	D5453	0.05 max wt.%	-
Sulfur	D2622/129	-	0.05 max wt.%
Copper strip corrosion	D130	No3 max	No3 max
Cetane number	D613	40min	47min
Aromaticity	D1319	35 max vol.%	-
Carbon residue	D4530	-	0.05 max mass%
Carbon residue	D524	0.35 max mass%	-
Distillation temp (90% volume recycle)	D1160	555K min- 611K max	-

Curriculum Vitae

Name: Mohamed Kaddour

Post-secondary Education and Degrees: The University of Western Ontario
London, Ontario, Canada

2014-2016 ME.Sc Candidate.

The University of Western Ontario
London, Ontario, Canada

2013-2014 M.Eng.

The University of Science and Technology Houari Boumediene
Bab-Ezzouar, Algiers, Algeria

1992-2000 State Engineer.

Honours and Awards Western Engineering Scholarship
2014-2016

Related Work Experience Teaching Assistant
The University of Western Ontario
2014-2016

Multiple Engineering, and Project Management Positions
Al Qanawat, and TACIR (U.A Emirates); NAFTEC, and EFTPH (Algeria)
2000-2012